



**UNIVERSIDAD AUTÓNOMA CHAPINGO**

**POSGRADO EN INGENIERÍA AGRÍCOLA  
Y USO INTEGRAL DEL AGUA**

**MODELING AND OPTIMIZATION OF A GREENHOUSE-TYPE SOLAR  
DRYER SYSTEM**

**TESIS DE GRADO  
COMO REQUISITO PARCIAL PARA OBTENER EL GRADO DE  
DOCTOR EN INGENIERÍA AGRÍCOLA Y USO INTEGRAL DEL AGUA**

**PRESENTA:  
JOSÉ OLAF VALENCIA ISLAS**

**BAJO LA SUPERVISIÓN DE:  
PHD. IRINEO L. LÓPEZ CRUZ**

**CO-DIRECTOR:  
PhD. MURAT KACIRA**



Chapingo, Estado de México, 18 de noviembre del 2022

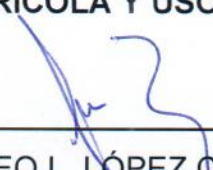


MODELING AND OPTIMIZATION OF A GREENHOUSE-TYPE SOLAR DRYER  
SYSTEM

Tesis realizada por **JOSÉ OLAF VALENCIA ISLAS** bajo la supervisión del  
Comité Asesor indicado, aprobada por el mismo y aceptada como requisito  
parcial para obtener el grado de:

**DOCTOR EN INGENIERÍA AGRÍCOLA Y USO INTEGRAL DEL AGUA**

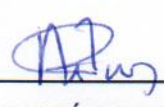
CO-DIRECTOR:

  
\_\_\_\_\_  
DR. IRINEO L. LÓPEZ CRUZ

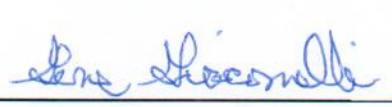
CO-DIRECTOR:

  
\_\_\_\_\_  
DR. MURAT KACIRA

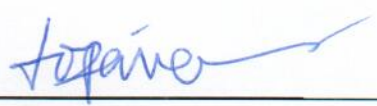
ASESOR:

  
\_\_\_\_\_  
DR. AGUSTÍN RUIZ GARCÍA

ASESOR:

  
\_\_\_\_\_  
DR. GENE GIACOMELLI

LECTOR EXTERNO:

  
\_\_\_\_\_  
DR. PEIWEN LI

# CONTENTS

<b>1</b>	<b>GENERAL INTRODUCTION .....</b>	<b>1</b>
<b>1.1</b>	<b>Background.....</b>	<b>1</b>
1.1.1	Drying .....	1
1.1.2	Water activity.....	1
1.1.3	Moisture content and moisture ratio.....	2
1.1.4	Drying rate.....	4
1.1.5	Drying rate constant .....	5
1.1.6	Solar Drying.....	5
1.1.7	Types of Solar Dryers .....	6
1.1.8	Most common Solar Dryers.....	7
	Cabinet dryer.....	7
	Greenhouse-type dryers .....	9
	In-house or Pilot plants .....	10
<b>1.2</b>	<b>Objectives.....</b>	<b>11</b>
<b>1.3</b>	<b>Dissertation structure and overview .....</b>	<b>11</b>
1.3.1	Overall Summary.....	12
	Thin layer models for tomato – Chapter 3.....	12
	Model Predictive Control for Greenhouse-type Solar Dryers -Chapter 4 .....	13
	Greenhouse-type Solar Dryer modeling with Computational Fluid Dynamics a review – Chapter 5.....	14
	Alternative Designs to Greenhouse-type Solar Dryer Air Distribution – Chapter 6 .....	14
1.3.2	Overall Conclusions and Outlook.....	15
	Thin-layer models for tomato – Chapter 4 .....	15
	Model Predictive Control for Greenhouse-Type Solar Dryers – Chapter 5 .....	16
	Greenhouse-type Solar Dryer modeling with Computational Fluid Dynamics a review – Chapter 6.....	16
	Alternative Designs to Greenhouse-type solar Dryer Air distribution – Chapter 7.....	17
<b>2</b>	<b>LITERATURE REVIEW.....</b>	<b>19</b>
<b>2.1</b>	<b>Thin-layer models for tomato drying.....</b>	<b>19</b>

2.2	Control of Greenhouse-type Solar Dryers .....	22
2.3	Computational Fluid Dynamics of Greenhouse-type Solar Dryers	23
3	REFERENCES.....	32
4	EVALUATION OF THIN LAYER MODELS IN A GREENHOUSE-TYPE SOLAR DRYER DURING DRYING OF TOMATO FRUITS.....	41
4.1	Abstract .....	41
4.2	Introduction.....	41
4.3	Materials and Methods .....	45
4.3.1	The Greenhouse Solar Dryer .....	45
4.3.2	Drying experiments and data collection .....	46
4.3.3	Mathematical modeling .....	47
4.4	Theory and calculations.....	50
4.5	Results.....	51
4.6	Discussion.....	55
4.7	Conclusions .....	57
4.8	Appendices .....	58
4.9	Acknowledgments .....	59
4.10	References .....	59
5	CONTROLLER DESIGN FOR A GREENHOUSE-TYPE SOLAR DRYER BASED ON PRODUCT TEMPERATURE MODEL .....	67
5.1	Abstract .....	67
5.2	Introduction.....	68
5.3	Materials and Methods .....	70
5.3.1	Greenhouse-type Solar Dryer .....	70
5.3.2	Experiment .....	71
5.3.3	Greenhouse-type Solar Prediction Model .....	72
5.3.4	MPC Problem Statement .....	73
5.3.5	Control Strategies.....	75

<b>5.4</b>	<b>Results.....</b>	<b>76</b>
5.4.1	Model simulations and Evaluation.....	76
5.4.2	MPC Simulations.....	79
<b>5.5</b>	<b>Discussion.....</b>	<b>81</b>
<b>5.6</b>	<b>Conclusions .....</b>	<b>83</b>
<b>5.7</b>	<b>Acknowledgments .....</b>	<b>84</b>
<b>5.8</b>	<b>References .....</b>	<b>84</b>
<b>6</b>	<b>ADVANCES IN MODELING WITH COMPUTATIONAL FLUID DYNAMICS OF GREENHOUSE-TYPE SOLAR DRYERS.....</b>	<b>88</b>
<b>6.1</b>	<b>Abstract .....</b>	<b>88</b>
<b>6.2</b>	<b>Introduction.....</b>	<b>89</b>
<b>6.3</b>	<b>Physical Phenomena that occur in Greenhouse-type Solar Dryers 92</b>	
<b>6.4</b>	<b>Computational Fluid Dynamics .....</b>	<b>96</b>
6.4.1	Pre-Processing stage.....	97
6.4.2	Solver .....	97
6.4.3	Post-Processing .....	97
<b>6.5</b>	<b>How to build a CFD model for Drying .....</b>	<b>98</b>
6.5.1	Radiation model .....	99
6.5.2	Species Model.....	100
6.5.3	Turbulence Model.....	100
6.5.4	Assumptions and Boundary Conditions .....	101
<b>6.6</b>	<b>State of Art WITH CFD APPLICATION IN SOLAR DRYING.....</b>	<b>102</b>
6.6.1	Products studied in Greenhouse-type solar Dryers .....	104
<b>6.7</b>	<b>CFD modeling of Greenhouse-type solar Dryers.....</b>	<b>116</b>
<b>6.8</b>	<b>Conclusions .....</b>	<b>124</b>
<b>6.9</b>	<b>References .....</b>	<b>124</b>

<b>7</b>	<b>TWO NEW AIR DISTRIBUTION SYSTEMS TO ENHANCE DRYING IN GREENHOUSES</b>	<b>139</b>
<b>7.1</b>	<b>Abstract</b>	<b>139</b>
<b>7.2</b>	<b>Introduction</b>	<b>140</b>
<b>7.3</b>	<b>Materials and Methods</b>	<b>141</b>
7.3.1	Experimental Setup	141
7.3.2	Instrumentation	142
7.3.3	Meshing and Simulations	143
<b>7.4</b>	<b>Theory/calculations</b>	<b>146</b>
7.4.1	Mathematical Models	146
7.4.2	Boundary conditions	147
<b>7.5</b>	<b>Results</b>	<b>150</b>
7.5.1	Evaluation	150
7.5.2	Air temperature	150
7.5.3	Air velocity	152
7.5.4	Air Density	153
<b>7.6</b>	<b>Discussion</b>	<b>154</b>
7.6.1	Case A	154
7.6.2	Case B	155
7.6.3	Case C	156
7.6.4	Comparison between Cases	157
<b>7.7</b>	<b>Conclusions</b>	<b>158</b>
<b>7.8</b>	<b>References</b>	<b>159</b>

## LIST OF TABLES

<b>TABLE 4-1.</b> THIN LAYER DRYING MODELS.....	48
<b>TABLE 4-2.</b> STATISTICS FOR THE BEST FIVE MODELS UNDER FIT AND TEST STAGES. ..	53
<b>TABLE 4-4.</b> PARAMETER VALUES FOR ALL 35 THIN LAYER MODELS TESTED IN THIS STUDY. .....	58
<b>TABLE 6-1.</b> PRODUCTS DEHYDRATED IN GREENHOUSE-TYPE SOLAR DRYERS AROUND THE WORLD.....	105
<b>TABLE 6-2.</b> CFD PAPERS FOUND IN A LITERATURE REVIEW. ....	119
<b>TABLE 7-1.</b> MESH QUALITY STATISTICS FOR ALL GEOMETRIES UNDER STUDY.....	145
<b>TABLE 7-2.</b> BOUNDARY CONDITIONS USED FOR THE SIMULATIONS. ....	148
<b>TABLE 7-3.</b> OPERATING CONDITIONS USED FOR THE SIMULATIONS.....	149
<b>TABLE 7-4.</b> EVALUATION POINTS BETWEEN MEASUREMENTS AND SIMULATIONS. ....	150

## LIST OF FIGURES

<b>FIGURE 1-1.</b> THE REACTION RATE OF THE DIFFERENT MICROORGANISMS AND PROCESSES IN AGRICULTURAL PRODUCTS AS A FUNCTION OF WATER ACTIVITY (LABUZA, 1977).....	2
<b>FIGURE 1-2.</b> CLASSIFICATION OF SOLAR DRYERS BY DIFFERENT CRITERIA. ....	6
<b>FIGURE 1-3.</b> GENERAL CHARACTERISTICS OF A CABINET DRYER (JANJAI & BALA, 2012). .....	8
<b>FIGURE 1-4.</b> CABINET DRYER WITHOUT A SOLAR CONCENTRATOR SEPARATED (SPALL & SETHI, 2020). ....	8
<b>FIGURE 1-5.</b> SOLAR CABINET DRYER WITH SOLAR CONCENTRATOR, MIXED TYPE, AND FORCED AIRFLOW (ARUN ET AL., 2019). ....	9
<b>FIGURE 1-6.</b> CABINET SOLAR DRYER, INDIRECT TYPE WITH A WATER HEATER WITH HEATER EXCHANGER (IRANMANESH ET AL., 2020). ....	9
<b>FIGURE 1-7.</b> GREENHOUSE-TYPE SOLAR DRYER WITH A POLYCARBONATE COVER AND PARABOLIC ROOF (JANJAI ET AL., 2009A). ....	10
<b>FIGURE 1-8.</b> GREENHOUSE-TYPE SOLAR DRYER WITH PLASTIC COVER AND VENLO GEOMETRY (BARNWAL & TIWARI, 2008A). ....	10
<b>FIGURE 1-9.</b> GREENHOUSE-TYPE SOLAR DRYER WITH SOLAR COLLECTOR AND PLASTIC COVER (ROMÁN-ROLDÁN ET AL., 2019).....	10
<b>FIGURE 1-10.</b> TUNNEL GREENHOUSE SOLAR DRYER (PATIL & GAWANDE, 2016). ....	10
<b>FIGURE 1-11.</b> SOLAR PILOT PLANT FOR DRYING AGRICULTURAL PRODUCTS (GARCÍA-VALLADARES ET AL., 2020). ....	11
<b>FIGURE 1-12.</b> DIMENSIONS OF THE GREENHOUSE-TYPE SOLAR DRYER. ....	13
<b>FIGURE 2-1.</b> INFRARED DRYER USED BY SADIN ET AL. (2017).....	21
<b>FIGURE 2-2.</b> SMALL TUNNEL DRYER USED BY MURUGAVELH ET AL. (2019). ....	21
<b>FIGURE 2-3.</b> GREENHOUSE SOLAR DRYER USED BY HAMDİ & KOOLİ (2018). ....	21
<b>FIGURE 2-4.</b> RECYCLABLE CAN SOLAR DRYER USED BY KISHK ET AL. (2019). ....	21

<b>FIGURE 2-5.</b> THE INCREASING TREND IN THE NUMBER OF DRYING PAPERS PER YEAR (DATA, SCOPUS, 2019).....	25
<b>FIGURE 2-6.</b> TRENDS IN PUBLICATIONS ON DRYING, CFD, AND GREENHOUSE-TYPE SOLAR DRYERS, (DATA SCOPUS, 2019).....	26
<b>FIGURE 2-7.</b> GREENHOUSE-TYPE SOLAR DRYER USED TO DRY SLUDGE (KRAWCZYK & BADYDA, 2011).....	27
<b>FIGURE 2-8.</b> AIR VELOCITY DISTRIBUTION INSIDE A GREENHOUSE-TYPE SOLAR DRYER STUDIED BY SOMSILA & TEEBOONMA (2014). ....	27
<b>FIGURE 2-9.</b> TEMPERATURE DISTRIBUTION FOR PARABOLIC AND SINUSOIDAL COVERS GEOMETRIES (SRICHAT ET AL., 2019).....	29
<b>FIGURE 2-10.</b> GREENHOUSE-TYPE SOLAR DRYER USED BY (ROMÁN-ROLDÁN ET AL., 2019).....	29
<b>FIGURE 2-11.</b> GREENHOUSE GEOMETRIES STUDIED BY PURUSOTHAMAN ET AL. (2019) AS SOLAR DRYERS. ....	29
<b>FIGURE 2-12.</b> GREENHOUSES USED BY VILLAGRAN ET AL. (2021) TO TEST AS SOLAR DRYERS. ....	30
<b>FIGURE 4-1.</b> DIMENSIONS OF THE GREENHOUSE-TYPE SOLAR DRYER.....	46
<b>FIGURE 4-2.</b> OUTSIDE AND INSIDE CONDITIONS OF DATASET 1. ....	52
<b>FIGURE 4-3.</b> OUTSIDE AND INSIDE CONDITIONS OF DATASET 2. ....	52
<b>FIGURE 4-4.</b> BEST FIVE THIN LAYER MODELS DURING THE FITTING WITH MEASUREMENTS. ....	54
<b>FIGURE 4-5.</b> COMPARISON OF MEASUREMENTS AND THE BEST FIVE THIN LAYER MODELS WITH THE NEW DATA. ....	54
<b>FIGURE 5-1.</b> GREENHOUSE SOLAR DRYER DIMENSIONS AND ORIENTATION.....	71
<b>FIGURE 5-2.</b> MATLAB SIMULINK MODEL OF THE GREENHOUSE-TYPE SOLAR DRYER WITH THE MPC CONTROL.....	74
<b>FIGURE 5-3.</b> BLOCK DIAGRAM FLOW FOR THE GREENHOUSE-TYPE SOLAR DRYER SYSTEM. ....	75

<b>FIGURE 5-4.</b> OUTDOOR DATA IS USED FOR MODEL IDENTIFICATION AND MODEL VALIDATION.....	77
<b>FIGURE 5-5.</b> INDOOR DATA OF THE GREENHOUSE FOR IDENTIFICATION AND VALIDATION. ....	77
<b>FIGURE 5-6.</b> RELATIVE HUMIDITY, PRODUCT AND AIR TEMPERATURE INSIDE THE GREENHOUSE, MEASUREMENTS, AND MODEL SIMULATIONS. ....	78
<b>FIGURE 5-7.</b> FLOOR AND COVER TEMPERATURE INSIDE THE GREENHOUSE, MODEL, AND MEASUREMENTS.....	78
<b>FIGURE 5-8.</b> MODEL STATISTICS BETWEEN THE MEASUREMENTS AND THE MODEL SIMULATIONS.....	79
<b>FIGURE 5-9.</b> CONTROLLERS' STRATEGIES WITH THE PRODUCT AND AIR TEMPERATURE. ....	80
<b>FIGURE 5-10.</b> FLOOR AND COVER TEMPERATURE AND RELATIVE HUMIDITY WITH THE CONTROLLERS.....	81
<b>FIGURE 5-11.</b> PRODUCT TEMPERATURE WITH THE TWO MPC STRATEGIES. ....	81
<b>FIGURE 6-1.</b> MOST WASTED AGRICULTURAL PRODUCTS AFTER HARVEST AND DURING DISTRIBUTION STAGES (ADAPTED FROM FAO, 2019).....	89
<b>FIGURE 6-2.</b> PHYSICAL PROCESSES INVOLVED IN DRYING WITHIN A GREENHOUSE-TYPE SOLAR DRYER SYSTEM (GTSDS). ....	95
<b>FIGURE 6-3.</b> A CLOSER LOOK AT THE HEAT AND MASS TRANSFER IN A PRODUCT UNDER DRYING.....	96
<b>FIGURE 6-4.</b> NUMBER OF DRYING PAPERS PER YEAR, DATA FROM SCOPUS, 2019...	103
<b>FIGURE 6-5.</b> PAPER GROWTH PUBLICATIONS PER YEAR IN DRYING, CFD, AND GREENHOUSE-TYPE SOLAR DRYERS, DATA FROM SCOPUS, 2019.....	104
<b>FIGURE 6-6.</b> VOLUME OF ALL GREENHOUSES USED IN RESEARCH, SO FAR. ....	114
<b>FIGURE 7-1.</b> GREENHOUSE-TYPE SOLAR DRYER USED FOR THIS STUDY. ORIENTATION AND DIMENSIONS. ....	142

<b>FIGURE 7-2.</b> SENSOR DISTRIBUTION IN THE GREENHOUSE-TYPE SOLAR DRYER. A) WINDSONIC4, B) CS215-L FLOOR, C) NORTH WALL 0.95 M, D) SOUTH WALL 0.95 M, E) Cs215-L 0.6M, F) CS215-L 0.95 M, G) CS215-L 1.9M, H) CS215-L 2.65 M, I) CMP3 PYRANOMETER AND J) SENSORS OUTSIDE THE GREENHOUSE. ....	143
<b>FIGURE 7-3.</b> EVALUATION CASE MESH.....	143
<b>FIGURE 7-4.</b> FIRST DESIGN PROPOSAL FOR AIR DISTRIBUTION SYSTEM WITH 2 LINES. CASE B. ....	144
<b>FIGURE 7-5.</b> SECOND DESIGN PROPOSAL FOR AIR DISTRIBUTION SYSTEM WITH 3 LINES. CASE C. ....	144
<b>FIGURE 7-6.</b> GREENHOUSE MESH WITH THE INLETS (BLUE) DONE BY THE FLUENT MESHING PROGRAM. ....	145
<b>FIGURE 7-7.</b> DIMENSIONS OF THE B AND C SYSTEMS. THE B SYSTEM IS LOCATED AT THE HALF OF THE GREENHOUSE WHILE THE C IS LOCATED AT THE SOUTH WALL. ....	145
<b>FIGURE 7-8.</b> AIR TEMPERATURE DISTRIBUTION INSIDE THE GREENHOUSE-TYPE SOLAR DRYER WITH THE DIFFERENT DESIGNS TESTED. ....	151
<b>FIGURE 7-9.</b> AIR VELOCITY DISTRIBUTION INSIDE THE GREENHOUSE-TYPE SOLAR DRYER. ....	153
<b>FIGURE 7-10.</b> AIR DENSITY DISTRIBUTION INSIDE THE GREENHOUSE-TYPE SOLAR DRYER. ....	154

## ABBREVIATION

<b>FAO:</b>	Organization of the United Nations for Food and Agriculture
<b>MPC:</b>	Model Predictive Control
<b>mm:</b>	Milimeters
<b>m:</b>	Meters
<b>m<sup>3</sup></b>	Cubic meters
<b>kg:</b>	Kilogram
<b>hr</b>	hour
<b>s</b>	seconds
<b>R<sup>2</sup>:</b>	Determination Coefficient
<b>RMSE:</b>	Root Mean Square Error
<b>MSE:</b>	Mean Square Error
<b>MAE:</b>	Mean Absolute Error
<b>EF:</b>	Model Efficiency
<b>CFD:</b>	Computational Fluid Dynamics
<b>e.g.:</b>	For example
<b>et al.:</b>	And others

## DEDICATION

*A mis padres Rufino y Judith*

*A mis hermanos, Katherine y Edwin*

*A J. Natalia Valencia*

*A mis co-directores, Dr. Irineo López y Dr. Murat Kacira*

*A mis amigos, que no podría enlistarlos a cada uno de ellos.*

*Por todo su apoyo y cariño,*

*Infinitas gracias.*

*Y al lector, espero que encuentre en esta tesis algo de su interés. En este doctorado aprendí que cuanto más cerca crees que estás de la respuesta, más preguntas surgen. Profundizar en el conocimiento significa reconocer a los que te han precedido, pero también encontrar tu voz en cada etapa de tu formación como científico. No te rindas, continúa e innova, el mundo te necesita.*

## ACKNOWLEDGMENTS

Al Consejo Nacional de Ciencia y Tecnología (CONACyT) por el apoyo económico para desarrollar mis estudios de posgrado. A la Universidad Autónoma Chapingo y al Posgrado en Ingeniería Agrícola y Uso Integral del Agua (IAUIA), por todo el apoyo y la gran educación que recibí durante esta etapa. Al Biosystems Engineering Department de la Universidad de Arizona, por hacerme sentir bienvenido y darme cursos de calidad.

A mis asesores en la Universidad Autónoma Chapingo, por su valioso apoyo y guía constante en todo el proceso de doctorado. Al Dr. Irineo L. López Cruz por todo su tiempo, amistad y apoyo; Dr. es usted un ejemplo a seguir y siempre tendré presente lo que me ha enseñado desde que lo conocí. Dr. Agustín, siempre estuvo al pendiente y siempre encontré en usted a alguien a quién seguir y continuar haciendo investigación.

A mis asesores en la Universidad de Arizona por todo su apoyo y tiempo. Thanks Dr. Gene Giacomelli, I found always interesting having some words with you, and I have learned a lot from all your experience; Dr. Peiwen Li thanks for all your advice and knowledge; Dr. Murat Kacira, thanks for all your support, advice, knowledge, and friendship, you are such an example to follow.

Gracias a mi familia, quienes más sufrieron el poco tiempo que tenía para dedicarles y que con su amor y apoyo logré concluir el máximo grado de estudios que me puede conferir una Universidad, mi amor y apoyo siempre para ustedes. Por último, gracias a Mayra, Dr. Mauricio Carillo, Dava, Dr. Kitt, Dr. Armando Barreto, Eduardo, Elena, Cynthia, Juan Gabriel, Juan José, Miguel, Marín y al Dr. Slack por todo su apoyo, palabras, compañía y tiempo durante todos estos años. A J. Natalia Valencia G. sin la cual no hubiera podido terminar esta etapa de mi vida.

## AUTHOR BIOGRAPHY



### Datos personales

Nombre	José Olaf Valencia Islas
Fecha de nacimiento	19 de noviembre de 1991
Lugar de nacimiento	Texcoco, México
Profesión	Ing. Mecánico Agrícola
No. Cédula	08741285
Correo electrónico	j.valencia.islas@outlook.com

### Desarrollo académico

Preparatoria	Universidad Autónoma Chapingo (UACH)
Licenciatura	Ing. Mecánica Agrícola (UACH)
Maestría	Ingeniería Agrícola y Uso Integral del Agua (UACH)

## MODELING AND OPTIMIZATION OF A GREENHOUSE-TYPE SOLAR DRYER SYSTEM

### RESUMEN GENERAL

El secado solar en invernaderos es una alternativa económica y segura para el secado, permite aumentar la vida de anaquel de productos de forma inocua. Los objetivos de la tesis fueron 1) modelar la cinética de secado de jitomate en un secador solar tipo invernadero; 2) modelar y controlar las condiciones internas en un secador solar tipo invernadero; 3) evaluar alternativas de diseño para mejorar el proceso de secado. El secador solar de tipo invernadero se ubica en la Universidad Autónoma Chapingo (México) y tiene una cubierta de policarbonato de 6 mm de espesor con forma parabólica; piso de concreto de 15 cm de espesor; dos ventiladores para extraer el aire y cuatro entradas de aire; con un volumen aproximado de 211 m<sup>3</sup>. Se probaron 35 modelos de capa fina para el secado de jitomate en rodajas. La innovación en esta etapa fue analizar los modelos en cuanto a su estructura, número de parámetros y evaluarlos con datos de otro experimento. El mejor modelo fue el de Page VI con un RMSE de 0.06 y un R<sup>2</sup> de 0.993. Para mejorar el secado, se modeló y diseñó un controlador basado en "Model Predictive Control" para el invernadero. La principal innovación fue el uso de identificación de sistemas con el algoritmo N4SID, la obtención de un modelo con la temperatura del producto como estado y el control basado en la temperatura del producto y no la del aire. Finalmente, se realizó una revisión de literatura en la modelación de secadores solares tipo invernadero usando CFD y se desarrolló un modelo computacional (CFD) para el secador. Se validó el modelo y se probaron dos diseños para recircular el aire y mejorar la distribución de temperatura dentro del invernadero. Ambos sistemas mostraron mayores temperaturas y una velocidad más uniforme en todo el volumen.

**Palabras clave:** Secado solar, Control, Modelación, CFD, Capa fina.

Tesis de Doctorado en IAUIA  
Universidad Autónoma Chapingo  
Autor: José Olaf Valencia Islas  
Director: Dr. Irineo L. Lopez Cruz / Dr. Murat Kacira

### ABSTRACT

Solar drying in greenhouses is an economical and safe alternative for drying, it allows to increase the shelf life of products in an innocuous way. The objectives of the thesis were 1) to model the drying kinetics of tomato in a greenhouse-type solar dryer; 2) to model and control the internal conditions in a greenhouse-type solar dryer; 3) to evaluate design alternatives to improve the drying process. The greenhouse-type solar dryer is located at the Universidad Autonoma Chapingo (Mexico) and has a 6-mm-thick parabolic-shaped polycarbonate cover; 15 cm thick concrete floor; two exhaust fans for the air and four air inlets; with an approximate volume of 211 m<sup>3</sup>. Thirty-five thin-layer models were tested for drying tomato slices. The innovation at this stage was to analyze the models in terms of their structure, and number of parameters and evaluate them with data from another experiment. The best model was the Page VI model with an RMSE of 0.06 and an R<sup>2</sup> of 0.993. To improve drying, a controller based on "Model Predictive Control" for the greenhouse was modeled and designed. The main innovation was the use of system identification with the N4SID algorithm, obtaining a model with product temperature as state and control based on product temperature and not air temperature. Finally, a literature review on the modeling of greenhouse-type solar dryers using CFD was carried out and a computational model (CFD) for the dryer was developed. The model was validated, and two designs were tested to recirculate the air and improve the temperature distribution inside the greenhouse. Both systems showed higher temperatures and a more uniform velocity throughout the volume.

**Keywords:** Solar drying, Control, Modeling, CFD, Thin-layer.

PhD Thesis in IAUIA  
Universidad Autonoma Chapingo  
Author: Jose Olaf Valencia Islas  
Major Professor: Dr. Irineo L. Lopez Cruz / Dr. Murat Kacira

# 1 GENERAL INTRODUCTION

## 1.1 BACKGROUND

### 1.1.1 Drying

Drying is the physical process by which, using heat, the moisture content of a product is extracted to a safe threshold at which microbial and fungal growth is stopped or retarded. To determine what the threshold is, the concept of water activity and moisture content in the product relative to dry weight can be used. Both concepts have their advantages and definitions that are mentioned below.

The only issue with drying is its energy consumption nature. As a highly consuming process, most industrial dryers use natural gas, coal, or diesel/gasoline as the main fuel for heat production. The process of drying has been used in the humankind for food preservation as well as clothing drying, but even with all those years of experience there is a lack of understanding the process and optimization based on the food and health requirements.

Drying can be done in several mediums as liquids and air, with the air drying as the most common. If the air is considered two main classifications can be done regarding the type of heat exchange that mostly dominates the process. There are convective dryers which based the process in the convection process between the air and the product to be dehydrated; there are also conductive dryers where the main heat exchange is due to convection between the solid benches and the product.

### 1.1.2 Water activity

The water activity criterion determines the thresholds for different agricultural products in which bacteria, fungi, and enzymes are present. The water contained within agricultural products is in equilibrium, given a temperature, with

other elements such as proteins, sugars, enzymes, etc. The water activity can be calculated as the ratio between the partial pressure of pure water at saturation and the partial pressure of water vapor in the wet product at the same temperature (Eq. 1-1) (Babalis et al., 2017).

$$a_w = \left( \frac{p_w}{p_w^*} \right)_T \quad (\text{Eq. 1-1})$$

where  $p_w$  (Pa) is the water vapor partial pressure in the wet product,  $p_w^*$  (Pa) is the partial pressure of pure water at saturation,  $T$  (°C) is the temperature at which the pressures of steam are calculated,  $a_w$  (dimensionless) is the water activity. The water activity values vary between 0 and 1. Closer to 0 value means a lower activity of enzymes, microbes, and bacteria (Labuza, 1977). The desired water activity values for drying range from 0.6 to 0.65 (Babalis et al., 2017), which would be equivalent to 15 to 20% final moisture content in the dehydrated product (Figure 1-1).

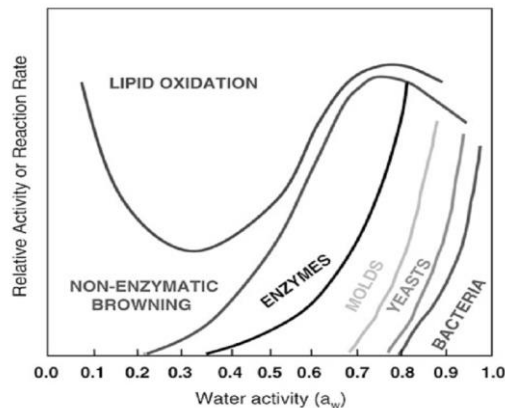


**Figure 1-1.** The reaction rate of the different microorganisms and processes in agricultural products as a function of water activity (Labuza, 1977).

### 1.1.3 Moisture content and moisture ratio

Moisture content is another significant variable for drying process. We can distinguish different moisture contents; for example, equilibrium moisture content

refers to the point at which the vapor pressure exerted by the moisture content of the product is equal to the partial vapor pressure of the surrounding air. There are two formulations to determine moisture content depending on whether it is calculated on a wet or dry basis. On a wet basis, the moisture content is the weight of water contained per unit of wet material (Eq. 1-2). If, on the contrary, the formulation is used on a dry basis, it is the ratio of the moisture content concerning the weight of the dry material (Eq. 1-3) (Vijayan et al., 2017):

$$W = \frac{m_w}{m_w + m_d} \quad (\text{kg of water per kg of wet matter}) \quad (\text{Eq. 1-2})$$

$$X = \frac{m_w}{m_d} \quad (\text{kg of water per kg of dry matter}) \quad (\text{Eq. 1-3})$$

where  $m_w$  is the mass of water and  $m_d$  is the mass of the dry solid,  $W$  is the moisture content on a wet basis,  $X$  is the moisture content on a dry basis. The relationship between moisture content on a dry and wet basis can be understood from Eqs. 1-4 and 1-5.

$$X = \frac{W}{1 - W} \quad (\text{kg}) \quad (\text{Eq. 1-4})$$

$$W = \frac{X}{1 + X} \quad (\text{kg}) \quad (\text{Eq. 1-5})$$

As there are two formulations, it is difficult to define in which case each one should be used, for example, it is common to find products expressed in moisture content on a wet basis for agricultural purposes, but for drying it is better to consider moisture on a dry basis. To facilitate the decision, the moisture ratio is used instead. The moisture ratio is a dimensionless value where the initial moisture of the product, the moisture content in equilibrium, and the moisture content at time  $t$  are considered, where  $t$  is the time in which sampling is carried out during drying, all of them in dry basis (Eq. 1-6).

$$MR = \frac{M_t - M_e}{M_0 - M_e} \quad (\text{dimensionless}) \quad (\text{Eq. 1-6})$$

where  $M_t$  is the moisture content at any time  $t$  on a dry basis and can be determined by Eq. 1-7 (El-Sebaili et al., 2002);  $M_e$  is the equilibrium moisture content and can be determined when the moisture no longer changes over time after drying;  $M_0$  is the initial moisture content of the product on a dry basis, it is calculated with Eq. 1-3 and MR is the moisture ratio.

$$M_t = \left[ \frac{(M_0 + 1)W_t}{W_0} - 1 \right] \quad (\text{dimensionless}) \quad (\text{Eq. 1-7})$$

where  $W_t$  is the weight of the product at each time step  $t$  (kg),  $W_0$  is the initial weight of the dry product (kg).

#### 1.1.4 Drying rate

The drying rate is defined as the mass of water that has been removed per unit of time per unit mass or unit area. The drying rate depends on factors such as the type of product, its transport properties, size, and initial moisture content. That is why, for each product, the drying rate will be different. The drying rate has three well-defined phases, the first is known as stable or constant drying rate, where the product is saturated with water and the moisture content is extracted through the diffusion process at a constant rate. The second phase is known as falling, in which the product has run out of moisture on the surface and requires more energy to move the water from inside the product to the surface to later be evaporated. The drying rate drops continuously and can almost form a straight line. Finally, the third stage is known as the second fall, the product is almost dry, and the movement of the remaining water is carried out slowly since more energy

is required. The moisture content at this stage continues to decrease until equilibrium has been reached and drying cannot continue (Vijayan et al., 2017). If heat is continuously applied at this point, then the product can be burnt. The drying rate can be defined with Eq. (1-8)

$$DR = \frac{M_{t+dt} - M_t}{dt} \quad (kg \text{ hr}^{-1}) \quad (\text{Eq. 1-8})$$

where  $DR$  is the drying rate,  $M_{t+dt}$  is the moisture content at time  $t + dt$  on a dry basis,  $dt$  is the time increment.

### 1.1.5 Drying rate constant

The kinetics of drying must be understood through the mass and heat transport equations that occur between the air and the product; however, a constant can be used that contains the combination of the transport properties of each material or product. That constant could then greatly simplify the modeling of the drying process, leading to thin-layer models. Normal values for the drying constant range from 0 to 1 (Vijayan et al., 2017).

### 1.1.6 Solar Drying

Solar drying is one of the oldest practices of humanity used for products as diverse as meat, fruits, vegetables, clothing, and even construction materials such as wood and bricks (Belessiotis & Delyannis, 2011). Solar dryers are devices that can improve solar drying known as open sun drying. This approach is more efficient in energy management and it also protects the product from the negative effects of the environment. The main factors limiting the full adoption of solar dryers have been the lack of cost-benefit, technical, and local practical experience information associated with solar dryers (Vijayavenkataraman et al., 2012). Solar dryers have different sizes, shapes, and types of covers. Depending on the type of material and shape, we can find solar dryers classified with different names,

and, in general, up to 500 types of dryers can be found in the literature, and 100 are commercially available (Mujumdar & Law, 2010).

### 1.1.7 Types of Solar Dryers

Considering the number of solar dryers reported by Mujumdar & Law (2010), the classification can be made based on certain distinctive characteristics in each dryer. Thus, the classification is based on temperature (Koyuncu, 2006) as high and low; by energy as direct, indirect, mixed, or hybrid (Patil & Gawande, 2016) by airflow as passive or active (Patil & Gawande, 2016) (Figure 1-2).

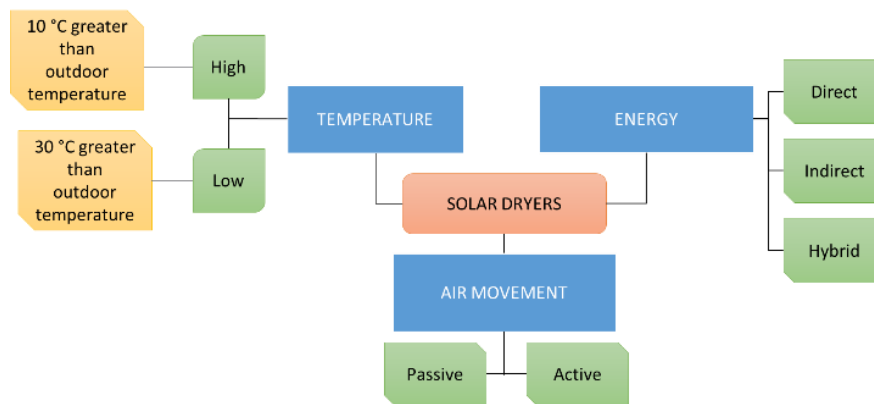


**Figure 1-2.** Classification of solar dryers by different criteria.

Here, it is worth mentioning that traditional solar drying is not considered since it does not use a specific device or design. The product is placed in the sun on a table, floor, or hanging and some care is performed to prevent the damage in case of rain or contamination by animals. The *classification by temperature* is very intuitive and separates only the designs between those that reach temperatures exceeding the ambient temperature by 30°C or only by 10°C. Koyuncu (2006) differentiates between solar heaters that can be used to prepare the air before entering the drying chamber. The *classification by airflow* opens the possibility of natural convection, in the case of passive flow, or forced convection, in the case of active flow. In passive flow dryers, the heated air is moved upwards

by the buoyancy force of changing the density or by stack effect due to wind pressure on the heated air. In general, they have a solar air heater, a drying chamber, and a chimney. These are low-cost dryers which are used in regions without electricity, and they can greatly improve traditional solar drying. Active flow dryers require an element that produces a forced air flow, they can be fans that extract the volume of air inside the dryer or fans inside the dryer that produces convection without extracting the air. *The classification by heat delivery* to the product for solar dryers are direct, indirect, or mixed. Direct dryers have a drying chamber with transparent materials that allow the passage of solar radiation while indirect dryers on the other hand have only the solar collector with a transparent cover, but the drying chamber is covered with opaque materials. The mixed solar dryers are equipped with solar collector and drying chamber with transparent materials.

Solar dryers today can extend to several classifications at once. For example, there are cabinet-type solar dryers with mixed-type forced convection and low-temperature solar heaters. Srinivasan & Muthukumar (2021) mentioned other types of solar dryers, for instance considering the type of storage material such as those based on latent heat exchange using paraffin and calcium chloride and based on sensible heat exchange with rocks and concrete.

### **1.1.8 Most common Solar Dryers**

#### **Cabinet dryer**

These are one of the most common types of solar dryers consisting of a solar collector to preheat the air, a drying chamber, and a chimney. The drying chamber can function with direct, indirect, or mixed energy. They are among the oldest dryers that have been worked on and their redesigns and studies to improve their efficiency are very popular. However, the size limits their scalability and the possibility of using them outside of experimentation or family projects.

Due to their design, most cabinet dryers have multiple layers of product to be dehydrated and arranged in trays.

Janjai & Bala (2012) present some of the indirect cabinet-type dryers whose main working mechanism is based on convection, for instance natural if fans are not added and a chimney is used or forced convection if fans are used to extract the air (Figure 1-3). If cabinet dryers are of the direct type without a solar collector apart from the drying chamber, they are also known as box dryers (Figure 1-4). This type of dryer is also a greenhouse type solar dryer, but due to its size, it should be distinguished as cabinet or box only. Spall & Sethi (2020) developed a cabinet dryer and found that, with the reflective element, size and design it is possible to decrease drying time and especially for applications for altitudes between 40 to 50°N (Figure 1-4).

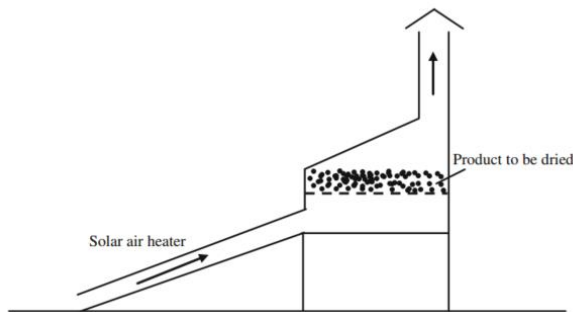


**Figure 1-3.** General characteristics of a cabinet dryer (Janjai & Bala, 2012).

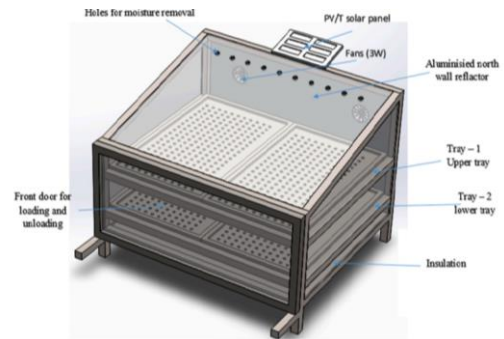
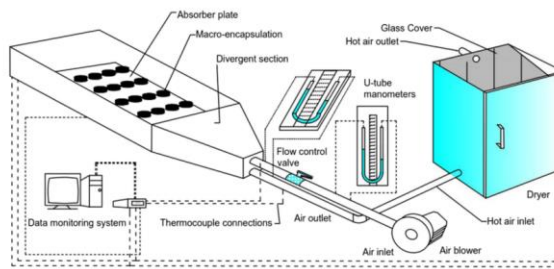


Fig. 1a. Isometric view of MRT solar dryer.

**Figure 1-4.** Cabinet dryer without a solar concentrator separated (Spall & Sethi, 2020).

Some dryers have more complex designs that have the solar concentrator separated from the drying chamber. The air is conditioned in a collector and piped to the drying chamber by forced flow (Figure 1-5). Alternatively, a fluid is used with a solar heater that elevates the fluid temperatures. Then, the higher temperature fluid is directed to a heat exchanger and is mixed with cold air in the drying chamber (Figure 1-6).



**Figure 1-5.** Solar cabinet dryer with solar concentrator, mixed type, and forced airflow (Arun et al., 2019).

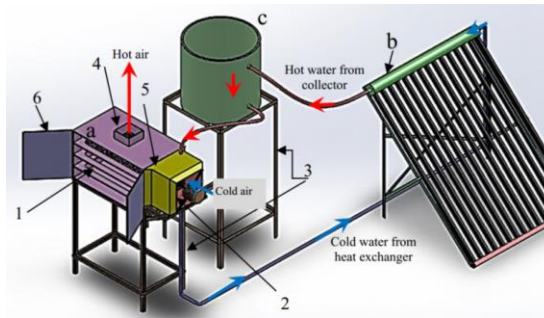


**Figure 1-6.** Cabinet solar dryer, indirect type with a water heater with heater exchanger (Iranmanesh et al., 2020).

### Greenhouse-type dryers

Greenhouse-type solar dryers are characterized by being larger than the cabinet type, with a solid structure to support the cover and to withstand the wind loads of the place where it will be built. Different types of materials can be used for the cover and this topic is still under development (Srinivasan & Muthukumar, 2021). Likewise, different types of structures such as metal, wood, and bamboo, among others, can be used. In most cases, the height is sufficient for one person to enter the greenhouse to perform work or supervise the drying process. The large volume of air allows a large amount of product to enter and dry in less time than traditional drying, with better quality and less contamination.

Various greenhouse designs with different geometries and temperature regimes have been developed over the years for solar drying (Srichat et al., 2019.; Verma, 2019). Among those studied, one of the most popular greenhouse designs is with parabolic roof shape. (Figure 1-7). The main advantage of this design is the ability to reach high temperatures by concentrating the greatest number of sun rays in the geometric center of the parabola. Its design is mainly developed for tropical climates, and it can support high wind loads (Janjai et al., 2009). However, there are also other designs proposed, which are originally used to grow crops, for solar drying (Figure 1-8). The air temperature and the addition of photovoltaic panels

have also been evaluated for solar drying (Barnwal & Tiwari, 2008) while some focused on solar collectors to increase air temperature (Román-Roldán et al., 2019a) (Figure 1-9).



**Figure 1-7.** Greenhouse-type solar dryer with a polycarbonate cover and parabolic roof (Janjai et al., 2009a).



**Figure 1-8.** Greenhouse-type solar dryer with plastic cover and Venlo geometry (Barnwal & Tiwari, 2008a).

Greenhouse-type dryers can also be found in the literature as tunnel type (Patil & Gawande, 2016) , although some authors separate them into two different categories with main difference being their height and length. The tunnels are smaller, but longer compared to greenhouses (Figure 1-10).

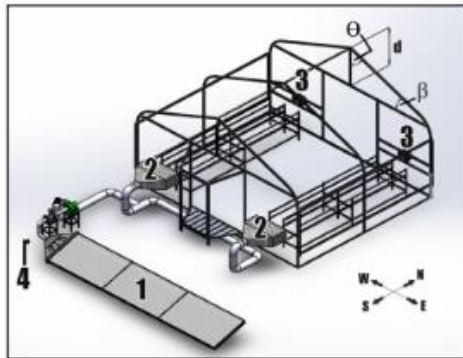


**Figure 1-9.** Greenhouse-type solar dryer with solar collector and plastic cover (Román-Roldán et al., 2019).

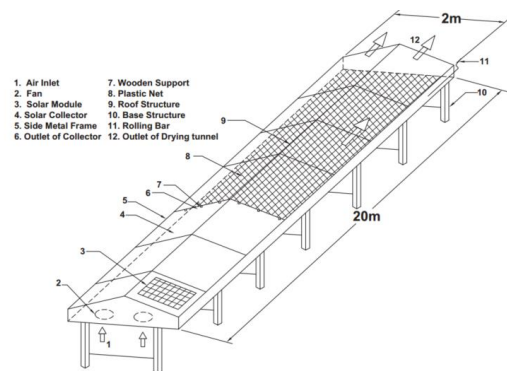


**Figure 1-10.** Tunnel greenhouse solar dryer (Patil & Gawande, 2016).

### In-house or Pilot plants

Pilot plants or drying houses are buildings in which the drying chamber is protected into a building. They can use solar energy mixed with other types of

energy sources such as electrical resistors, natural gas, coal, or radiated tubes. The new plants make use of alternative energies to reduce the impact of the large amount of energy needed for drying (Figure 1-11). Drying plants usually have high-end sensors to measure the variables involved in drying. The advancement and study of these dryers are still under development; however, García-Valladares et al. (2020), have developed drying studies in a plant located in Morelos, Zacatecas (latitude 22° 53' N, longitude 102° 39' W) with a maximum temperature of 70.9 °C showing a thermal efficiency of 60.7%.



**Figure 1-11.** Solar pilot plant for drying agricultural products (García-Valladares et al., 2020).

## 1.2 OBJECTIVES

The objectives of this dissertation were 1) to model the drying kinetics of sliced tomato in a greenhouse-type solar dryer; 2) to model and control the indoor environment of a greenhouse-type solar dryer during the drying process; 3) to evaluate two alternative air distribution system designs to enhance the drying process.

## 1.3 DISSERTATION STRUCTURE AND OVERVIEW

The dissertation is based on papers which means, each chapter presents a whole paper submitted to journals and subject to peer review. This document contains seven chapters. The first chapter is the general introduction with an overview of the problem, concepts necessary to understand the subject studied,

and a summary of what was done in each step of the research with its general conclusions. The second chapter consists of a literature review of each of the topics that were used as steps to complete the investigation. The third chapter contains the references of the first two chapters; For later chapters, the references are found at the end of each chapter, so the references are related to each topic. The fourth chapter presents the study of the drying kinetics of sliced tomatoes through the use and evaluation of thin-layer models. The fifth chapter presents the development and testing of a controller for a Greenhouse-type Solar Dryer using Model Predictive Control and System Identification techniques. The sixth chapter deals with a review of the modeling of Greenhouse-type Solar Dryers through Computational Fluid Dynamics (CFD), previous studies, products studied, and the processes needed to consider for modeling the drying process. Finally, the seventh chapter deals with the development of a numerical model with CFD for the Greenhouse-type Solar Dryer located at the Universidad Autonoma Chapingo; Once the model was evaluated using data, new air circulation designs were tested to improve air homogenization and optimize drying.

### **1.3.1 Overall Summary**

#### **Thin layer models for tomato – Chapter 3**

The Greenhouse-type Solar Dryer used for this dissertation was located at the Universidad Autonoma Chapingo, Mexico (19°29' N, 98°53 W, and 2250 m of altitude). The structure is of galvanized steel, the cover is a double wall polycarbonate of 6 mm thickness, and it has a parabolic shape roof. The floor is covered with a concrete layer of 0.15 m thickness (Figure 1-12).

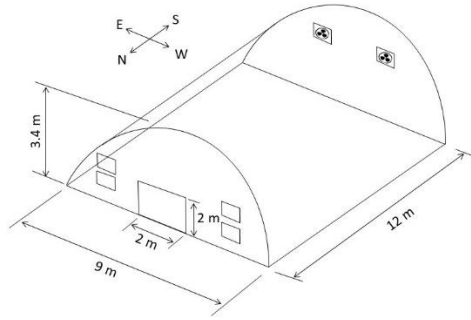


**Figure 1-12.** Dimensions of the greenhouse-type solar dryer.

For this study, 35 thin-layer models were tested during an experiment with tomato slices of 5 mm thickness. The thin-layer models have a different number of parameters, mathematical structures, and are based on different types of approximations. The methodology followed was the following: 1) two experiments were done with tomato slices in the greenhouse-type solar dryer at the Universidad Autonoma Chapingo (Figure 1-12) with 75 kg of tomato each (Saladette variety, Roma-type); 2) The Moisture ratio content was calculated as specified by Eq. 1-6; 3) the moisture ratio calculated with one experiment was used to calibrate the thin-layer models; 4) the moisture ratio calculated with the second experiment was used to test the performance of each calibrated model through the statistics root mean square error, mean square error, mean average error and model efficiency; 5) the models were compared to find which one best describes the drying kinetics of tomato slices in the greenhouse-type solar dryers.

#### **Model Predictive Control for Greenhouse-type Solar Dryers -Chapter 4**

A new strategy for controlling the greenhouse-type solar dryer (Figure 1-12) air was developed. The new strategy is based on the product temperature instead of the air temperature. A thermocouple type T was inserted into the tomato slices. The air temperature, air humidity, floor temperature, cover temperature, and solar radiation were recorded and used with the model identification methodology N4SID (Dosiek et al., 2013) to find a state space model of the

greenhouse dryer. With the model, an optimal linear Model Predictive Control was developed using the model to predict the product temperature, and the optimal strategy is calculated each time step. Two different strategies of using two exhaust fans separately or together were tested. The use of an MPC is completely new as many of the studies found in the literature are related to artificial neural networks, fuzzy logic, or PID controllers.

### **Greenhouse-type Solar Dryer modeling with Computational Fluid Dynamics a review – Chapter 5**

A literature review of the state of the art in modeling Greenhouse-type solar dryers using Computational Fluid Dynamics was done. The focus was to investigate the state-of-art with CFD modeling, the products studied, and identify the need for CFD modeling for greenhouse solar dryers. Some theories describing the physics and models that should be used specifically for drying were stated as part of the research.

### **Alternative Designs to Greenhouse-type Solar Dryer Air Distribution – Chapter 6**

One of the advantages of using modeling through Computational Fluid Dynamics (CFD) is the possibility of carrying out virtual experiments to determine the behavior of a fluid in each volume. Using the Greenhouse-type solar dryer geometry (Figure 2-1) a computational model was developed following the CFD methodology. The geometry was settled into a CAD 3D model and used to discretize the volume domain and approach the Navier-Stokes equations. The boundary conditions, mesh quality, and model structure was studied to get a trustworthy model. The experimental data obtained from previous greenhouse solar dryer study was used to validate the CFD model developed and compared with CFD predicted results. With the validated CFD model, three new strategies and system designs to distribute the air from the greenhouse attic directed below

the product drying tables to the drying product were developed and virtually tested for environmental uniformity, air temperature and air velocities obtained.

### **1.3.2 Overall Conclusions and Outlook**

#### **Thin-layer models for tomato – Chapter 4**

The best model for the Moisture ratio of tomato slices in a greenhouse-type solar dryer was found to be the Page modified VI which is equivalent to the Overhults et al. model. The Page model is a Semi-theoretical model and is highly used and found in other research regarding drying, it has two parameters and could be fit relatively without trouble. Other authors have found the Midilli Kucuk as the best model (Sadin et al., 2017; Hamdi and Kooli, 2018). However, the Midilli model is much less accurate than the first five models (Regression, Haghi & Angiz IV, Overhults et al., Weibull III and Page modified VI) and compared to the Page models it has more parameters to be fitted. Although the recommendation is to use the Page model VI, the best five models during the test stage are suitable to be used for tomato slices in greenhouse-type solar dryers. The present study has shown that several models can be found in the literature to be used in thin-layer modeling. However, no major discussions have been found on testing the models with new data. The study showed that the best models during calibration may not always be the best models with highest prediction accuracy.

The variability of the conditions significantly affects the behavior of the models due to the high abstraction of the moisture ratio concept and the assumption of constant temperature during drying. Thin layer models only depend on time and not on temperature, an important parameter that would be considered within the drying constant. Other investigations with different products within greenhouse-type solar dryers should be established. Still, there is no need to add more models to the existing ones given their wide repertoire in the literature and the similarity between the mathematical structure reflected in the estimated values when calibrating the models using experimental data.

## **Model Predictive Control for Greenhouse-Type Solar Dryers – Chapter 5**

The Model Predictive Controller designed in this study simulated the behavior of the system within the set points considered. The main difference between both control strategies considered was the total operation time the fans were activated to achieve the product temperature. Model Predictive Control, based on product temperature, can improve control strategy with energy savings and enhanced dried product quality. System Identification can serve as a starting point for complex systems such as greenhouse-type solar dryers. The setpoint should be carefully considered as the uncertainty of the model can affect the behavior of the MPC. A model with better adjustment could be used to improve the Model Predictive Controller as it is essential for the optimization process. Perhaps, a Kalman Filter could be a better option if this controller is implemented in a real greenhouse with the data introduced to the Kalman filter.

With analog actuators, the controller should be less restricted and thus, offering a better tool for controlled environments. The product temperature was successfully used to control a greenhouse-type solar dryer rather than the air temperature. Future studies can also consider combining multiple inputs and multiple outputs into the Model Predictive Control.

## **Greenhouse-type Solar Dryer modeling with Computational Fluid Dynamics a review – Chapter 6**

The Greenhouse-type Solar Dryer is a complex system, and its study involves multiphase and multiscale phenomena that need to be considered when modeling. More research is needed on Computational Fluid Dynamics modeling in greenhouse-type solar dryers. The great variability of types of solar dryers is the result of a lack of knowledge in the general drying process. Due to the nature of drying, scaling the results obtained with small-volume greenhouses to high-

volume dryers is not so easy, it is necessary to consider turbulence in the models and the behavior of the indoor air to obtain better results. Using small greenhouses does not impact enough industrial-scale drying research. The models developed so far are based on data, and few use theoretical and CFD models. Although alternatives have been proposed to solve the problem of simultaneous transfer processes, involving various phases and scales, so far, the behavior of the product and the air have not been modeled together. It is necessary to pay attention to the most wasted products, not only those that are of economic importance so drying can be used to preserve the most wasted products.

## **Alternative Designs to Greenhouse-type solar Dryer Air distribution – Chapter 7**

The numerical model was validated, and the following conclusions were obtained from the air recirculation proposals: The density of the original system varies concerning the volume, thus using the Boussinesq approximation could lead to an error during the simulation of greenhouse-type solar dryers when it is not known if the temperature difference is greater than 15°C. For the greenhouse solar dryer system evaluated in this study, the temperature distribution inside the greenhouse is improved when a recirculation system with three lines is used with a fan that can provide a speed of 5 m s<sup>-1</sup>. If a system with two lines is used, better air distribution is observed compared to the original system, but there are still areas with temperature stratification. The temperature near the ground is lower than the one reached in the upper part at the height of the drying tables. It would be more desirable to introduce the product at dawn to use the solar radiation effectively.

The average speed of the air in the three systems is 0.3 m s<sup>-1</sup>, which is desirable for a good quality product when drying. An improvement can be made to the system by reducing the size of the holes and changing the layout to three

holes per tube. However, the factor of the tables and the product must be added to investigate the reduction in air velocity due to the obstruction of both.

## 2 LITERATURE REVIEW

### 2.1 THIN-LAYER MODELS FOR TOMATO DRYING

It is very common for produce to be prepared for dehydration either by chemical pretreatment or volume reduction to reduce drying time, achieve better uniformity, and have better product handling after drying. Vast number of fruits are cut into thin slices; thus, this simple process means that mathematical approximations can be used to determine the kinetics of drying.

One of the most common approaches is known as the thin layer. To consider that a layer is thin, it must be a maximum of 200 mm thick, which means that the conditions of the air around the slice in terms of mass and heat exchange are negligible (Patil & and Gawande, 2017). As the thickness in the slices is so small, usually around 5 mm, and considering a generally circular geometry, the moisture rate can be approximated using simplified solutions of Fick's second law, also known as the law of Diffusion, law of Newton's cooling and empirically, to exponential equations.

The thin-layer model equations have parameters that involve the drying constant. As described previously, the drying constant considers the information on the exchange of mass and energy of each product, so that, when obtained using experimental data, the variable related to the moisture ratio is the drying time. This approach can greatly simplify the mathematical modeling of drying, but since it only depends on the drying time, in the presence of variable temperature or humidity, unreliable results are obtained (Patil & and Gawande, 2017).

Each product has its characteristics and heat and mass transfer coefficients. In this study, tomato of the Saladette variety was used for the experiments, so the review will focus solely on thin-layer modeling in tomatoes. Patil and Gawande (2017) provides a review of the models' mathematical structure and the assumptions that lead to the thin layer models.

Azeez et al. (2019) used an oven-type vacuum dryer with temperatures of 50, 60, and 70 °C to investigate the antioxidant, polyphenolic, and carotene content activity, as well as the drying kinetics using the Page, Lewis, and Henderson and Pabis models, and identified that the Page model was the best to fit the conditions. Sadin et al., (2017) used an electric tray dryer that works with hot air at temperatures of 60, 70, and 80 °C to model the dehydration process (Figure 1-12). In the study, they used the Midilli-Kucuk, Logarithmic model, Henderson and Pabis, Binomial model, and Lewis models. They found that all the models predicted well but the Midilli-Kucuk model provided the most accuracy.

Kocabiyik et al. (2016), investigated the properties of the dehydrated tomato with infrared radiation and used the Newton, Page, Henderson & Pabis, Logarithmic model, and Wang & Singh, models. They found that the best fit of the drying kinetics of tomatoes in an infrared radiation oven was with the Logarithmic model.

Murugavelh et al. (2019), used a tunnel solar dryer (Figure 1-13) to investigate drying kinetics and perform an exergy analysis of the drying process. They fitted the Newton, Page, Modified Page, Henderson and Pabis, Logarithmic model, Two Term Exponential, Verma, Wang and Singh, Midilli-Kucuk, and Approximation of Diffusion. They found that the drying kinetics helped to understand the thermophysical parameters involved in the process, with the Midilli-Kucuk model as the best model for their specific conditions evaluated.

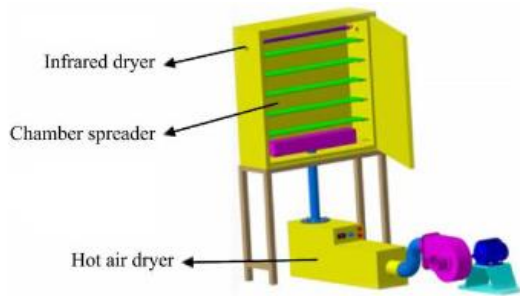


**Figure 2-1.** Infrared dryer used by Sadin et al. (2017).

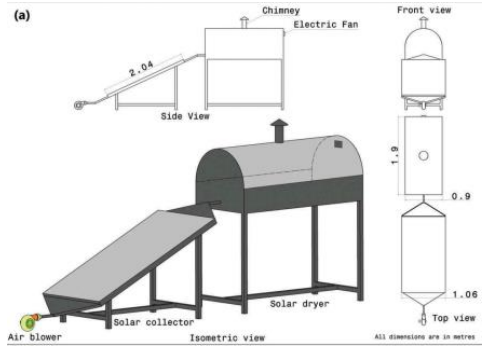


**Figure 2-2.** Small tunnel dryer used by Murugavelh et al. (2019).

Hamdi and Kooli (2018) investigated a greenhouse-type solar dryer (Figure 1-14) and compared it to open-air drying. They adjusted the Page, Modified Page, Wang and Singh, and Midilli-Kucuk models, and found the best model for both scenarios, drying in open-air and covering, the Midilli-Kucuk model. Kishk et al. (2019), proposed a solar dryer based on recyclable aluminum cans (Figure 1-15). The cans were used to build the solar collector and the drying process occur in a separate drying chamber. They evaluated Page, Henderson & Pabis, Newton, Logarithmic, Wang, and Singh, two terms, Two Terms Exponential, and Approximation of Diffusion models to fit the results with their proposed dryer. The study indicated that the model that best describes tomato drying in this tray dryer was the Wang and Singh model.



**Figure 2-3.** Greenhouse solar dryer used by Hamdi & Kooli (2018).

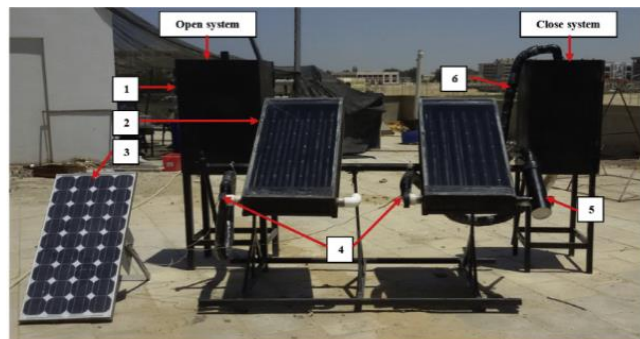


**Figure 2-4.** Recyclable can solar dryer used by Kishk et al. (2019).

There is still great opportunity for research on solar dryers, where incident radiation dominates the behavior of the dryer. The variability in radiation due to other environmental disturbances such as rain, season, or hour of the day, makes the use of thin-layer models a challenge. It is important to investigate the drying process and performance under varying conditions and test models with different mathematical structures and parameters. Furthermore, the dimensions of most dryers allow conditions to be more homogeneous, however this still pose a problem for industrial scale-up. Despite having a model that fits the data, there is no test stage using a case study for the models listed in each study reviewed. Finally, the best thin layer model in each research is not always the same. The Midilli Kucuk model has been demonstrated as the most common and the best model to describe the tomato drying kinetics.

## **2.2 CONTROL OF GREENHOUSE-TYPE SOLAR DRYERS**

The drying process in greenhouses is complex and the control involves the air characteristics inside the system. The interior conditions in a greenhouse are complex to model due to their non-linearity and the nature of the system with multiple inputs and multiple outputs, also known as MIMO system (Iddio et al., 2020). Greenhouse control can be divided into classical control, usually referred to as Proportional-Integral-Derivative (PID) algorithms, and advanced control, with model predictive control (MPC) algorithms, feedback/feedforward, adaptive and robust controls are implemented.

The Model Predictive Control approach (MPC) uses a mathematical model of the system to predict the variables of interest in a specified time period. Then, based on the behavior, a set of control strategies are used to minimize a cost function subject to constraints. Because the optimization and prediction are calculated in every step, the MPC can lead to the unstable behavior of the system (Camacho & Bordons, 2007b; Ouammi, 2021).

Linear MPCs have parameters that must be tuned for the controller to work properly. These parameters are the weights Q and R, which serve to penalize the objective function based on the variables considered in the controller (Eq. 1-9). The next parameter is the sampling period, the time interval in which the control actions remain constant. They depend on the time constant of the controlled system. The prediction period is the number of steps in time that, when multiplied by the sampling period, gives the length of the window in which the MPC calculates the model's predictions. Finally, the control period represents the number of steps in time for which the MPC calculates the optimal control actions that minimize the objective function (Eq 1-9) (Camacho & Bordons, 2007a; Drgoňa et al., 2020).

$$J^*(x_k) = \min_{u_{k+j|k}} \sum_{j=0}^{N-1} \left( \|x_{k+j|k}\|_Q^2 + \|u_{k+j|k}\|_R^2 \right) + \|x_{k+N|k}\|_Q^2 \quad (\text{Eq. 1-9})$$

Unlike the ON/OFF and Proportional Integral Derivative (PID) Controllers, the MPC can overcome important disturbances in solar drying systems due to unexpected outdoor weather, and then optimizes the response based on the specific greenhouse physical and technological constraints (Chen & You, 2020; Petersen et al., 2017). In addition, the possibility to add variables of economic impact in the cost function makes MPC a great option for a controller of greenhouse-type solar dryers (Ciglera et al., 2013). Even with the high advantages of using an MPC to control the greenhouse for the process of drying, the complexity has not been addressed in other studies. The possibility to use the information about the product can lead to better control based on an MPC strategy.

### 2.3 COMPUTATIONAL FLUID DYNAMICS OF GREENHOUSE-TYPE SOLAR DRYERS

Most of the models developed for greenhouse-type solar dryers are based on energy balances, using ordinary differential equations (ODEs) to model the humidity and temperature behavior of the air inside the dryer (Jain & and Tiwari, 2004; Janjai et al., 2011, 2014; Kumar & and Tiwari, 2006). However, when the product is involved, the so-called “thin layer” models are the most widely used. Thin layer models are based on regressions over data taken from the dehydration process during certain days and fitted with exponential or algebraic expressions that are based on Newton’s law of cooling, diffusion, or exponential decay behavior approximations (Defraeye, 2014; Verma, 2019). Both ODEs and Thin-layer models consider no spatial variation in the inner conditions of the greenhouse. Therefore, this assumption could be valid for small-volume greenhouses but not for volumes greater than 10 m<sup>3</sup> since a greater heat and mass exchange occur inside the dryer at the same time as heat is collected from the sun radiation. Therefore, a different modeling approach is needed that can address the problem when variations in the air inside the greenhouse are considered.

The behavior of fluid flow, heat transfer, and associated chemical reactions can be described by three fundamental principles: conservation of mass, conservation of momentum, and conservation of energy. Computational Fluid Dynamics (CFD) is a finite difference-based method solving Navier-Stokes equations numerically with computer simulations. The CFD approach replaces the governing equations with numbers and those approximations advance through time and space to find the final numerical description of the fluid field under study (Anderson, 2009). Some benefits of CFD simulations include the ability to simulate systems that are difficult to understand and that involve expensive or hazardous experiments; testing alternative designs in real systems; understanding the physics behind the fluid flow. A CFD code has three main modules i) Pre-processing, ii) Solver, and iii) post-processing. These codes can be introduced in the same software or could need a specific computer program for each step.

A Scopus literature database search with (Spiroski, 2013) the keywords “drying” resulted 207,450 papers published from 1826 to 2021 (Figure 1-16). There is an increasing trend in the articles published related to drying since the year 1971. However, this result contains not only drying articles in the food area but also Medicine, Health Sciences, Chemistry, and Materials. That is why it is necessary to apply another filter to the areas that correspond to Agronomic Sciences or Agriculture and discard those that do not correspond to the subject. Figure 1-17 shows the search results for literature with combined keywords "CFD, solar, greenhouse, drying." Among all drying studies, only 0.007% corresponds to CFD modeling of greenhouse-type solar dryers with 15 publications. This reveals that the literature still lacks research on CFD modeling for greenhouse solar dryers.

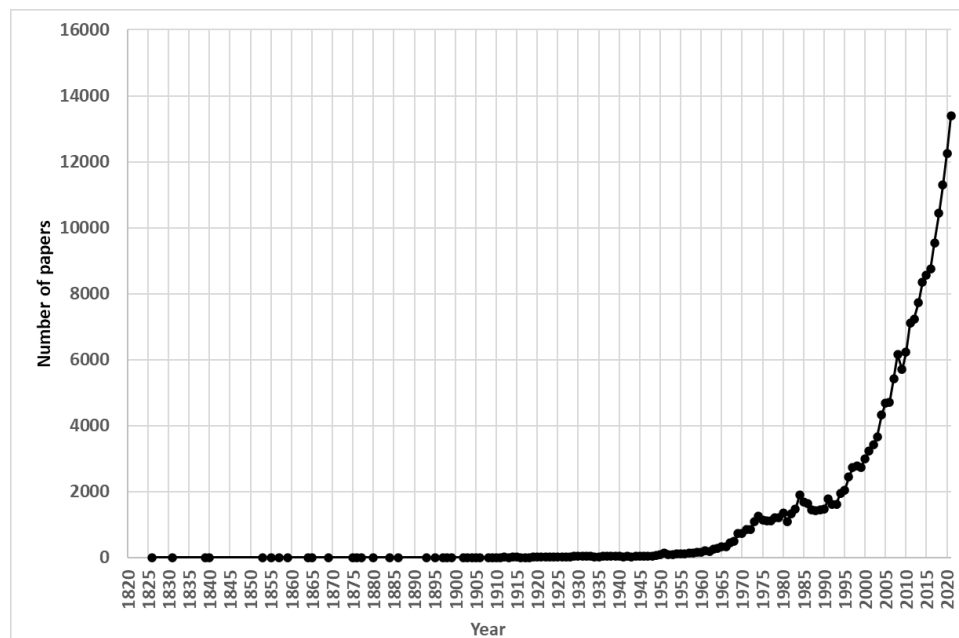


**Figure 2-5.** The increasing trend in the number of drying papers per year (data, Scopus, 2019).

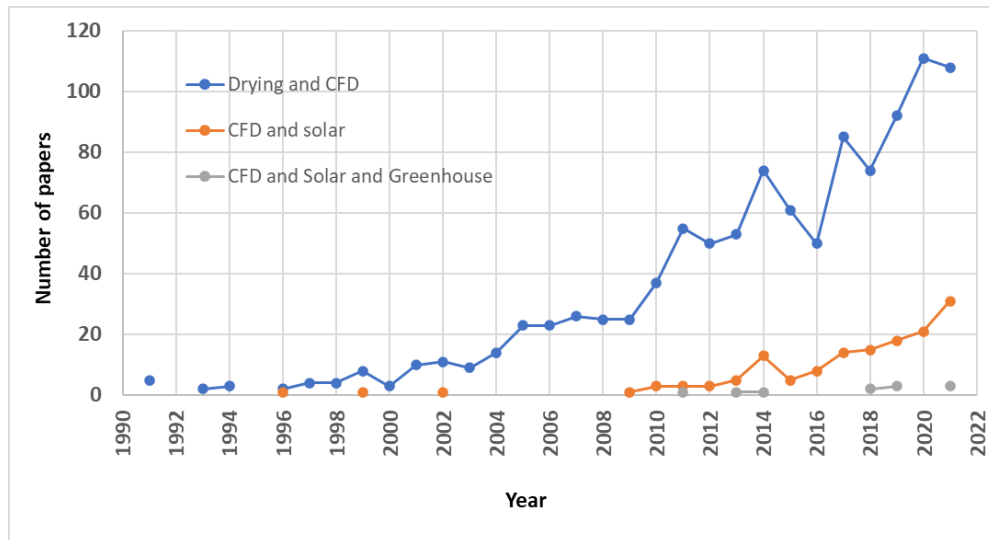


**Figure 2-6.** Trends in publications on drying, CFD, and greenhouse-type solar dryers, (data Scopus, 2019).

The applications of CFD for greenhouse aerodynamics have reached a maturity (Aguilar-Rodríguez et al., 2021; Fatnassi et al., 2021; Kim, Hong, et al., 2017; Kim, Lee, et al., 2017; Li et al., 2020; Piscia et al., 2012; Tong et al., 2018). Therefore, it is possible to implement some of the established methodologies and models for evaluating greenhouse solar dryers. New proposals in greenhouse-type dryers, as Kumar and Shrivastava (2017) point out, are focused on specifically designing geometries and equipment that can produce a better energy conservation effect and a more homogeneous distribution of temperature and air-wind profiles with constant speeds.

The main challenge when analyzing the macroscopic scale of the dryers is that even the simplest processes involved in drying are highly non-linear, and therefore, it is difficult to scale the results in small dryer experiments to dryers with scaled up structures (Strumillo, 2007). Therefore, CFD can address this issue effectively as it allows studying designs with their true sizes considered and help evaluating what-if scenarios. Furthermore, the CFD modeling can generate results with environmental variables in a detailed granularity for the whole problem domain offering a better understanding of the drying process (Bakker et al., 2001).

Up to now, CFD studies have focused only on the moving air inside the greenhouse-type dryer. Krawczyk and Badyda (2011) studied the process of drying sludge from the waste inside a chapel-type greenhouse with dimensions of 3 m high, and 3.12 m long, the width is not reported (Figure 1-18). This two-dimensional CFD study simulated the behavior of humidity, the temperature of sludge, and air within the dryer using FLUENT software. They reported the difficulty of solving simultaneously the phenomena of transport and the use of fine mesh in the vicinity of the greenhouse walls.

Lokeswaran and Eswaramoorthy (2013), analyzed a hemicylindrical greenhouse with a concrete floor with an area of 40 m<sup>2</sup>, transparent polyethylene covering 200 microns thick. They used FLUENT 6.3.26 with a mesh of 914,905 elements. They found that the behavior of the air inside the dryer is not homogeneous, and to improve it is necessary to add a fan so that temperatures do not vary so much. Somsila and Teeboonma (2014), evaluated the behavior of a greenhouse with a sloping roof for drying para rubber (Figure 1-19). The study revealed that the air speeds were almost constant throughout the dryer resulting in no temperature stratification. The temperature inside the dryer was between 55-60 °C, and the highest temperature was found in the ceiling.

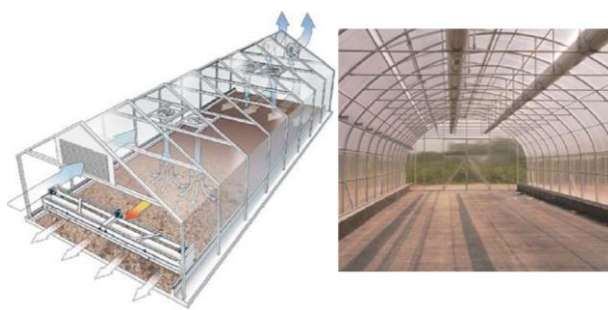


**Figure 2-7.** Greenhouse-type solar dryer used to dry sludge (Krawczyk & Badyda, 2011).

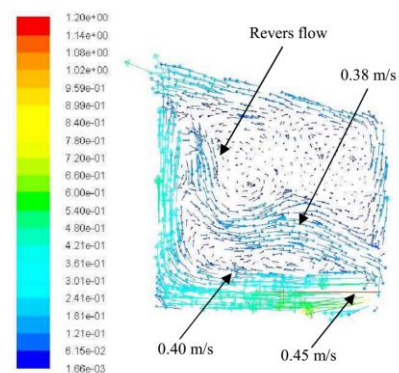


**Figure 2-8.** Air velocity distribution inside a greenhouse-type solar dryer studied by Somsila & Teeboonma (2014).

Gupta et al. (2018) simulated the behavior of the air inside a chapel-type greenhouse with natural ventilation, produced by a small hole located in the opposite wall of the air inlet. They used ANSYS 15.0 software for simulation. The results indicated that the air could circulate throughout the geometry at an almost constant speed; however, the temperature has significant differences, being higher in the side walls. Noh et al. (2018) studied an industrial-scale solar dryer that consists of evacuated tubes, a heat exchanger blower, and a drying chamber. The dimensions of the drying chamber were 1.25 m in height, 1.7 m in width, and 17 m long. For simulation, five pallets were stacked up on top of each other, and three different ventilations were considered: the first being passive, passive with active combination, and passive with intermittent active ventilation. They found that the optimal condition was passive with intermittent active ventilation which produce the highest temperature inside the sericite mica.

Using CFD simulations, Srichat et al. (2019) tested a hypothesis about dryer geometry. They compared a roof with sinusoidal geometry and the parabolic shape (Figure 1-20). The results indicated that the sinusoidal shape had higher temperatures in any of the axes where the solution is simulated. Thus, this indicated that sinusoidal geometry would be an improved design of a solar greenhouse-type solar dryer, reducing drying time and increasing product quality. Román-Roldán et al. (2019) studied the behavior of a chapel-type greenhouse, with a plastic cover and a coupled air heater (Figure 1-21). They tested the number of elements in the mesh, going from 1 to 7 million, to determine the quality of the mesh in the geometry. The better results were with 6 million mesh. Furthermore, the study revealed that when the volume is reduced by 36.5%, the temperature distribution and the air speed inside the dryer were improved.

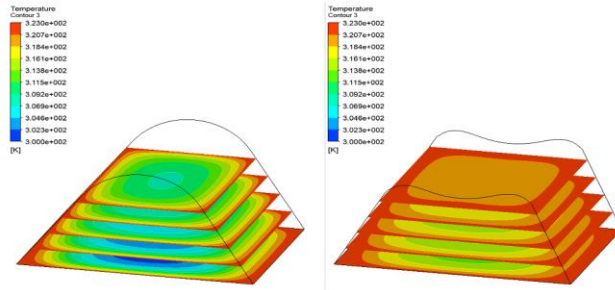


**Figure 2-9.** Temperature distribution for parabolic and sinusoidal covers geometries (Srichat et al., 2019).

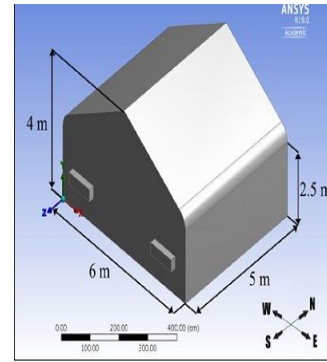


**Figure 2-10.** Greenhouse-type solar dryer used by (Román-Roldán et al., 2019).

Purusothaman et al. (2019) studied three different roof shapes in greenhouse dryers for free and forced convection. The research simulated the period from 10 am to noon. They found that the trapezoidal roof greenhouse achieves a higher temperature than the triangle or hemispherical roof greenhouses (Figure 1-22). Vivekanandan et al. (2021) researched six different small greenhouse dryers. The CFD predicted results were compared with experimental data of 7.5 hours for winter and summer sessions. They found that the Quonset shape was the ideal shape among others with order of best designs with Quonset, Tropical, Pyramid, Parabola, Modified Quonset, and Igloo.

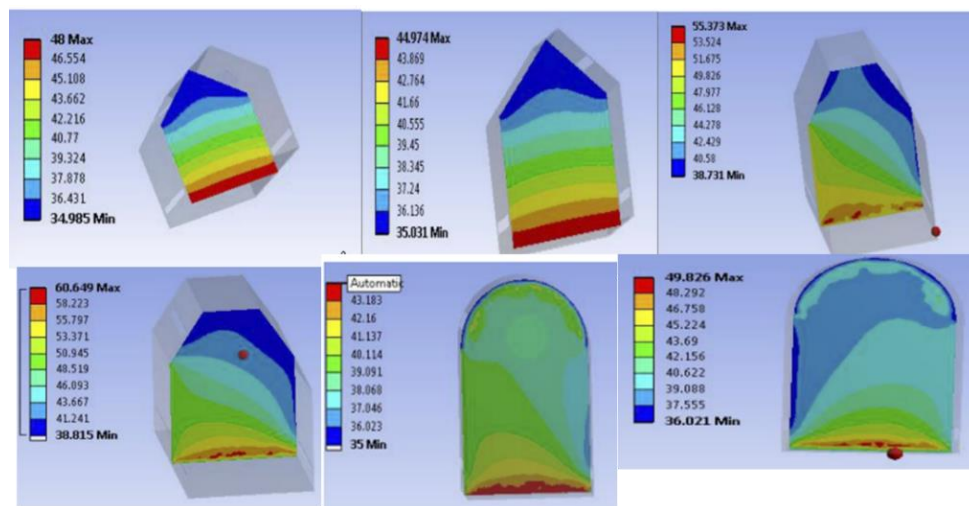


**Figure 2-11.** Greenhouse geometries studied by Purusothaman et al. (2019) as solar dryers.

Villagran et al. (2021) studied four different greenhouse dryer designs (Figure 2-12). Three of them had polyethylene covers and the last one uses insect-proof porous mesh inside the greenhouse. All greenhouses were placed in a computational domain around the greenhouse, it is a small box with a minimum of 10 times the height of the greenhouse. A wind profile was used as an inlet, solar radiation was considered at the top, and as an outlet a pressure equal to the atmospheric pressure. The results found by the researchers were that the greenhouse with a double polyethylene film has the highest microclimate dynamics and thus the highest temperature and lowest relative humidity.

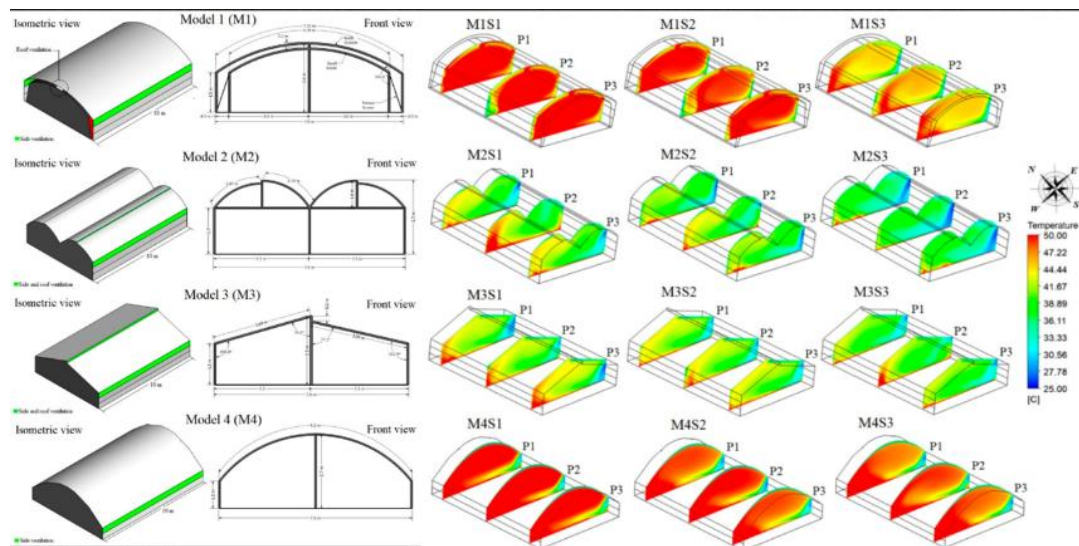


**Figure 2-12.** Greenhouses used by Villagran et al. (2021) to test as solar dryers.

Finally, Román-Roldán et al. (2021) researched a new prototype for air recirculation of a chapel-type greenhouse dryer with a polyethylene cover. Six different configurations with fans were tested by the authors and compared to experimental results. The two main objectives were to study air distribution and air temperature in each configuration. They found that fans above 15 m/s are required to improve a better distribution of air, also if fan velocity was kept between 5 to 20 m/s the temperature of the drying chamber varies from 51 to 81°C.

There is still a greater need for further research which involves the kinetics of drying with the psychrometric kinetics of the humid air inside the greenhouse, with alternative air distribution system designs to improve the uniformity of the greenhouse air temperature and air current speeds especially at the product drying tables leading to improved drying process. Furthermore, a complete understanding of the drying process can lead to better system designs and strategies for controlling the quality of dried fruits.

### 3 REFERENCES

Aguilar-Rodríguez, C. E., Flores-Velázquez, J., Rojano, F., Flores-Magdaleno, H., & Panta, E. R. (2021). Simulation of water vapor and near infrared radiation to predict vapor pressure deficit in a greenhouse using cfd. *Processes*, 9(9). <https://doi.org/10.3390/PR9091587>

Anderson, J. D. (2009). Basic philosophy of CFD. *Computational Fluid Dynamics*, 3–14. [https://doi.org/10.1007/978-3-540-85056-4\\_1/COVER/](https://doi.org/10.1007/978-3-540-85056-4_1/COVER/)

Arun, K. R., Srinivas, M., Saleel, C. A., & Jayaraj, S. (2019). Active drying of unripened bananas (*Musa Nendra*) in a multi-tray mixed-mode solar cabinet dryer with backup energy storage. *Solar Energy*, 188, 1002–1012. <https://doi.org/10.1016/J.SOLENER.2019.07.001>

Azeez, L., Adebisi, S. A., Oyedeji, A. O., Adetoro, R. O., & Tijani, K. O. (2019). Bioactive compounds' contents, drying kinetics and mathematical modelling of tomato slices influenced by drying temperatures and time. *Journal of the Saudi Society of Agricultural Sciences*, 18(2), 120–126. <https://doi.org/10.1016/J.JSSAS.2017.03.002>

Babalis, S., Papanicolaou, E., & Belessiotis, V. (2017). Fundamental mathematical relations of solar drying systems. *Green Energy and Technology*, 0(9789811038327), 89–175. [https://doi.org/10.1007/978-981-10-3833-4\\_4/FIGURES/22](https://doi.org/10.1007/978-981-10-3833-4_4/FIGURES/22)

Bakker, A., Haidari, A. H., & Oshinowo, L. M. (2001). Realize greater benefits from CFD. *Chemical Engineering Progress*, 97(3), 45–53.

Barnwal, P., & Tiwari, G. N. (2008). Grape drying by using hybrid photovoltaic-thermal (PV/T) greenhouse dryer: An experimental study. *Solar Energy*, 82(12), 1131–1144. <https://doi.org/10.1016/J.SOLENER.2008.05.012>

Belessiotis, V., & Delyannis, E. (2011). Solar drying. *Solar Energy*, 85(8), 1665–1691. <https://doi.org/10.1016/J.SOLENER.2009.10.001>

Camacho, E. F., & Bordons, C. (2007a). Introduction to model predictive control. *Advanced Textbooks in Control and Signal Processing*, 9781852336943, 1–11. [https://doi.org/10.1007/978-0-85729-398-5\\_1](https://doi.org/10.1007/978-0-85729-398-5_1)

Camacho, E. F., & Bordons, C. (2007b). Model predictive controllers. *Advanced Textbooks in Control and Signal Processing*, 9781852336943, 13–30. [https://doi.org/10.1007/978-0-85729-398-5\\_2](https://doi.org/10.1007/978-0-85729-398-5_2)

Chen, W. H., & You, F. (2020). Efficient Greenhouse Temperature Control with Data-Driven Robust Model Predictive. *Proceedings of the American Control Conference*, 2020-July, 1986–1991. <https://doi.org/10.23919/ACC45564.2020.9147701>

Ciglera, Í., Gyalistrasb, D., Tietd, V.-N., Luká, & Ferkla. (2013). Beyond theory : the challenge of implementing Model Predictive Control in buildings Ji ř.

Defraeye, T. (2014). Advanced computational modelling for drying processes – A review. *Applied Energy*, 131, 323–344. <https://doi.org/10.1016/J.APENERGY.2014.06.027>

Dosiek, L., Zhou, N., Pierre, J. W., Huang, Z., & Trudnowski, D. J. (2013). Mode shape estimation algorithms under ambient conditions: A comparative review. *IEEE Transactions on Power Systems*, 28(2), 779–787. <https://doi.org/10.1109/TPWRS.2012.2210570>

Drgoňa, J., Arroyo, J., Cupeiro Figueroa, I., Blum, D., Arendt, K., Kim, D., Ollé, E. P., Oravec, J., Wetter, M., Vrabie, D. L., & Helsen, L. (2020). All you need to know

about model predictive control for buildings. *Annual Reviews in Control*, 50, 190–232. <https://doi.org/10.1016/J.ARCONTROL.2020.09.001>

El-Sebaili, A. A., Aboul-Enein, S., Ramadan, M. R. I., & El-Gohary, H. G. (2002). Experimental investigation of an indirect type natural convection solar dryer. *Energy Conversion and Management*, 43(16), 2251–2266. [https://doi.org/10.1016/S0196-8904\(01\)00152-2](https://doi.org/10.1016/S0196-8904(01)00152-2)

Fatnassi, H., Boulard, T., Poncet, C., Katsoulas, N., Bartzanas, T., Kacira, M., Giday, H., & Lee, I. B. (2021). Computational fluid dynamics modelling of the microclimate within the boundary layer of leaves leading to improved pest control management and low-input greenhouse. *Sustainability (Switzerland)*, 13(15). <https://doi.org/10.3390/SU13158310>

García-Valladares, O., Ortiz, N. M., Pilatowsky, I., & Menchaca, A. C. (2020). Solar thermal drying plant for agricultural products. Part 1: Direct air heating system. *Renewable Energy*, 148, 1302–1320. <https://doi.org/10.1016/J.RENENE.2019.10.069>

Gupta, V., Sharma, A., & Gupta, K. S. (2018). Numerical Analysis of Direct Type Greenhouse Dryer. *ASME 2017 Gas Turbine India Conference, GTINDIA 2017*, 2. <https://doi.org/10.1115/GTINDIA2017-4784>

Hamdi, I., & Kooli, S. (2018). Exergy and energy analysis of the solar drying processes of tomatoes in Tunisia. *2018 9th International Renewable Energy Congress, IREC 2018*, 1–6. <https://doi.org/10.1109/IREC.2018.8362493>

Iddio, E., Wang, L., Thomas, Y., McMorrow, G., & Denzer, A. (2020). Energy efficient operation and modeling for greenhouses: A literature review. *Renewable and Sustainable Energy Reviews*, 117, 109480. <https://doi.org/10.1016/J.RSER.2019.109480>

Iranmanesh, M., Samimi Akhijahani, H., & Barghi Jahromi, M. S. (2020). CFD modeling and evaluation the performance of a solar cabinet dryer equipped with evacuated tube solar collector and thermal storage system. *Renewable Energy*, 145, 1192–1213. <https://doi.org/10.1016/J.RENENE.2019.06.038>

Jain, D., & Tiwari, G. N. (2004). Effect of greenhouse on crop drying under natural and forced convection I: Evaluation of convective mass transfer coefficient. *Energy Conversion and Management*, 45(5), 765–783. [https://doi.org/10.1016/S0196-8904\(03\)00178-X](https://doi.org/10.1016/S0196-8904(03)00178-X)

Janjai, S., & Bala, B. K. (2012). Solar drying technology. *Food Engineering Reviews*, 4, 16–54. <https://doi.org/10.1007/s12393-011-9044-6>

Janjai, S., Intawee, P., Kaewkiew, J., Sritus, C., & Khamvongsa, V. (2011). A large-scale solar greenhouse dryer using polycarbonate cover: Modeling and testing in a tropical environment of Lao People's Democratic Republic. *Renewable Energy*, 36(3), 1053–1062. <https://doi.org/10.1016/J.RENENE.2010.09.008>

Janjai, S., Lamlert, N., Intawee, P., Mahayothee, B., Bala, B. K., Nagle, M., & Müller, J. (2009). Experimental and simulated performance of a PV-ventilated solar greenhouse dryer for drying of peeled longan and banana. *Solar Energy*, 83(9), 1550–1565. <https://doi.org/10.1016/J.SOLENER.2009.05.003>

Janjai, S., Phusampao, C., Nilnont, W., & Pankaew, P. (2014). Experimental performance and modeling of a greenhouse solar dryer for drying macadamia nuts. *International Journal of Scientific & Engineering Research*, 5(6). <http://www.ijser.org>

Kim, R. woo, Hong, S. woon, Lee, I. bok, & Kwon, K. seok. (2017). Evaluation of wind pressure acting on multi-span greenhouses using CFD technique, Part 2:

Application of the CFD model. *Biosystems Engineering*, 164, 257–280.  
<https://doi.org/10.1016/J.BIOSYSTEMSENG.2017.09.011>

Kishk, S. S., ElGamal, R. A., & ElMasry, G. M. (2019). Effectiveness of recyclable aluminum cans in fabricating an efficient solar collector for drying agricultural products. *Renewable Energy*, 133, 307–316.  
<https://doi.org/10.1016/J.RENENE.2018.10.028>

Kocabiyik, H., Yilmaz, N., Tuncel, N. B., Sumer, S. K., & Buyukcan, M. B. (2016). Quality properties, mass transfer characteristics and energy consumption during shortwave infrared radiation drying of tomato. *Http://Dx.Doi.Org/10.3920/QAS2014.0550*, 8(3), 447–456.  
<https://doi.org/10.3920/QAS2014.0550>

Koyuncu, T. (2006). Performance of various design of solar air heaters for crop drying applications. *Renewable Energy*, 31(7), 1073–1088.  
<https://doi.org/10.1016/J.RENENE.2005.05.017>

Krawczyk, P., & Badyda, K. (2011). Two-dimensional CFD modeling of the heat and mass transfer process during sewage sludge drying in a solar dryer. *Archives of Thermodynamics*, 32(4), 3–16. <https://doi.org/10.2478/V10173-011-0028-Y>

Kumar, A., & Shrivastava, V. (2017). Historical Trends and Recent Developments in Solar Greenhouse Dryer Operated Under Active Mode: A Review. *Indian Journal of Science and Technology*, 10(33), 1–16.  
<https://doi.org/10.17485/IJST/2017/V10I33/116988>

Kumar, A., & Tiwari, G. N. (2006). Thermal Modeling and Parametric Study of a Forced Convection Greenhouse Drying System for Jaggery: An Experimental Validation. *International Journal of Agricultural Research*, 1(3), 265–279.  
<https://doi.org/10.3923/IJAR.2006.265.279>

Labuza, T. P. (1977). THE PROPERTIES OF WATER IN RELATIONSHIP TO WATER BINDING IN FOODS: A REVIEW<sup>1,2</sup>. *Journal of Food Processing and Preservation*, 1(2), 167–190. <https://doi.org/10.1111/J.1745-4549.1977.TB00321.X>

Li, H., Li, Y., Yue, X., Liu, X., Tian, S., & Li, T. (2020). Evaluation of airflow pattern and thermal behavior of the arched greenhouses with designed roof ventilation scenarios using CFD simulation. *PLoS ONE*, 15(9), e0239851–e0239851. <https://doi.org/10.1371/JOURNAL.PONE.0239851>

Lokeswaran, S., & Eswaramoorthy, M. (2013). An Experimental Analysis of a Solar Greenhouse Drier: Computational Fluid Dynamics (CFD) Validation. <Http://Dx.Doi.Org/10.1080/15567036.2010.532195>, 35(21), 2062–2071. <https://doi.org/10.1080/15567036.2010.532195>

Mujumdar, A. S., & Law, C. L. (2010). Drying Technology: Trends and Applications in Postharvest Processing. *Food and Bioprocess Technology*, 3(6), 843–852. <https://doi.org/10.1007/S11947-010-0353-1/TABLES/1>

Murugavelh, S., Anand, B., Midhun Prasad, K., Nagarajan, R., & Azariah Pravin Kumar, S. (2019). Exergy analysis and kinetic study of tomato waste drying in a mixed mode solar tunnel dryer. <Https://Doi.Org/10.1080/15567036.2019.1679289>. <https://doi.org/10.1080/15567036.2019.1679289>

Noh, A. M., Mat, S., & Ruslan, M. H. (2018). CFD simulation of temperature and air flow distribution inside industrial scale solar dryer. *Journal of Advanced Research in Fluid Mechanics and Thermal Sciences*, 45(1), 156–164.

Ouammi, A. (2021). Model predictive control for optimal energy management of connected cluster of microgrids with net zero energy multi-greenhouses. *Energy*, 234, 121274. <https://doi.org/10.1016/J.ENERGY.2021.121274>

Patil, R. C., & Gawande, R. R. (2017). Mathematical modeling of solar drying systems. *Green Energy and Technology*, 0, 265–316. [https://doi.org/10.1007/978-981-10-3833-4\\_9/FIGURES/3](https://doi.org/10.1007/978-981-10-3833-4_9/FIGURES/3)

Patil, R., & Gawande, R. (2016). A review on solar tunnel greenhouse drying system. *Renewable and Sustainable Energy Reviews*, 56, 196–214. <https://doi.org/10.1016/J.RSER.2015.11.057>

Petersen, L. N., Poulsen, N. K., Niemann, H. H., Utzen, C., & Jørgensen, J. B. (2017). Comparison of three control strategies for optimization of spray dryer operation. *Journal of Process Control*, 57, 1–14. <https://doi.org/10.1016/J.JPROCONT.2017.05.008>

Piscia, D., Montero, J. I., Baeza, E., & Bailey, B. J. (2012). A CFD greenhouse night-time condensation model. *Biosystems Engineering*, 111(2), 141–154. <https://doi.org/10.1016/J.BIOSYSTEMSENG.2011.11.006>

Purusothaman, M., Valarmathi, T. N., & Santhosh, P. S. (2019). CFD Analysis of Greenhouse Solar Dryer with Different Roof Shapes. 5th International Conference on Science Technology Engineering and Mathematics, ICONSTEM 2019, 408–412. <https://doi.org/10.1109/ICONSTEM.2019.8918788>

Román-Roldán, N. I., Ituna Yudsonago, J. F., López-Ortiz, A., Rodríguez-Ramírez, J., & Sandoval-Torres, S. (2021). A new air recirculation system for homogeneous solar drying: Computational fluid dynamics approach. *Renewable Energy*, 179, 1727–1741. <https://doi.org/10.1016/J.RENENE.2021.07.134>

Román-Roldán, N. I., López-Ortiz, A., Ituna-Yudsonago, J. F., García-Valladares, O., & Pilatowsky-Figueroa, I. (2019). Computational fluid dynamics analysis of heat transfer in a greenhouse solar dryer “chapel-type” coupled to an air solar

heating system. *Energy Science and Engineering*, 7(4), 1123–1139.  
<https://doi.org/10.1002/ESE3.333>

Sadin, R., Chegini, G., & Khodadadi, M. (2017). Drying characteristics and modeling of tomato thin layer drying in combined infrared-hot air dryer. *Agricultural Engineering International: CIGR Journal*, 19(1), 150–157.  
<https://cigrjournal.org/index.php/Ejournal/article/view/3780>

Somsila, P., & Teeboonma, U. (2014). Investigation of temperature and air flow inside Para rubber greenhouse solar dryer incline roof type by using CFD technique. *Advanced Materials Research*, 931–932, 1238–1242.  
<https://doi.org/10.4028/WWW.SCIENTIFIC.NET/AMR.931-932.1238>

Spall, S., & Sethi, V. P. (2020). Design, modeling and analysis of efficient multi-rack tray solar cabinet dryer coupled with north wall reflector. *Solar Energy*, 211, 908–919. <https://doi.org/10.1016/J.SOLENER.2020.10.012>

Srichat, A., Vengsungnle, P., Hongtong, K., Kaewka, W., & Jongpluempiti, J. (2019). A Comparison of Temperature for Parabola and Sinusoidal Greenhouse Solar Dryer by CFD. *IOP Conference Series: Materials Science and Engineering*, 501(1), 012006. <https://doi.org/10.1088/1757-899X/501/1/012006>

Srinivasan, G., & Muthukumar, P. (2021). A review on solar greenhouse dryer: Design, thermal modelling, energy, economic and environmental aspects. *Solar Energy*, 229, 3–21. <https://doi.org/10.1016/J.SOLENER.2021.04.058>

Strumillo, C. (2007). Perspectives on Developments in Drying. *https://Doi.Org/10.1080/07373930600778056*, 24(9), 1059–1068.  
<https://doi.org/10.1080/07373930600778056>

Tong, G., Christopher, D. M., & Zhang, G. (2018). New insights on span selection for Chinese solar greenhouses using CFD analyses. *Computers and Electronics in Agriculture*, 149, 3–15. <https://doi.org/10.1016/J.COMPAG.2017.09.031>

Verma, P. (2019). A Review Paper on Solar Greenhouse Dryer. *Journal of Mechanical and Civil Engineering*. Retrieved July 12, 2022, from <https://www.iosrjournals.org/iosr-jmce/papers/Conf15010/Vol-2/8.%2043-48.pdf>

Vijayan, S., Arjunan, T. v., & Kumar, A. (2017). Fundamental concepts of drying. *Green Energy and Technology*, 0(9789811038327), 3–38. [https://doi.org/10.1007/978-981-10-3833-4\\_1/FIGURES/10](https://doi.org/10.1007/978-981-10-3833-4_1/FIGURES/10)

Vijayavenkataraman, S., Iniyan, S., & Goic, R. (2012). A review of solar drying technologies. *Renewable and Sustainable Energy Reviews*, 16(5), 2652–2670. <https://doi.org/10.1016/J.RSER.2012.01.007>

Villagran, E., Henao-Rojas, J. C., & Franco, G. (2021). Thermo-Environmental Performance of Four Different Shapes of Solar Greenhouse Dryer with Free Convection Operating Principle and No Load on Product. *Fluids* 2021, Vol. 6, Page 183, 6(5), 183. <https://doi.org/10.3390/FLUIDS6050183>

Vivekanandan, M., Periasamy, K., Babu, C. D., Selvakumar, G., & Arivazhagan, R. (2021). Experimental and CFD investigation of six shapes of solar greenhouse dryer in no load conditions to identify the ideal shape of dryer. *Materials Today: Proceedings*, 37(Part 2), 1409–1416. <https://doi.org/10.1016/J.MATPR.2020.07.062>

## 4 EVALUATION OF THIN LAYER MODELS IN A GREENHOUSE-TYPE SOLAR DRYER DURING DRYING OF TOMATO FRUITS

FOR SUBMISSION TO BIOSYSTEMS ENGINEERING JOURNAL

Jose Olaf Valencia Islas, Irineo Lorenzo López Cruz\*, Murat Kacira, Agustín Ruiz García, Jose Francisco Marín Camacho and David de Martín  
Santiago

### 4.1 ABSTRACT

The objectives of this study were: 1) to evaluate 35 thin layer models in a greenhouse-type solar dryer to determine which model best describes the tomato's drying kinetics and 2) to compare the accuracy of the model predictions against experimental data. The greenhouse-type solar dryer has dimensions of 9 (W) x 12 m (L) and 3.4 m (H) with a parabolic roof shape of 6 mm thick polycarbonate cover, a concrete floor, four inlets at the north wall, and two exhaust fans at the south wall. The thin-layer models were fitted and tested with data from sliced tomato drying experiments. The best five models for the calibration stage had an  $R^2$  over 0.999 whereas in the test stage is over 0.993. From all the models in both stages, the recommended model was the Page modified VI as it is a semi-theoretical model with few parameters needed and an RMSE of 0.06 and an  $R^2$  of 0.993.

**Keywords:** solar drying, black-box modeling, thin-layer models, greenhouse

### 4.2 INTRODUCTION

Tomato (*Solanum Lycopersicum* L.) is considered one of the most important crops in the world, not only because it is an integral part of the human diet (Kumar et al., 2015) but also, due to its high content of vitamin A (Djebli et al., 2019),

lycopene, and antioxidant substances present in the fruits (Khama et al., 2016) (Khama et al., 2016). Globally, the tomato yield is 177 million tons in a total of 4.8 million hectares (Kishk et al., 2019), making it the second most cultivated vegetable. However, despite the importance of tomatoes, being a highly perishable product, losses in developed countries range from 22 to 50% (Correia et al., 2015) mainly due to their high water content.

A way to preserve perishable foods is drying, through which the water content of the product is reduced to the point where microbial activity stops (Valta et al., 2019). Nevertheless, drying is one of the most intense processes in energy consumption in the food industry, especially in hot air dryers in which a large percentage of thermal energy is lost at the air outlets (Dorouzi et al., 2018). As a renewable energy source, solar energy, if abundant in a given region, can help reducing energy demand from fossil fuel-based sources lowering operating cost, and can be implemented in any area, especially in rural areas (Fterich et al., 2018; Mohsen et al., 2019). One of the main disadvantages of solar drying is the inconsistency of the drying process as it depends on dynamics of irradiance over time, for instance during cloud pass or nighttime drying, affecting the drying time and quality of the product. Also, if it is done in the open field, the drying product can be exposed to contamination by animals, bacteria, or fungi (Julián Molina Mosquera et al., 2018; Samimi-Akhijahani & Arabhosseini, 2018). To avoid the issues and enhance energy conservation and usage, drying has been studied indoors with cabinets, greenhouses, or other structures that use solar drying as the main heat source.

In drying, the relationship between the process used and the product quality achieved is a solid basis for improving the process (Jorge et al., 2014), yet it is known that different crops have different moisture content, specific heat capacity, latent heat of vaporization, and other parameters (Nwakuba et al., 2018) that difficult the understanding of drying and it is only through the insight of drying kinetics and modeling that such a complex process can be analyzed and optimized (das Purkayastha et al., 2013). Studies in drying kinetics are characterized by fitting measurements of drying properties with empirical equations to predict drying parameters and behavior of the material under different conditions (López-Cerino et al., 2018).

In the literature, considering the thin layer drying, the following studies are related to tomatoes and modeling: Azeez et al. (2019), used an oven-type vacuum dryer with temperatures of 50, 60, and 70 °C to investigate the antioxidant, polyphenolic, and carotene content activity, as well as the drying kinetics using the Page, Lewis, and Henderson and Pabis models, being the Page model the one that best fits the conditions. Sadin et al. (2017), used an electric tray dryer that works with hot air at temperatures of 60, 70, and 80 °C to model the dehydration process, they used the Midilli-Kucuk, Logarithmic model, Henderson & Pabis, Binomial model, and Lewis models. They found that all the models fitted well but the best was the Midilli-Kucuk model. Kocabiyik et al. (2016), investigated the properties of the dehydrated tomato with infrared radiation and used the Newton, Page, Henderson & Pabis, Logarithmic model, and Wang & Singh, models. They found that the best fit of the drying kinetics of tomatoes in an infrared radiation oven was with the Logarithmic model. Murugavelh et al. (2019), used a

tunnel solar dryer to investigate drying kinetics and perform an exergy analysis of the drying process. They fitted the Newton, Page, Modified Page, Henderson and Pabis, Logarithmic model, Two Term Exponential, Verma, Wang and Singh, Midilli-Kucuk, and Approximation of Diffusion. They found that the drying kinetics help to understand the thermophysical parameters involved in the process, with the Midilli-Kucuk model as the best model for their specific conditions. Hamdi & Kooli (2018), investigated a greenhouse-type solar dryer and compared it to open-air drying. They adjusted the Page, Modified Page, Wang and Singh, and Midilli-Kucuk models, and found the best model for both scenarios, drying in open-air and covering, the Midilli-Kucuk model. Kishk et al. (2019), proposed a solar dryer based on recyclable aluminum cans. The cans were used to build the solar collector and the drying process occur in a separate drying chamber. They evaluated Page, Henderson and Pabis, Newton, Logarithmic, Wang, and Singh, Two terms, Two Terms Exponential, and Approximation of Diffusion models to fit the results with their proposed dryer. The study indicated that the model that best describes tomato drying in this tray dryer was the Wang and Singh model.

There is a significant opportunity for research on solar dryers, where incident radiation dominates the behavior of the dryer. The variability in radiation due to conditions such as rain, season, or hour of the day, makes it a problem for the use of thin-layer models. It is important to investigate the drying process and performance under varying conditions and test models with different mathematical structures and models with different parameters. Furthermore, the dimensions of most dryers allow conditions to be more homogeneous but pose a problem for industrial scale-up. Despite having a model that fits the data there is no test stage,

using a case study, for the models listed in each study. Finally, the best thin layer model in each research is not always the same, the Midilli Kucuk model is identified to be the most common as it describes best the tomato drying kinetics.

The objectives of this study were: 1) to evaluate 35 thin layer models in a greenhouse-type solar dryer to determine which model best describes the tomato's drying kinetics and 2) to compare the accuracy of the model predictions against experimental data.

### **4.3 MATERIALS AND METHODS**

#### **4.3.1 The Greenhouse Solar Dryer**

The Greenhouse-type Solar Dryer is located at the Universidad Autonoma Chapingo, Mexico (19°29' N, 98°53 W, and 2250 m of altitude). It is oriented in the North-South direction and has dimensions of 9 (W) x 12 m (L) and 3.4 m (H). It has a ground surface area of 108 m<sup>2</sup> and an approximate volume of 211 m<sup>3</sup>. The structure is of galvanized steel, the cover is a double wall polycarbonate of 6 mm thickness, and it has a parabolic shape roof. The floor is covered with a concrete layer of 0.15 m thickness (Figure 4-1).

The dryer has four air inlets of 1.23 m in width and 0.53 m in height, the door is 2 x 2 m, all with an anti-aphid mesh of 40 x 26 threads. In the south wall, there are two exhaust fans with a capacity of 9,435 m<sup>3</sup> h<sup>-1</sup> each, powered by single-phase motors of 0.5 HP and allowing renewal of air inside the dryer in approximately 40 s (measured).

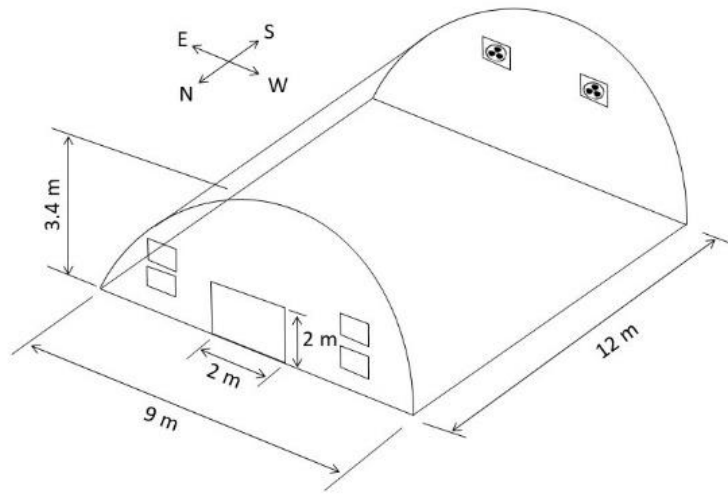


**Figure 4-1.** Dimensions of the greenhouse-type solar dryer.

#### 4.3.2 Drying experiments and data collection

Seventy kilograms of tomatoes (*Saladette* variety, Roma-type) were freshly purchased from the local market in Mexico City, Mexico. They were washed and sliced into a thickness of 5 mm. Two experiments were carried out in the greenhouse-type solar dryer. The first was conducted on December 4<sup>th</sup>, 2018, hereinafter called Dataset 1; the second was carried out on July 19<sup>th</sup>, 2019, hereinafter called Dataset 2. Both experiments began at 8:00 a.m., and the span of the experiments was different given the conditions of the weather; the first one lasted 11.5 hours and the tomato was withdrawn the same day, and the second lasted 16.25 hours and was withdrawn the next day. Samples of tomato slices, randomly distributed in small trays inside the drying tables, were weighed at 15 minutes intervals, the weight loss was recorded by a digital balance (VELAB VE-1000, Velab Mexico, Mexico) of  $\pm 0.1$  g accuracy. Drying continued until the measured weight was constant for four consecutive measurements. When drying

was completed, the samples were dried at 130 °C for 16 hours in an electric drying oven (Felisa fe-291ad series 1507045) (Bala, 2016).

To measure the air temperature inside the greenhouse, five CS215-L digital sensors (Campbell Scientific, Utah, USA,  $\pm 2\%$ ,  $\pm 0.4^{\circ}\text{C}$  accuracies) were used and the measured values were averaged; for radiation measurements a pyranometer CMP3 was used (Kipp & Zonen 102885, Sterling, USA,  $5 \mu\text{V} / \text{W} / \text{m}^2$  accuracy). For the external environment variables, the air temperature was measured with an HMP60 digital sensor (Vaisala, Vantaa, Finland,  $\pm 3\%$ ,  $\pm 0.6^{\circ}\text{C}$ , accuracy), and solar radiation was measured with a pyranometer (Hukseflux LP02-L, Campbell Scientific, Utah, USA,  $15 \mu\text{V} / \text{W} / \text{m}^2$ , accuracy).

### **4.3.3 Mathematical modeling**

The moisture ratio curves of the second experiment (Dataset 2) were fitted with 35 empirical and semi-theoretical thin-layer drying models (Table 4-1). These models were selected from a literature review of models used, so far, in thin layer drying of tomatoes and other models which has not been used before for this fruit. After fitting the adjusted models, they were tested with new data from the first experiment (Dataset 1). All models were fitted using the function non-linear least squares (lsqnonlin) in Matlab, minimizing the sum of the squared difference between the predicted and measured moisture ratio, computed with Dataset 2.

**Table 4-1.** Thin layer drying models.

	<b>Name</b>	<b>Equation</b>	<b># of parameters</b>	<b>Type</b>	<b>Reference</b>
1	Newton	$MR = \exp(-kt)$	1	ST	(Kesavan et al., 2019)
2	Page	$MR = \exp(-kt^n)$	2	ST	(López-Cerino et al., 2019)
3	Page modified VI	$MR = \exp(kt^n)$	2	ST	(Kurozawa et al., 2012)
4	Overhults et al.	$MR = \exp(-(kt)^n)$	2	ST	(Sonmete et al., 2016)
5	Page modified	$MR = \exp((-kt)^n)$	2	ST	(Kesavan et al., 2019)
6	Weibull Distribution III	$MR = \exp\left(-\left(\frac{t}{a}\right)^n\right)$	2	E	(López-Cerino et al., 2019)
7	Aghbashlo model	$MR = \exp\left(-\frac{k_1 t}{1 + k_2 t}\right)$	2	E	(Ezeanya et al., 2018)
8	Henderson & Pabis	$MR = a * \exp(-kt)$	2	ST	(Ezeanya et al., 2018)
9	Regression	$MR = \exp(-(at^2 + bt))$	2	E	(Shi et al., 2008)
10	Vega-Galvez et al.	$MR = n + k\sqrt{t}$	2	E	(Vega-Gálvez et al., 2008)
11	Wang & Singh	$MR = 1 + at + bt^2$	2	E	(Kesavan et al., 2019)
12	Two terms exponential	$MR = a * \exp(-kt) + (1 - a)\exp(-kat)$	2	ST	(Ezeanya et al., 2018)
13	Midilli modified III	$MR = a * \exp(-kt) + bt$	3	ST	(Doymaz, 2009)
14	Haghi & Angiz IV	$MR = a * \exp\left(\frac{-(t - b)^2}{2c^2}\right)$	3	E	(López-Cerino et al., 2019)
15	Two terms modified III	$MR = a * \exp(-k_0 t) + a * \exp(-k_1 t)$	3	ST	(Baini & Langrish, 2007)
16	Page modified VII	$MR = \exp\left(-k\left(\frac{t}{L^2}\right)^n\right)$	3	ST	(Artnaseaw et al., 2010)
17	Logistic	$MR = \frac{a_0}{[1 + a * \exp(kt)]}$	3	E	(López-Cerino et al., 2019)
18	Verma et al.	$MR = a * \exp(-k_0 t) + (1 - a)\exp(-k_1 t)$	3	ST	(Badaoui et al., 2019)

19	Midilli modified	$MR = \exp(-kt^n) + bt$	3	ST	(López-Cerino et al., 2019)
20	Approximation of Diffusion	$MR = a * \exp(-kt) + (1 - a)\exp(-kbt)$	3	ST	(Ezeanya et al., 2018)
21	Logarithmic model	$MR = a * \exp(-kt) + b$	3	ST	(Kesavan et al., 2019)
22	Khazaei & Daneshmandi	$MR = a + \exp(-bt) - ct$	3	E	(Khazaei & Danaeshmandi, 2007)
23	Henderson & Perry modified	$MR = a * \exp(-kt^n)$	3	E	(Corzo et al., 2011)
24	Demir et al.	$MR = a * \exp((-kt)^n) + b$	4	E	(Demir et al., 2007)
25	Midilli-Kucuk	$MR = a * \exp(-kt^n) + bt$	4	ST	(Kesavan et al., 2019)
26	Two terms	$MR = a * \exp(-k_0t) + b * \exp(-k_1t)$	4	ST	(Kesavan et al., 2019)
27	Sripinyowanich & Noomhorn	$MR = \exp(-kt^n) + bt + c$	4	E	(López-Cerino et al., 2019)
28	Wang et al. Two terms	$MR = (1 - a) \exp(bkt) + a * \exp(ckt)$	4	E	(Wang et al., 2007)
29	Jena & Das	$MR = a * \exp(-kt + b\sqrt{t}) + c$	4	E	(Jena & Das, 2007)
30	Two terms modified IV	$MR = a * \exp(-k_0t^n) + b * \exp(-k_1t)$	5	ST	(Tirawanichakul et al., 2008)
31	Hii et al.	$MR = a * \exp(-kt^n) + c * \exp(-gt^n)$	5	E	(López-Cerino et al., 2019)
32	Alibas model	$MR = a * \exp((-kt^n) + bt) + g$	5	E	(Alibaş, 2012)
33	Henderson and Pabis modified	$MR = a * \exp(-kt) + b * \exp(-gt) + c * \exp(-ht)$	6	ST	(Kesavan et al., 2019)
34	Wang et al. Three terms	$MR = (1 - a - b) \exp(ckt) + a * \exp(dkt) + b * \exp(fkt)$	6	E	(Wang et al., 2007)

35	Henderson and Pabis modified II	$MR = a * \exp(-kt^n) + b * \exp(-gt) + c * \exp(-ht)$	7	ST	(Ameri et al., 2018)
----	---------------------------------	--	---	----	----------------------

where: a, b, c, d, f, g, h,  $k_0$ ,  $k_1$ ,  $k_2$ , k, n = parameters, L = thickness.

#### 4.4 THEORY AND CALCULATIONS

The moisture ratio (MR, dimensionless) is defined as:

$$MR = \frac{M_t - M_e}{M_0 - M_e} \quad (\text{Eq- 4-1})$$

where  $M_0$  (decimal),  $M_e$  (decimal) and  $M_t$  (decimal) are initial moisture content, equilibrium moisture content, and moisture content at any time, respectively (Hasan et al., 2014).

Moisture ratio is the amount of water content that a product has in a dimensionless value based on the moisture of equilibrium. The drying rate is the change in the moisture content over time and has three main phases. Phase I is defined by a constant rate of drying driven mainly by the diffusion of water vapor on the surface of the thin surface of the material. Phase II corresponds to the first falling rate period where the surface of the thin slice is no longer saturated with water and the humidity is transferred from the interior to the surface by the capillary forces; in this phase, the drying rate decreases over time. Finally, the Phase III, also known as the second falling rate period, the process depends on the properties of the material rather than the external conditions. The hygroscopic and porosity behaviour highly affect the drying time and moisture content. The process depends more on the heat transferred from the surrounding air as more

energy is needed to move the water from inside to the surface of the product (Babalís et al., 2017).

Models' predictions were evaluated using Dataset 1, in terms of coefficients of determination ( $R^2$ ), root mean square error (RMSE), mean absolute error (MAE), and modeling efficiency (EF), defined as (Patil & Gawande, 2017):

$$R^2 = \frac{(\sum M_{obs} M_{pre})^2}{\sum M_{obs}^2 \sum M_{pre}^2} \quad (\text{Eq- 4-2})$$

$$RMSE = \sqrt{\frac{\sum (M_{pre} - M_{obs})^2}{N}} \quad (\text{Eq- 4-3})$$

$$MAE = \frac{1}{N} \sum |MR_{pre} - MR_{obs}| \quad (\text{Eq- 4-4})$$

$$EF = 1 - \frac{\sum (MR_{obs} - MR_{pre})^2}{\sum (MR_{obs} - \overline{MR})^2} \quad (\text{Eq- 4-5})$$

Where

$$\overline{MR} = \frac{1}{N} \sum MR_{obs} \quad (\text{Eq- 4-6})$$

$MR_{obs}$ , is the moisture ratio observed (decimal),  $MR_{pre}$ , is the moisture ratio predicted (decimal),  $N$ , is the quantity of data (an integer).

## 4.5 RESULTS

During both drying experiments, the outdoor air temperature ranged between 15 to 25°C whereas the inner temperature reached a maximum temperature of 55 °C, 30 to 35°C higher than outdoor temperatures. Radiation

levels were very different for the two experiments and clouds play an important role in the amount of radiation that reaches the greenhouse (Figures 4-2 and 4-3). The temperature distribution through time differs in both experiments due to the solar radiation variability.

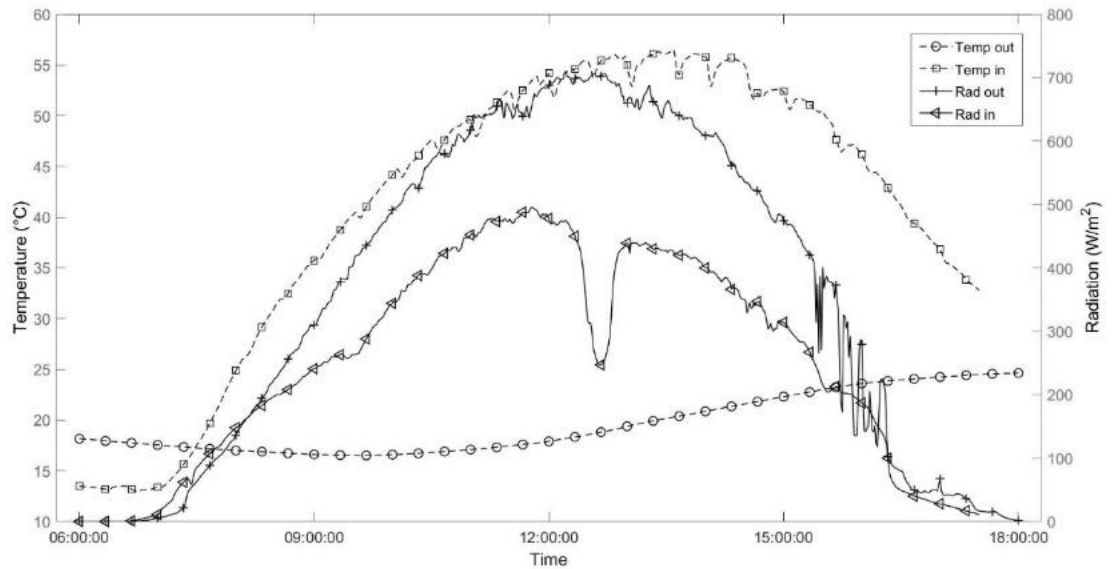


**Figure 4-2.** Outside and inside conditions of Dataset 1.

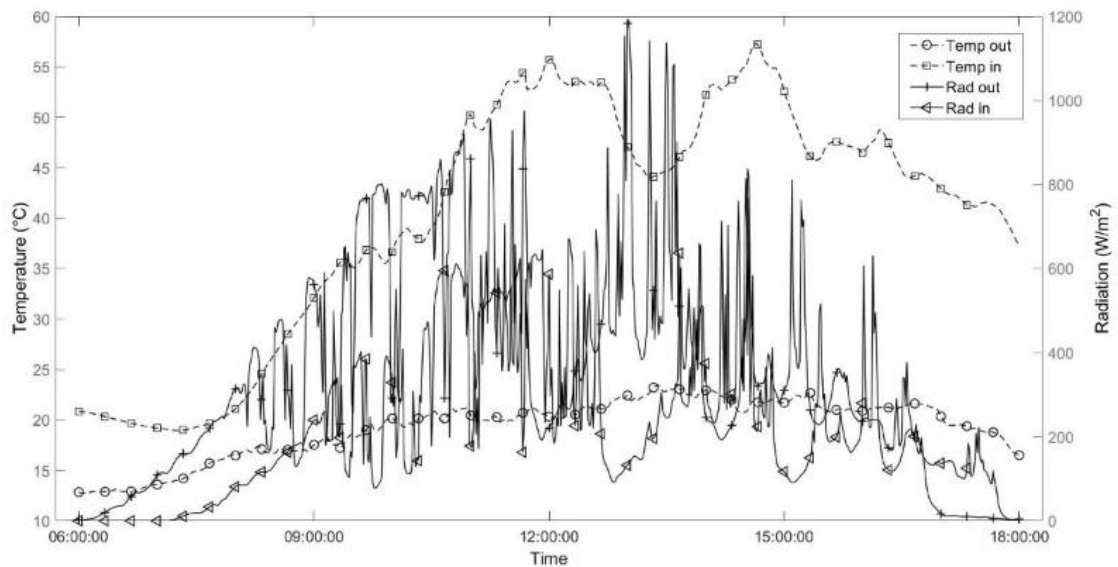


**Figure 4-3.** Outside and inside conditions of Dataset 2.

The best five models for each stage were compared through the RMSE,  $R^2$ , MAE, MSE, and EF values (Table 4-2) the remaining models were not listed here but the worst model in the fit stage was the Vega-Gálvez et al., (2008) model with  $R^2=0.945$ , an RMSE=0.105, and an EF=0.91; the worst model in the test stage was Demir et al., (2007) with  $R^2=0.942$ , an RMSE=0.1452 and EF=0.849; all other models are above in  $R^2$  and EF with fewer values of RMSE.

**Table 4-2.** Statistics for the best five models under fit and test stages.

#	Parameters	$R^2$	MSE	RMSE	MAE	EF
<b>Fit stage best models</b>						
Henderson and Pabis modified II		1.000	0.0001	0.008	0.018	0.999
Wang three terms		1.000	0.0001	0.010	0.023	0.999
Henderson and Pabis modified		1.000	0.0001	0.010	0.024	0.999
Hii et al.		0.999	0.0001	0.011	0.027	0.999
Alibas		0.999	0.0001	0.011	0.023	0.999
<b>Test stage best models</b>						
Regression		0.994	0.003	0.059	0.045	0.975
Haghi & Angiz IV		0.993	0.003	0.059	0.045	0.975
Overhults et al.		0.993	0.004	0.060	0.047	0.974
Weibull III		0.993	0.004	0.060	0.047	0.974
Page modified VI		0.993	0.004	0.060	0.047	0.974

The measurements and the fitted curves are shown for each stage in Figures 4-3 and 4-4. In general, all models sub estimates the moisture content

during Phase II of the drying rate in the test scenario. In terms of the fit stage, all models follow exactly the behaviour of the data-calculated moisture ratio.

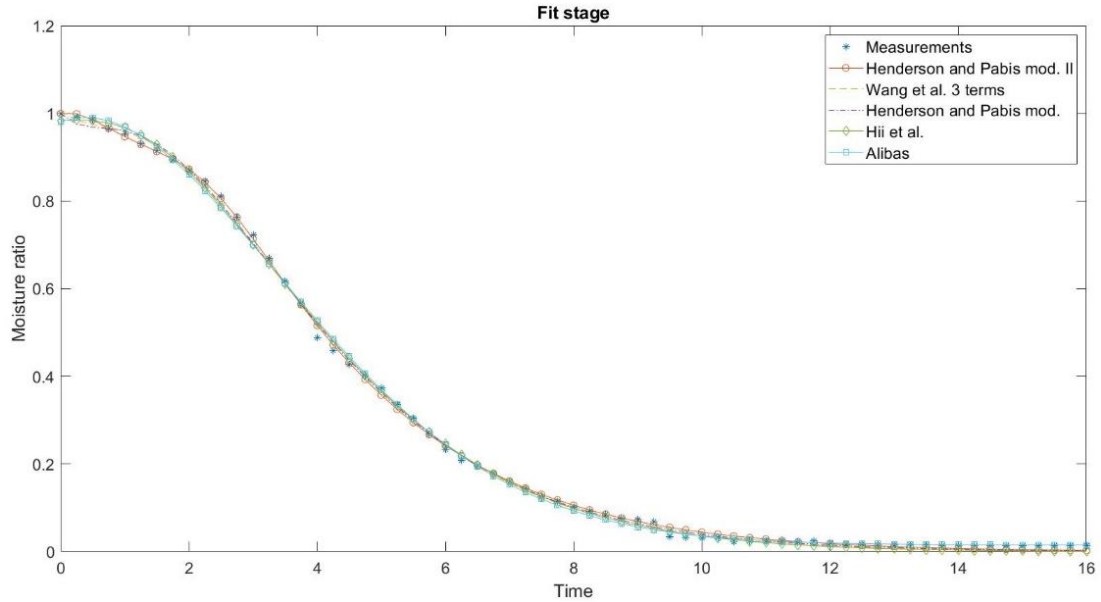


**Figure 4-4.** Best five thin layer models during the fitting with measurements.

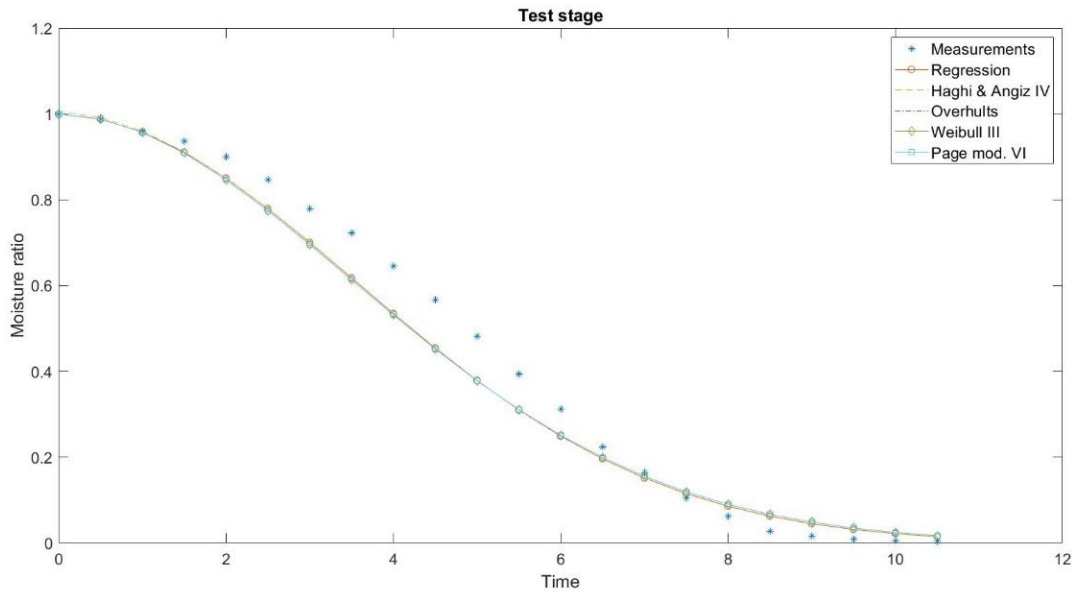


**Figure 4-5.** Comparison of measurements and the best five thin layer models with the new data.

The parameter values for all the models are summarized in Table 4-3 under the Appendices section of this paper.

#### **4.6 DISCUSSION**

The best models at the fit stage are those with a higher number of parameters (Table 4-2) but for the test stage, the best performance is achieved with models with less than 4 parameters. In general, it is desirable to use models with few parameters avoiding overfitting or complex models that can lead to parameters that cannot be physically explained.

Semi-theoretical models are superior to empirical models as they have a physical meaning and can also be used regardless of the experiment. The use of empirical models is limited when the system changes, because new data are required to adjust the model or greater disparities may arise when using them.

The drying rate depends highly on the characteristics of the product and the air temperature. The shape factor highly affects Phase II on the drying rate and the drying constant affects Phase III. In this study, some of the models have the same or close values as the structure could be similar or based on the same model. The five best models in the adjustment stage have very similar behaviour to the moisture ratio obtained from the data, that is, phases I and II are well captured by the model during the adjustment; however, in the test stage, it is observed that Phase II is underestimated. This may be due to the difference in

temperature in the new data, it is observed that there is a fluctuation in temperature over the day (Figures 4-2 and 4-3) due to the large radiation variability. Phases I and III are well represented by the models but the time to reach the desired moisture will be overestimated by the difference in the wide drop in moisture ratio during Phase II.

The semi-theoretical models, such as Henderson and Pabis derived from Fick's Second Law of Diffusion, the Page and Overhults based on the Newton law of cooling, are models that have the structure based on approximations to the solution of physical models. Thus, the parameters can be related to a physical understanding of the problem. The modifications for both kinds of models are not always related to the solution of the physical laws but still preserve some of the structure and could lead to conclusions related to the physics of drying.

The main difference between the structure of the Newton and the Henderson and Pabis original models is the constant multiplying the exponential term. In general,  $k$  is the drying constant ( $s^{-1}$ ),  $t$  is the time ( $s$ ) and  $A$  or  $a$  is the shape factor (dimensionless). The drying constant is associated with the drying parameters such as heat and mass transfer, depends on temperature, and is simplified through the thin layer models. The values range from 0 to 1 for all models used in this study, as expected.

## 4.7 CONCLUSIONS

The best model to predict the moisture ratio of tomato slices in a greenhouse-type solar dryer was found to be the Page modified VI (Model 3, Table 4-1). This model was also found to be equivalent to the Overhults et al. model. The Page model is a Semi-theoretical model and is highly used and found in other research regarding drying, it has two parameters and could be fit relatively without trouble. Other authors found the Midilli Kucuk as the best model but for this study, the Midilli model was not as accurate as the first five models (Regression, Haghi and Angiz IV, Overhults, Weibull II and Page modified VI models), and compared to the Page models it has more parameters to be fitted. Although the the Page model was identified to be the most accurate among others evaluated, the Regression, Haghi and Angiz IV, Overhults, Weibull II and Page modified VI models are also suitable to predict moisture content of tomato slices dried in greenhouse-type solar dryers.

The present study has shown that some of the models found in the literature identified to be ideal for use in thin-layer modeling. However, no major discussions have been found on testing the models with new data. This is recommended since, as observed in the results, the best-fitting models does not always mean that they would offer the most accurate predictions. The variability of the conditions significantly affects the behavior of the models due to the high abstraction of the moisture ratio concept and the assumption of constant temperature during drying.

Thin layer models only depend on time and not on temperature, an important parameter that would be considered within the drying constant. Other investigations with different products within greenhouse-type solar dryers should be established. Still, more models should not be developed given their wide repertoire in the literature and the similarity between the mathematical structure reflected in the estimated values when adjusting the models with data.

#### 4.8 APPENDICES

**Table 4-3.** Parameter values for all 35 thin layer models tested in this study.

Model name	Parameters
1 Newton	$k = 0.208$
2 Page	$k = 0.043, n = 1.930$
3 Page modified VI	$k = -0.043, n = 1.930$
4 Page modified	$k = 0.197, n = 1.930$
5 Page modified VII	$k = 21.698, n = 1.930$
6 Overhults et al. Weibull Distribution	$k = 0.197, n = 1.930$
7 III	$a = 5.076, n = 1.930$
8 Henderson & Pabis	$a = 1.222, k = 0.247$
9 Regression Two terms	$a = 0.038, b = 0.005$
10 exponential	$a = 2.242, k = 0.355$
11 Wang & Singh	$a = -0.152, b = 0.006$
12 Aghbashlo model	$k_1 = 0.126, k_2 = -0.062$
13 Vega-Galvez et al. Henderson & Perry	$n = 1.181, k = -0.335$
14 modified	$a = 1.009, k = 0.046, n = 1.900$
15 Midilli modified	$k = 0.041, n = 1.980, b = 0.001$
16 Midilli modified III	$a = 1.186, k = 0.216, b = -0.005$
17 Logarithmic	$a = 1.283, k = 0.197, n = -0.104$
18 Hagui & Angiz IV	$a = 1.007, b = -0.130, c = 3.670$
19 Two terms modified Two terms modified	$a_0 = 1.140, a = 0.108, k = 0.587$
20 III	$a = 0.611, k_0 = 0.247, k_1 = 0.247$

---

21	Verma et al. Approximation of	$a = 32.084, k_0 = 0.482, k_1 = 0.502$
22	Diffusion Khazaei &	$a = -45.659, k = 0.499, b = 0.972$
23	Daneshmandi Sripinyowanich &	$a = 0.150, b = 0.236, c = 0.015$
24	Noomhorn	$k = 0.043, n = 1.965, b = 0.001, c = 0.007$
25	Midilli-Kucuk	$a = 1.003, k = 0.042, n = 1.967, b = 0.001$
26	Two terms	$a = 36.265, k_0 = 0.495, b = -35.325, k_1 = 0.515$
27	Jena & Das Wang et al. Two	$a = 0.899, k = 0.416, b = 0.561, c = -0.027$
28	terms	$a = 3.106, b = 9.519, k = -0.07, c = 5.627$
29	Demir et al. Two terms modified	$a = -15.950, k = -0.0002, n = 0.435, b = 17.202$
30	IV	$a = -14.829, k_0 = 0.301, n = 0.955, b = 15.738, k_1 = 0.273$
31	Hii et al.	$a = -0.440, k = 0.435, n = 1.458, c = 1.424, g = 0.129$
32	Alibas model Henderson and	$a = 0.965, k = 0.079, b = 0.067, n = 1.759, g = 0.015$
33	Pabis modified Wang et al. Three	$a = 16.007, k = 0.873, b = 19.992, g = 0.585, c = -34.993, h = 0.730$
34	terms Henderson and	$a = 11.029, b = 1.626, c = -1.741, k = 0.384, d = -1.385, f = -3.329$
35	Pabis modified II	$a = -0.324, k = 0.189, n = 2.631, b = 17.751, g = 0.507, c = -16.427, h = 0.551$

---

## 4.9 ACKNOWLEDGMENTS

This work was supported by the National Council of Science and Technology (CONACyT, [grant number CB-2015-254055])

## 4.10 REFERENCES

Alibaş, İ. (2012). Microwave Drying of Grapevine (*Vitis vinifera* L.) Leaves and Determination of Some Quality Parameters. *Journal of Agricultural Sciences*, 18(1), 43–53. [https://doi.org/10.1501/TARIMBIL\\_0000001191](https://doi.org/10.1501/TARIMBIL_0000001191).

Artnaseaw, A., Theerakulpisut, S., & Benjapiyaporn, C. (2010). Drying characteristics of Shiitake mushroom and Jinda chili during vacuum heat pump

drying. *Food and Bioproducts Processing*, 88(2–3), 105–114.  
<https://doi.org/10.1016/J.FBP.2009.09.006>.

Azeez, L., Adebisi, S. A., Oyedeji, A. O., Adetoro, R. O., & Tijani, K. O. (2019). Bioactive compounds' contents, drying kinetics and mathematical modelling of tomato slices influenced by drying temperatures and time. *Journal of the Saudi Society of Agricultural Sciences*, 18(2), 120–126.  
<https://doi.org/10.1016/J.JSSAS.2017.03.002>.

Babalis, S., Papanicolaou, E., & Belessiotis, V. (2017). Fundamental mathematical relations of solar drying systems. *Green Energy and Technology*, 0(9789811038327), 89–175. [https://doi.org/10.1007/978-981-10-3833-4\\_4/COVER](https://doi.org/10.1007/978-981-10-3833-4_4/COVER).

Badaoui, O., Hanini, S., Djebli, A., Haddad, B., & Benhamou, A. (2019). Experimental and modelling study of tomato pomace waste drying in a new solar greenhouse: Evaluation of new drying models. *Renewable Energy*, 133, 144–155.  
<https://doi.org/10.1016/J.RENENE.2018.10.020>.

Baini, R., & Langrish, T. A. G. (2007). Choosing an appropriate drying model for intermittent and continuous drying of bananas. *Journal of Food Engineering*, 79(1), 330–343. <https://doi.org/10.1016/J.JFOODENG.2006.01.068>.

Bala, B. K. (2016). Drying and Storage of Cereal Grains. In *Drying and Storage of Cereal Grains*. John Wiley & Sons, Ltd. <https://doi.org/10.1002/9781119124207>.

Correia, A. F. K., Loro, A. C., Zanatta, S., Spoto, M. H. F., & Vieira, T. M. F. S. (2015). Effect of temperature, time, and material thickness on the dehydration process of tomato. *International Journal of Food Science*, 2015.  
<https://doi.org/10.1155/2015/970724>.

Corzo, O., Bracho, N., & Alvarez, C. (2011). DETERMINATION OF SUITABLE THIN LAYER MODEL FOR AIR DRYING OF MANGO SLICES (*Mangifera indica* L.) AT DIFFERENT AIR TEMPERATURES AND VELOCITIES. *Journal of Food Process Engineering*, 34(2), 332–350. <https://doi.org/10.1111/J.1745-4530.2009.00360.X>.

das Purkayastha, M., Nath, A., Deka, B. C., & Mahanta, C. L. (2013). Thin layer drying of tomato slices. *Journal of Food Science and Technology*, 50(4), 642. <https://doi.org/10.1007/S13197-011-0397-X>.

Demir, V., Gunhan, T., & Yagcioglu, A. K. (2007). Mathematical modelling of convection drying of green table olives. *Biosystems Engineering*, 98(1), 47–53. <https://doi.org/10.1016/J.BIOSYSTEMSENG.2007.06.011>.

Djebli, A., Hanini, S., Badaoui, O., & Boumahdi, M. (2019). A new approach to the thermodynamics study of drying tomatoes in mixed solar dryer. *Solar Energy*, 193, 164–174. <https://doi.org/10.1016/J.SOLENER.2019.09.057>.

Dorouzi, M., Morteza pour, H., Akhavan, H. R., & Moghaddam, A. G. (2018). Tomato slices drying in a liquid desiccant-assisted solar dryer coupled with a photovoltaic-thermal regeneration system. *Solar Energy*, 162, 364–371. <https://doi.org/10.1016/J.SOLENER.2018.01.025>.

Doymaz, I. (2009). MATHEMATICAL MODELLING OF THIN-LAYER DRYING OF KIWIFRUIT SLICES. *Journal of Food Processing and Preservation*, 33(SUPPL. 1), 145–160. <https://doi.org/10.1111/J.1745-4549.2008.00289.X>.

Ezeanya, N., Akubuo, C., Chilakpu, K., & Iheonye, A. (2018). Modeling of thin-layer solar drying kinetics of cassava noodles (Tapioca). *Agricultural Engineering International: CIGR Journal*, 20, 193–200. [https://www.researchgate.net/publication/326173054\\_Modeling\\_of\\_thin-layer\\_solar\\_drying\\_kinetics\\_of\\_cassava\\_noodles\\_Tapioca/citation/download](https://www.researchgate.net/publication/326173054_Modeling_of_thin-layer_solar_drying_kinetics_of_cassava_noodles_Tapioca/citation/download).

Fterich, M., Chouikhi, H., Bentaher, H., & Maalej, A. (2018). Experimental parametric study of a mixed-mode forced convection solar dryer equipped with a PV/T air collector. *Solar Energy*, 171, 751–760. <https://doi.org/10.1016/J.SOLENER.2018.06.051>.

Hamdi, I., & Kooli, S. (2018). Exergy and energy analysis of the solar drying processes of tomatoes in Tunisia. 2018 9th International Renewable Energy Congress, IREC 2018, 1–6. <https://doi.org/10.1109/IREC.2018.8362493>.

Hasan, A. A. M., Bala, B. K., & Rowshon, M. K. (2014). Thin layer drying of hybrid rice seed. *Engineering in Agriculture, Environment and Food*, 7(4), 169–175. <https://doi.org/10.1016/J.EAEF.2014.06.002>.

Jena, S., & Das, H. (2007). Modelling for vacuum drying characteristics of coconut presscake. *Journal of Food Engineering*, 79(1), 92–99. <https://doi.org/10.1016/J.JFOODENG.2006.01.032>.

Jorge, A., Almeida, D. M., Canteri, M. H. G., Sequinel, T., Kubaski, E. T., & Tebcherani, S. M. (2014). Evaluation of the chemical composition and colour in long-life tomatoes (*Lycopersicon esculentum* Mill) dehydrated by combined drying methods. *International Journal of Food Science & Technology*, 49(9), 2001–2007. <https://doi.org/10.1111/IJFS.12501>.

Julián Molina Mosquera, J., Salgado Patrón, J., & Sendoya-Losada, D. F. (2018). DESIGN AND IMPLEMENTATION OF A DRYER TO CONTROL AND MONITOR THE DEHYDRATION PROCESS OF TOMATOES. 13(16). [www.arpnjournals.com](http://www.arpnjournals.com).

Kesavan, S., Arjunan, T. v., & Vijayan, S. (2019). Thermodynamic analysis of a triple-pass solar dryer for drying potato slices. *Journal of Thermal Analysis and Calorimetry*, 136(1), 159–171. <https://doi.org/10.1007/S10973-018-7747-0>.

Khama, R., Aissani, F., Alkama, R., Bennamoun, L., Fraikin, L., Salmon, T., Plougonven, E., & Leonard, A. (2016). CONVECTIVE DRYING OF CHERRY TOMATO: STUDY OF SKIN EFFECT. *Journal of Engineering Science and Technology*, 11(3), 443–457..

Khazaei, J., & Danaeshmandi, S. (2007). Modeling of thin-layer drying kinetics of sesame seeds: Mathematical and neural networks modeling. *International Agrophysics*, 21(4), 335–348.  
[https://www.researchgate.net/publication/26551883\\_Modeling\\_of\\_thin-layer\\_drying\\_kinetics\\_of\\_sesame\\_seeds\\_Mathematical\\_and\\_neural\\_networks\\_modeling](https://www.researchgate.net/publication/26551883_Modeling_of_thin-layer_drying_kinetics_of_sesame_seeds_Mathematical_and_neural_networks_modeling).

Kishk, S. S., ElGamal, R. A., & ElMasry, G. M. (2019). Effectiveness of recyclable aluminum cans in fabricating an efficient solar collector for drying agricultural products. *Renewable Energy*, 133, 307–316.  
<https://doi.org/10.1016/J.RENENE.2018.10.028>.

Kocabiyik, H., Yilmaz, N., Tuncel, N. B., Sumer, S. K., & Buyukcan, M. B. (2016). Quality properties, mass transfer characteristics and energy consumption during shortwave infrared radiation drying of tomato. *Http://Dx.Doi.Org/10.3920/QAS2014.0550*, 8(3), 447–456.  
<https://doi.org/10.3920/QAS2014.0550>.

Kumar, V., Singh, B. R., Chandra, Suresh, & Singh, S. (2015). A Review on Tomato Drying by Different Methods with Pretreatments. *International Journal of Food and Fermentation Technology*, 5, 15–24.

Kurozawa, L. E., Azoubel, P. M., Murr, F. E. X., & Park, K. J. (2012). DRYING KINETIC OF FRESH AND OSMOTICALLY DEHYDRATED MUSHROOM (AGARICUS BLAZEI). *Journal of Food Process Engineering*, 35(2), 295–313.  
<https://doi.org/10.1111/J.1745-4530.2010.00590.X>.

López-Cerino, I., López-Cruz, I. L., Janjai, S., Mahayothee, B., Nagle, M., Müller, J., López-Cerino, I., López-Cruz, I. L., Janjai, S., Mahayothee, B., Nagle, M., & Müller, J. (2019). Mathematical modelling of the thin layer of Pineapple (*Ananas comosus*, L.): experiment at Village-scale greenhouse-type solar dryer. *Ingeniería, Investigación y Tecnología*, 20(2), 0–0. <https://doi.org/10.22201/FI.25940732E.2019.20N2.016>.

López-Cerino, I., López-Cruz, L. I., Nagle, M., Mahayothee, B., Müller, J., López-Cerino, I., López-Cruz, L. I., Nagle, M., Mahayothee, B., & Müller, J. (2018). Thin layer drying of Pineapple (*Ananas comosus*, L.). *Ingeniería, Investigación y Tecnología*, 19(3), 329–342. <https://doi.org/10.22201/FI.25940732E.2018.19N3.028>.

Mohsen, H. A., Abd El-Rahmam, A. A., Hassan, H. E., & Mohsen, A. (2019). DRYING OF TOMATO FRUITS USING SOLAR ENERGY. *Agricultural Engineering International: CIGR Journal*, 21(2), 204–215. <https://cigrjournal.org/index.php/Ejournal/article/view/5401>.

Murugavelh, S., Anand, B., Midhun Prasad, K., Nagarajan, R., & Azariah Pravin Kumar, S. (2019). Exergy analysis and kinetic study of tomato waste drying in a mixed mode solar tunnel dryer. <https://doi.org/10.1080/15567036.2019.1679289>.

Nwakuba, N. R., Chukwuezie, C. O., Asoegwu, S. N., Nwandikom, G. I., & Okereke, N. A. A. (2018). Energy Requirements and Effective Moisture Diffusivity of Tomato Slices in a Hybrid Convective Dryer. *ASABE 2018 Annual International Meeting*, 1-. <https://doi.org/10.13031/AIM.201800038>.

Patil, R. C., & Gawande, R. R. (2017). Mathematical modeling of solar drying systems. *Green Energy and Technology*, 0(9789811038327), 265–316. [https://doi.org/10.1007/978-981-10-3833-4\\_9/COVER/](https://doi.org/10.1007/978-981-10-3833-4_9/COVER/).

Sadin, R., Chegini, G., & Khodadadi, M. (2017). Drying characteristics and modeling of tomato thin layer drying in combined infrared-hot air dryer. *Agricultural Engineering International: CIGR Journal*, 19(1), 150–157. <https://cigrjournal.org/index.php/Ejournal/article/view/3780>.

Samimi-Akhijahani, H., & Arabhosseini, A. (2018). Accelerating drying process of tomato slices in a PV-assisted solar dryer using a sun tracking system. *Renewable Energy*, 123, 428–438. <https://doi.org/10.1016/j.renene.2018.02.056>.

Shi, J., Pan, Z., McHugh, T. H., Wood, D., Hirschberg, E., & Olson, D. (2008). Drying and quality characteristics of fresh and sugar-infused blueberries dried with infrared radiation heating. *LWT - Food Science and Technology*, 41(10), 1962–1972. <https://doi.org/10.1016/J.LWT.2008.01.003>.

Sonmete, M. H., Mengeş, H. O., Ertekin, C., & Özcan, M. M. (2016). Mathematical modeling of thin layer drying of carrot slices by forced convection. *Journal of Food Measurement and Characterization* 2016 11:2, 11(2), 629–638. <https://doi.org/10.1007/S11694-016-9432-Y>.

Tirawanichakul, S., Tirawanichakul, Y., & Sniso, E. (2008). Paddy dehydration by adsorption: Thermo-physical properties and diffusion model of agriculture residues. *Biosystems Engineering*, 99(2), 249–255. <https://doi.org/10.1016/J.BIOSYSTEMSENG.2007.11.001>.

Valta, K., Sotiropoulos, A., Malamis, D., Kosanovic, T., Antonopoulou, G., Alexandropoulou, M., Jonuzay, S., Lyberatos, G., & Loizidou, M. (2019). Assessment of the effect of drying temperature and composition on the

biochemical methane potential of in-house dried household food waste. *Waste Management and Research*, 37(5), 461–468. <https://doi.org/10.1177/0734242X18823943>.

Vega-Gálvez, A., Lemus-Mondaca, R., Bilbao-SÁinz, C., Yagnam, F., & Rojas, A. (2008). MASS TRANSFER KINETICS DURING CONVECTIVE DRYING OF RED PEPPER VAR. HUNGARIAN (CAPSICUM ANNUUM L.): MATHEMATICAL MODELING AND EVALUATION OF KINETIC PARAMETERS. *Journal of Food Process Engineering*, 31(1), 120–137. <https://doi.org/10.1111/J.1745-4530.2007.00145.X>.

Wang, D. C., Fon, D. S., Fang, W., & Sokhansanj, S. (2007). Development of a Visual Method to Test the Range of Applicability of Thin Layer Drying Equations Using MATLAB Tools. *Drying Technology*, 22(8), 1921–1948. <https://doi.org/10.1081/DRT-200032878>.

# **5 CONTROLLER DESIGN FOR A GREENHOUSE-TYPE SOLAR DRYER BASED ON PRODUCT TEMPERATURE MODEL**

FOR SUBMISSION TO APPLIED THERMAL ENGINEERING JOURNAL

Valencia-Islas J. O., Kacira M., Lopez-Cruz I.L.\*, Giacomelli G., Ruiz-Garcia A.,  
Li P.

## **5.1 ABSTRACT**

Greenhouse-type solar dryers provide dehydration of fruits with high quality and without contamination from external conditions. The renewable energy use has not only promoted their use in drying but also technology development and research. However, problems still exist regarding optimization, control strategy, and the challenge of maintaining a desirable inner environment regardless of external disturbances. The control systems currently known are based on the local climate inside the greenhouse and assume that the product will have the same temperature as the air driving the drying process. However, the large amount of water content of the product (tomato) causes a significant difference between the air and the product temperature. Therefore, this study developed a model predictive controller with a focus on product temperature. The model was designed using system identification methods and with a model structure based on air temperature, relative humidity, floor temperature, cover temperature, and product temperature as state variables. Solar radiation, external air temperature, and relative humidity were model inputs. The accuracy of the model to predict

product temperature was greater than 87%. The simulated product temperature was used to define the setpoint for the control strategy. Two control strategies were considered; 1) both greenhouse wall exhaust fans were activated with a single control signal, and 2) both fans were activated independently with two stages of ventilation. Both control strategies maintained the product temperature below 50°C during the drying process which is desired to preserve lycopene and vitamins in the tomato. The second strategy required 22% less energy. This strategy successfully achieved an effective control to provide the desired product temperature.

**Keywords:** Greenhouses, MPC, Mathematical modeling, Systems Identification, Solar Dryers.

## 5.2 INTRODUCTION

Greenhouse-type solar dryers have become popular due to the use of renewable energy, controllability, size, reduction in product contamination, and the possibility of use in remote locations (Patil & Gawande, 2016; Tiwari, 2016). However, there is a great variety of designs with unique environmental controls for greenhouse conditions (Janjai et al., 2009; Kaewkiew et al., 2012). The best-dried product quality in less time can be achieved with a high level of ventilation and when the greenhouse's internal conditions are homogenous (Choab et al., 2019; Tham et al., 2017; Verma, n.d.).

The majority of control strategies for greenhouse-type solar dryers have been ON/OFF control with air temperature and relative humidity setpoints (Hamdi et al., 2018; Singh et al., 2022; Vengsungnle et al., 2020) and Pulse Width Modulation control with air temperature setpoint (Aprillia et al., 2022) controlling the exhaust fans speed. Even though both control strategies are less complex to implement in greenhouses, they lack optimal control abilities and energy savings when compared to Model Predictive Control (Achour et al., 2020).

The Model Predictive Control approach (MPC) is a type of control that uses a mathematical model of the system to predict, in a specified time horizon, the variables of interest. Then, based on the behavior a set of control strategies are used to minimize a cost function subject to constraints. Because the optimization and prediction are calculated in every step, the MPC could lead to the unstable behavior of the system (Camacho & Bordons, 2007a; Ouammi, 2021).

Linear MPCs have parameters that must be tuned for the controller to work properly. These parameters are the weights  $Q$  and  $R$ , which serve to penalize the objective function based on the variables considered in the controller. The next parameter is the sampling period, the time interval in which the control actions remain constant. They depend on the time constant of the controlled system. The prediction horizon is the number of steps in time that, when multiplied by the sampling period, gives the length of the window in which the MPC calculates the model's predictions. Finally, the control horizon represents the number of steps in time for which the MPC will calculate the optimal control actions that minimize the objective function (Camacho & Bordons, 2007b; Drgoňa et al., 2020).

Unlike the ON/OFF and Proportional Integral Derivative (PID) Controllers, the MPC can overcome important disturbances in solar drying systems due to unexpected outdoor weather, and then optimize the response based on the specific greenhouse physical and technological constraints (Chen & You, 2020; Petersen et al., 2017). In addition, the possibility to add variables of economic impact in the cost function makes MPC a great option for a controller of greenhouse-type solar dryers (Ciglera et al., 2013). There is a lack of research on applying MPC for greenhouse solar dryers. The objective of this study was to design a model predictive controller for a greenhouse-type solar dryer based on product temperature rather than greenhouse air temperature, and then design the controller with the existing equipment in the greenhouse for the drying process and evaluate the energy usage.

## **5.3 MATERIALS AND METHODS**

### **5.3.1 Greenhouse-type Solar Dryer**

The greenhouse used in this study has a 6 mm thick polycarbonate cover with a galvanized steel structure. It has a concrete floor with a thickness of 150 mm; two exhaust fans are located on the south wall and serve to extract and renew the air inside the greenhouse, the ventilation rate of each fan is  $2.6 \text{ m}^3 \text{ s}^{-1}$ . The greenhouse has four inlets of  $0.65 \text{ m}^2$  each, that are always open and located in the north wall at 0.85 and 1.4 m in height above the floor (Figure 5-1). The greenhouse is located at the Universidad Autónoma Chapingo ( $19^\circ 29' \text{ N}$ ,  $98^\circ 53' \text{ W}$ ) in Texcoco, Mexico with an altitude of 2250 m above sea level.

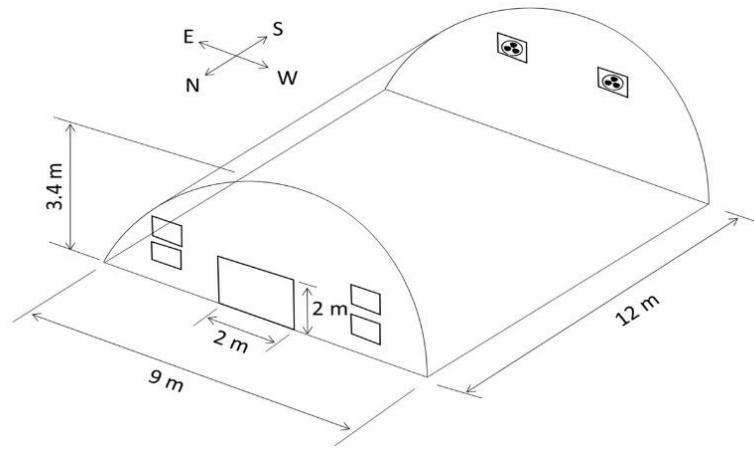


**Figure 5-1.** Greenhouse solar dryer dimensions and orientation.

### 5.3.2 Experiment

The experiments of this study were completed from May 2<sup>nd</sup> to May 10<sup>th</sup>, 2021. The data was then split into Dataset1 for developing the model from May 2<sup>nd</sup> to May 6<sup>th</sup> and Dataset2 to develop the controller from May 6<sup>th</sup> to May 10<sup>th</sup>. The dried product was a sliced saladette tomato of 5 mm thickness. Since the control application considered the product temperature, the moisture content of the product was not considered, and thus, every day new tomato slices were introduced regardless of the moisture content of the previous tomato slices. To measure the tomato slice temperatures, thermocouples type T (HOBOWare, Bourne, USA,  $\pm 0.6$  °C accuracy, 0.02 °C resolution, and Range of -260° to 400 °C) were inserted into the product and the mean temperature was considered as the true temperature of the whole tomato. The temperature and relative humidity outside the greenhouse were measured using an HMP60 digital sensor (Vaisala,

Vantaa, Finland,  $\pm 3\%$ ,  $\pm 0.6$  °C, accuracy) and solar radiation with a Hukseflux pyranometer (LP02-L, Campbell Scientific, Utah, USA,  $15 \mu\text{V} / \text{W} / \text{m}^2$ , accuracy). For the indoor variables, a CS215L (Campbell Scientific, Utah, USA,  $\pm 2\%$ ,  $\pm 0.4$ °C accuracies) and a CMP3 pyranometer (Kipp & Zonen 102885, Sterling, USA,  $5 \mu\text{V} / \text{W} / \text{m}^2$  accuracy) were used for temperature, relative humidity, and solar radiation, respectively. The data were recorded each minute for indoor conditions and five minutes for outdoor conditions. During the experiment, an ON-OFF control was used to reduce the temperature inside the greenhouse based on the product temperature. Whenever the slice temperature exceeds 50°C both greenhouse exhaust fans were turned ON and OFF when the product temperature was below 45 °C.

### 5.3.3 Greenhouse-type Solar Prediction Model

A mathematical model for air and product temperature inside the greenhouse was developed. The state-space representation was selected as it contains information about past behavior inside the greenhouse. The model considers as control input the ventilation rate; as inputs (disturbances) outdoor temperature, relative humidity, and solar radiation; as outputs, air temperature, relative humidity, cover temperature, product temperature, and floor temperature.

The linear subspace identification method NS4ID algorithm was used to identify the plant in a discrete-time state-space model. The linear discrete model is described by (Eq. 5-1) without noise.

$$\begin{bmatrix} \hat{x}(t+1) \\ y(t) \end{bmatrix} = \begin{bmatrix} A & B \\ C & D \end{bmatrix} \begin{bmatrix} x(t) \\ u(t) \end{bmatrix} \quad (\text{Eq. 5-1})$$

where  $\hat{x}(t + 1)$  is the one-step ahead state prediction,  $x(t)$  is the state at time  $t$ ,  $y(t)$  is the output vector,  $A, B, C$  and  $D$  are the state space matrices representation and  $u(t)$  is the input vector.

The best model was selected among several hundred models by selecting the one with the minimum Final prediction error (FPE) and the mean square error (MSE) statistics (Hamidane et al., 2021).

From Dataset1, 60% were used to identify the model and the rest for model evaluation. The statistics Root Mean Squared Error (RMSE), Mean Absolute Error (MAE), and model Efficiency (EF) were used to measure the agreement between the model and the measurements of the real system. A detailed explanation of the statistics can be found in (Martínez-Ruiz et al., 2021).

### 5.3.4 MPC Problem Statement

Given the mathematical model of the greenhouse dryer, the controller relies only on the product temperature, so the other states inside the greenhouse are not considered and serve only as estimations of the greenhouse conditions. The constraints of the controller are given by (Eq. 5-2) and (Eq. 5-3) regarding the ventilation rate and the number of exhaust fans and the product temperature

$$q_{min}n \leq q \leq q_{max}n \quad \text{with } n = \{0,1,2\}, q_{min} = 0, q_{max} = 2.6 \quad (\text{Eq. 5-2})$$

$$T_{min} \leq T \leq T_{max}, \quad \text{with } T_{min} = T_{amb}, T_{max} = 70 \quad (\text{Eq. 5-3})$$

The maximum ventilation rate is considered as the maximum physical constraint given by the exhaust fans, then, the controller considers a maximum ventilation rate as 5.2 given by the two fans and the maximum ventilation rate of each fan.

For the constraint over the product temperature, it is considered to vary within the boundaries of  $T_{amb}$  and up to 70 °C, the idea is to observe the behavior of the controller without a rigid constraint, changing the boundaries with a small percentage around the setpoint will over-constrain the optimization. The optimization is defined as (Eq. 5-4) with cost function (Eq. 5-5) and then becomes a linear quadratic optimization problem.

$$u_k^* = \operatorname{argmin} J(x_k, u_k) \quad (\text{Eq. 5-4})$$

$$\operatorname{minimize} J = \sum_{k=1}^N x_k' Q x_k + u_k' R u_k \quad (\text{Eq. 5-5})$$

The MPC and model were programmed into the MATLAB Simulink environment (Figure 5-2) and the flow of information is shown in Figure (5-3) in a simplified version.

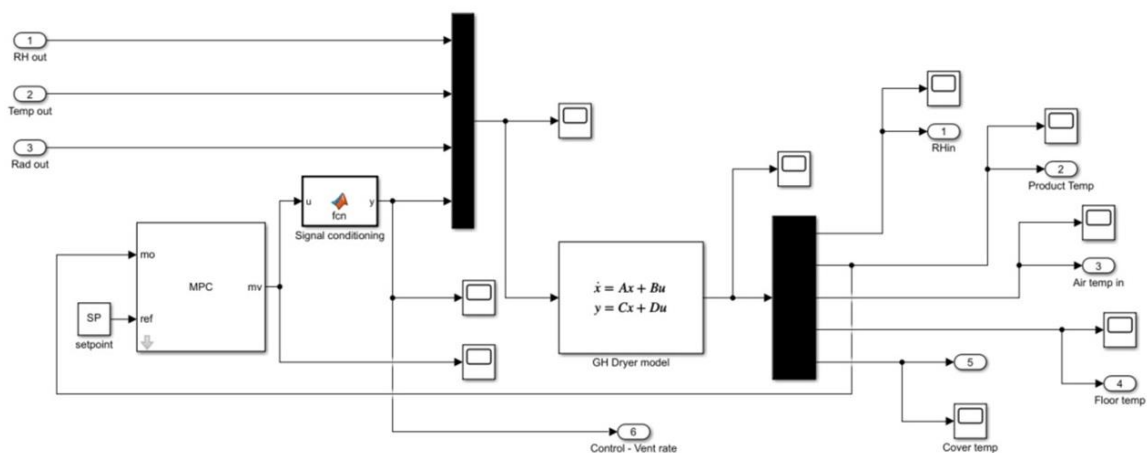


**Figure 5-2.** Matlab Simulink model of the greenhouse-type solar dryer with the MPC control.

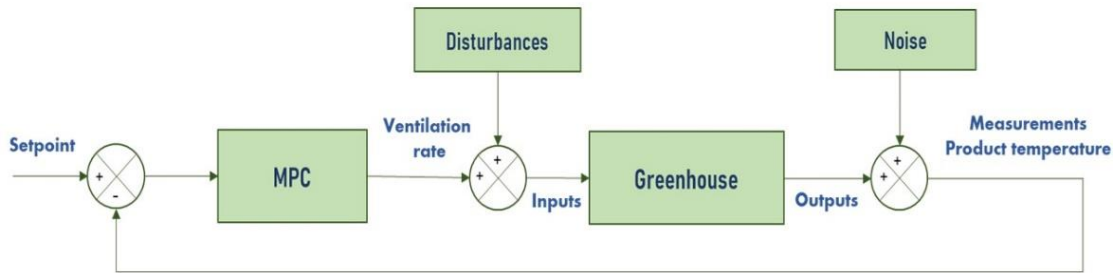


**Figure 5-3.** Block diagram flow for the greenhouse-type solar dryer system.

### 5.3.5 Control Strategies

Two different scenarios were tested for the controller design. The first is to place the two fans activated at the same time, i.e., the controller will have the values of 0 or  $5.2 \text{ m}^3 \text{ s}^{-1}$ , called MPC1. The second strategy is using the fans independently, then the possibilities are 0, 2.6 or  $5.2 \text{ m}^3 \text{ s}^{-1}$  called MPC2. Both scenarios lead to different optimal strategies as both have different physical constraints. Although the actuators are ON/Off devices, it is important to notice that using the ventilation rate as a step variable with fixed values could be used to design a model predictive controller.

The MPC used is tuned with different parameters and the best one is selected. The Sample time was found to be two, the prediction horizon is considered five and the control horizon is two. As the model was developed on a time scale of minutes, both, the control, and prediction horizons were considered in minutes. Values greater in all parameters either made the system become unstable or did not make any improvement to the controller.

## 5.4 RESULTS

### 5.4.1 Model simulations and Evaluation

The data used for model identification contained the outdoor relative humidity, temperature, and solar radiation (Figure 5-4) and the indoor air temperature, relative humidity, product, floor, and cover temperatures (Figure 5-5). The identified model is represented by the A, B, C, and D matrices (Eq. 5-6) with 5 outputs and 4 inputs (1 control signal and 3 disturbances).

$$A = \begin{bmatrix} -0.1789 & 0.0367 & -0.2752 & 0.1820 & 0.0256 \\ -0.0073 & 0.0098 & 0.0217 & 0.1075 & -0.1395 \\ -0.0245 & -0.0752 & -0.1661 & -0.0129 & 0.0856 \\ -0.0067 & -0.0096 & -0.0102 & 0.0496 & -0.1157 \\ 0.0465 & 0.0569 & 0.1726 & 0.0802 & -0.2126 \end{bmatrix}$$

$$B = \begin{bmatrix} -0.1774 & -1.2907 & -0.0088 & 2.1670 \\ 0.0159 & -0.1982 & 0.0000 & -0.5576 \\ -0.0174 & -0.0351 & 0.0056 & 0.8999 \\ 0.0268 & -0.0795 & 0.0000 & -0.3815 \\ 0.0448 & 0.0845 & -0.0023 & 1.5500 \end{bmatrix}$$

$$C = \begin{bmatrix} 0.4305 & 0.6035 & 0.4614 & 0.2228 & -0.0689 \\ -0.2207 & 0.1406 & -0.1914 & -0.1380 & -0.2749 \\ -0.4123 & -0.1619 & -0.3584 & 0.0045 & 0.5996 \\ -0.2335 & 0.1085 & -0.1625 & 0.0548 & -0.0871 \\ -0.2368 & 0.0913 & 0.0788 & 0.3050 & -0.1545 \end{bmatrix}$$

(Eq. 5-6)

$$D = [0]$$

The model overpredicted sometimes the floor and product temperature (Figures 5-6 and 5-7) but overall, the model predictions were good. The RMSE and MAE are less than 3 for product temperature and air temperature as both variables are important for the drying process. Model efficiency is greater than

0.87 for all the variables so the model is considered to be a good representation of the greenhouse (Figure 5-8).

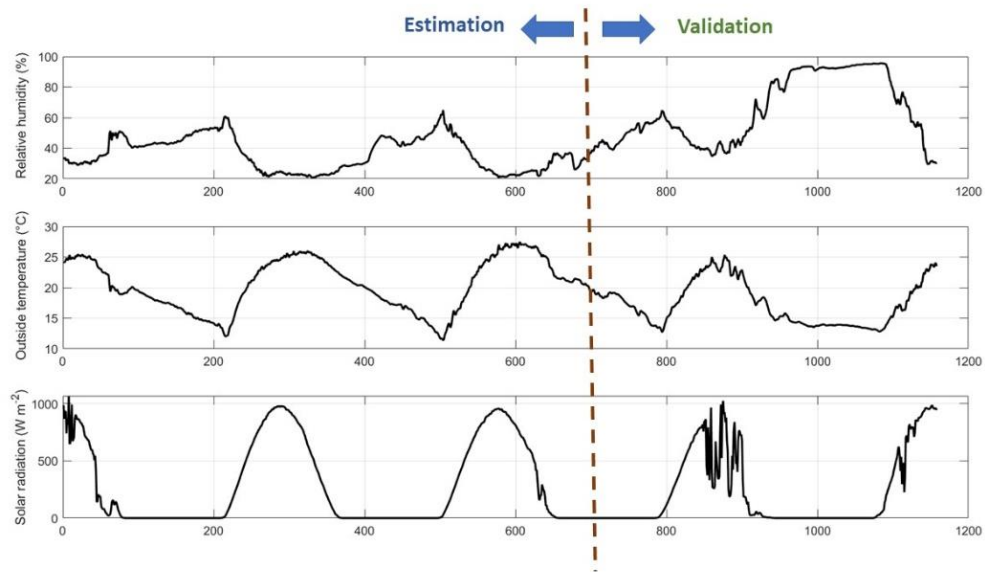


**Figure 5-4.** Outdoor data is used for model identification and model validation.

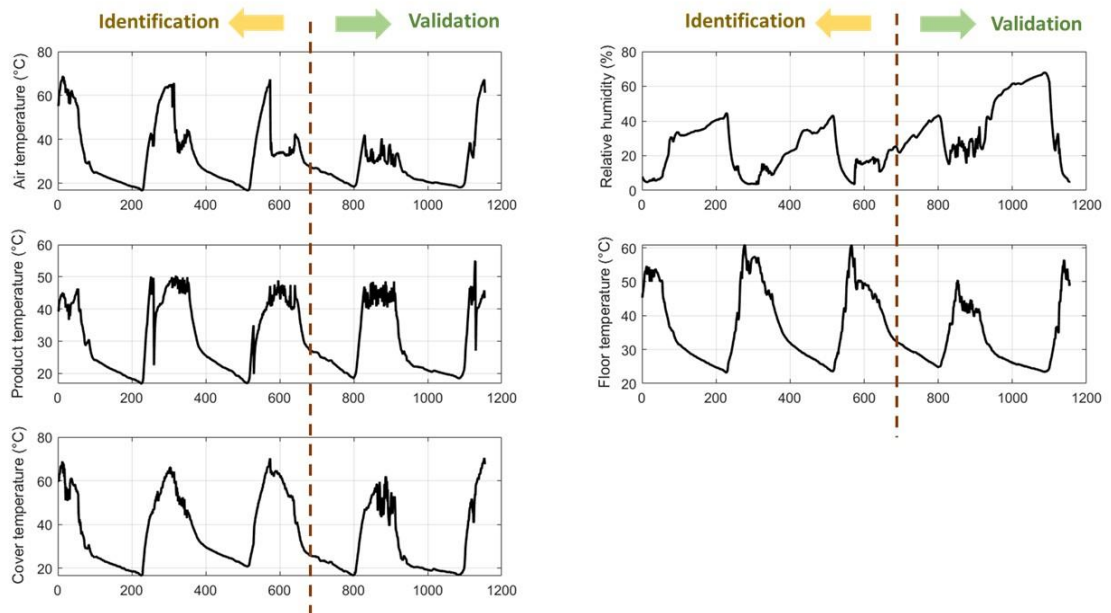


**Figure 5-5.** Indoor data of the greenhouse for identification and validation.

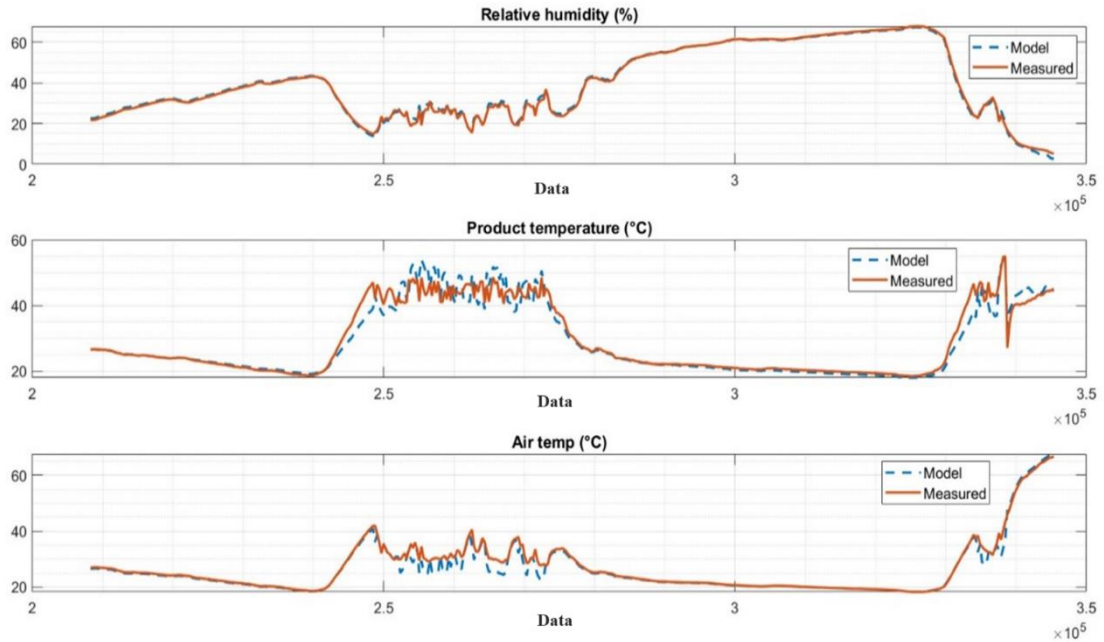


**Figure 5-6.** Relative humidity, product and air temperature inside the greenhouse, measurements, and model simulations.

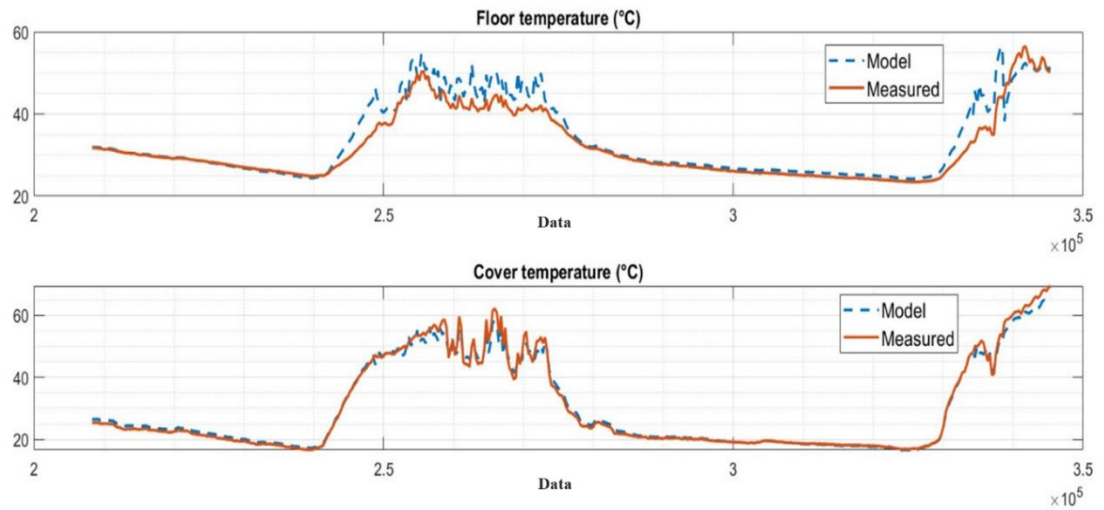


**Figure 5-7.** Floor and cover temperature inside the greenhouse, model, and measurements.

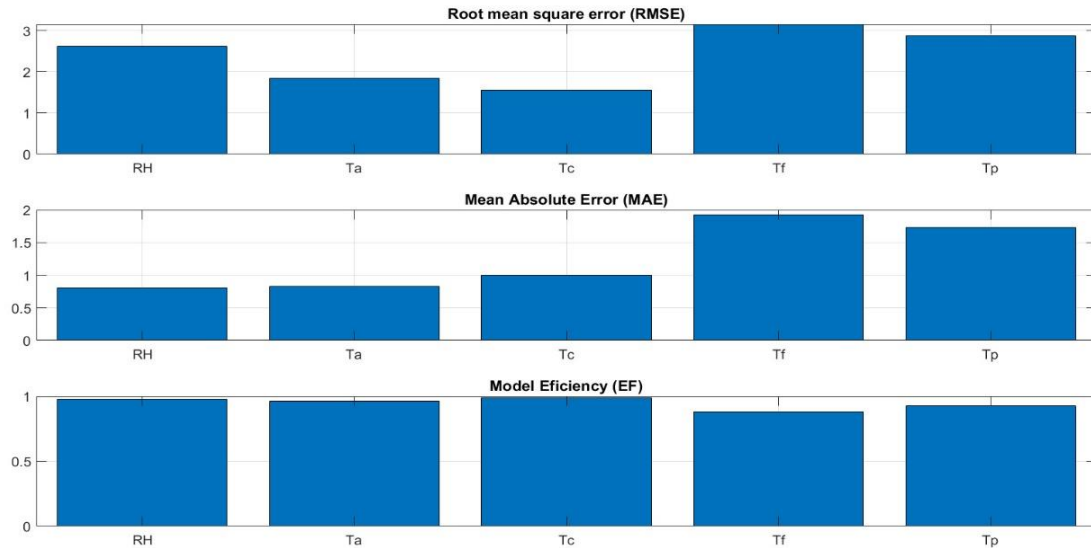


**Figure 5-8.** Model statistics between the measurements and the model simulations.

#### 5.4.2 MPC Simulations

The state space model was used for the Model Predictive Controller. The difference between the setpoint and measurement of the product temperature was used as input in the MPC. The only output of the MPC was the ventilation rate ranging from 0 to  $5.2 \text{ m}^3 \text{ s}^{-1}$ . The ventilation rate and the disturbances (relative humidity, air temperature, and solar radiation outside the greenhouse) were the inputs to the mathematical model. To simulate the real greenhouse operation, some noise was added to the model outputs as random variables, and a variation of 20% of temperatures and relative humidity was used to simulate the noise and was randomly summed or subtracted. The product temperature simulated as a measurement was subtracted from the setpoint and introduced again to the MPC.

The MPC1 controller was considered as the one with the strategy of two fans working separately. The MPC2 was the controller with both fans activated simultaneously. Both controllers were enough to keep the product temperature below 50°C (Figures 5-9 and 5-11). The difference in the strategies as well as the difference in the temperature due to the controller is small. The main difference was regarding the time and possible amount of energy used for controlling. There was a reduction in the air temperature, floor temperature, and increased relative humidity due to the MPC action (Figure 5-10).

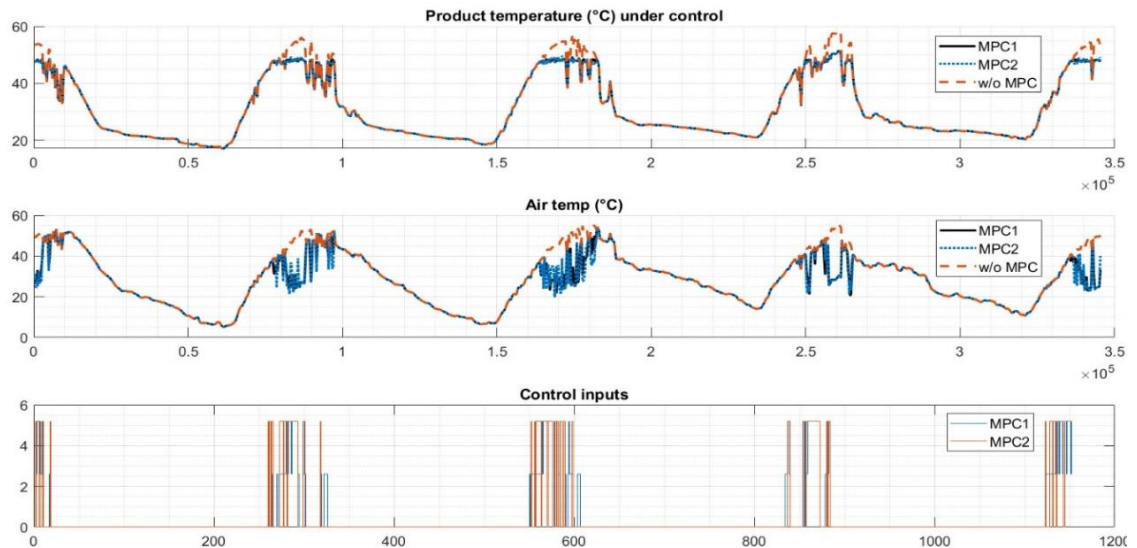


**Figure 5-9.** Controllers' strategies with the product and air temperature.

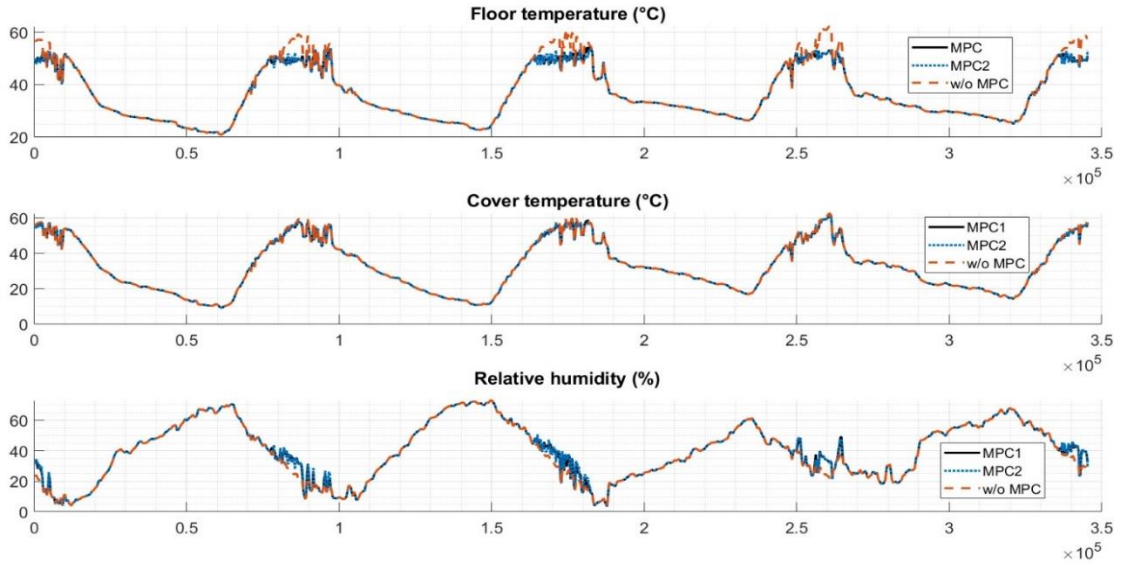


**Figure 5-10.** Floor and cover temperature and relative humidity with the controllers.

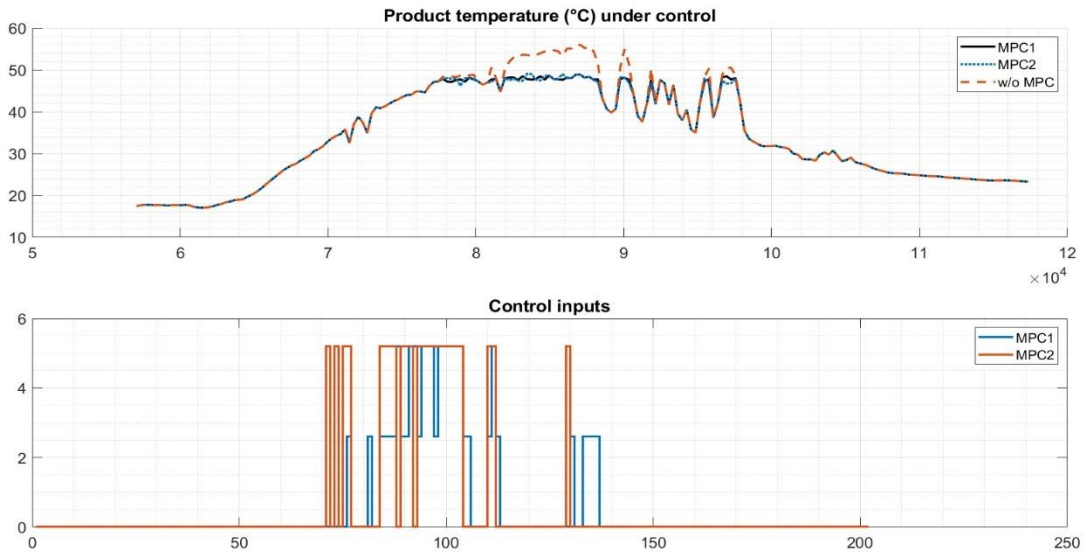


**Figure 5-11.** Product temperature with the two MPC strategies.

## 5.5 DISCUSSION

The two control strategies (both fans activated at the same time, MPC1, and using the fans independently, MPC2) differ in the constraints over the ventilation rate.

The signals are treated as pulse signals which, helps using ON/OFF actuators to optimize the controller. Usually, MPC is designed for analog actuators as they offer a non-stiff optimization to achieve a better optimal trajectory. The MPC designed in this study was found to be a good controller for maintaining the desired product temperature with ON/OFF exhaust fan controls.

The exhaust fans were activated before the setpoint is reached, as expected from a model predictive controller, these optimal strategies led to a smooth control instead of the dead bands showed by an on/off control. The ON/OFF control triggers the actuators when the setpoint is reached and thus, the tomato slice can be close to the undesirable temperature. With the MPC1 and MPC2 controllers, the set point is never reached, thus the product is always kept below 50 °C which is desirable to ensure the vitamins and lycopene are conserved during drying. The change in the restrictions on the ventilation rate changes the optimal strategies as shown in Figure (5-11). The MPC2 activates the fans before the MPC1.

It is noticed that the two-stage control is a better strategy and can reduce the energy needed for controlling the product temperature (Figure 5-11). To our knowledge, this is the first time the product temperature is used to control a dryer instead of the air temperature. According to the experimental data, the air temperature could be greater than 50°C before the product temperature reaches 50°C.

The future study should implement MPC in a real greenhouse setting to determine the system's behavior under external noise and inputs. The RMSE of the model is 2°C and 3°C for air and product temperature, respectively. This

means that the set point should be carefully considered as the uncertainty of the model can affect the behavior of the MPC. If the set point is 50°C, then it is also expected that at some points product temperature greater than 50°C can be observed due to the model predictions.

## **5.6 CONCLUSIONS**

The Model Predictive Controller designed in this study simulated the behavior of the system within the set points considered. The main difference between both control strategies considered was the total operation time the fans were activated to achieve the product temperature.

Model Predictive Control, based on product temperature, can improve control strategy with energy savings and enhanced dried product quality. System Identification can serve as a starting point for complex systems such as greenhouse-type solar dryers. The setpoint should be carefully considered as the uncertainty of the model can affect the behavior of the MPC. A model with better adjustment could be used to improve the Model Predictive Controller as it is essential for the optimization process. Perhaps a Kalman Filter could be a better option if this controller is implemented in a real greenhouse with the data introduced to the Kalman filter.

With analog actuators, the controller should be less restricted and thus, offering a better tool for controlled environments. The product temperature was successfully used to control a greenhouse-type solar dryer rather than the air

temperature. Future studies can also consider combining multiple inputs and multiple outputs.

## 5.7 ACKNOWLEDGMENTS

This work was supported by the Mexican National Council of Science and Technology (CONACyT) [grant number: CB-2015-254055].

## 5.8 REFERENCES

Achour, Y., Ouammi, A., Zejli, D., & Sayadi, S. (2020). Supervisory Model Predictive Control for Optimal Operation of a Greenhouse Indoor Environment Coping with Food-Energy-Water Nexus. *IEEE Access*, 8, 211562–211575. <https://doi.org/10.1109/ACCESS.2020.3037222>.

Aprillia, B. S., Pramudita, B. A., & Megantoro, P. (2022). Temperature control system on greenhouse effect gablek dryer. *JURNAL INFOTEL*, 14(1), 50–56. <https://doi.org/10.20895/INFOTEL.V14I1.736>.

Camacho, E. F., & Bordons, C. (2007a). Introduction to model predictive control. *Advanced Textbooks in Control and Signal Processing*, 9781852336943, 1–11. [https://doi.org/10.1007/978-0-85729-398-5\\_1](https://doi.org/10.1007/978-0-85729-398-5_1).

Camacho, E. F., & Bordons, C. (2007b). Model predictive controllers. *Advanced Textbooks in Control and Signal Processing*, 9781852336943, 13–30. [https://doi.org/10.1007/978-0-85729-398-5\\_2](https://doi.org/10.1007/978-0-85729-398-5_2).

Chen, W. H., & You, F. (2020). Efficient Greenhouse Temperature Control with Data-Driven Robust Model Predictive. *Proceedings of the American Control*

Conference, 2020-July, 1986–1991.  
<https://doi.org/10.23919/ACC45564.2020.9147701>.

Choab, N., Allouhi, A., el Maakoul, A., Kousksou, T., Saadeddine, S., & Jamil, A. (2019). Review on greenhouse microclimate and application: Design parameters, thermal modeling and simulation, climate controlling technologies. *Solar Energy*, 191, 109–137. <https://doi.org/10.1016/J.SOLENER.2019.08.042>.

Ciglera, Í., Gyalistrasb, D., Tietd, V.-N., Luká, & Ferkla. (2013). Beyond theory : the challenge of implementing Model Predictive Control in buildings Ji ř.

Drgoňa, J., Arroyo, J., Cupeiro Figueroa, I., Blum, D., Arendt, K., Kim, D., Ollé, E. P., Oravec, J., Wetter, M., Vrabie, D. L., & Helsen, L. (2020). All you need to know about model predictive control for buildings. *Annual Reviews in Control*, 50, 190–232. <https://doi.org/10.1016/J.ARCONTROL.2020.09.001>.

Hamdi, I., Kooli, S., Elkhadraoui, A., Azaizia, Z., Abdelhamid, F., & Guizani, A. (2018). Experimental study and numerical modeling for drying grapes under solar greenhouse. *Renewable Energy*, 127, 936–946. <https://doi.org/10.1016/J.RENENE.2018.05.027>.

Hamidane, H., el Faiz, S., Lachhab, A., Guerbaoui, M., & Ed-Dahhak, A. (2021). Constrained Discrete Model Predictive Control of a Greenhouse Relative Humidity. *E3S Web of Conferences*, 229, 01001. <https://doi.org/10.1051/E3SCONF/202122901001>.

Janjai, S., Lamlert, N., Intawee, P., Mahayothee, B., Bala, B. K., Nagle, M., & Müller, J. (2009). Experimental and simulated performance of a PV-ventilated solar greenhouse dryer for drying of peeled longan and banana. *Solar Energy*, 83(9), 1550–1565. <https://doi.org/10.1016/J.SOLENER.2009.05.003>.

Kaewkiew, J., Nabnean, S., & Janjai, S. (2012). Experimental investigation of the performance of a large-scale greenhouse type solar dryer for drying chilli in Thailand. *Procedia Engineering*, 32, 433–439. <https://doi.org/10.1016/J.PROENG.2012.01.1290>.

Martínez-Ruiz, A., Ruiz-García, A., Prado-Hernández, J. V., López-Cruz, I. L., Valencia-Islas, J. O., & Pineda-Pineda, J. (2021). Global sensitivity analysis and calibration by differential evolution algorithm of HORTSYST crop model for fertigation management. *Water* (Switzerland), 13(5). <https://doi.org/10.3390/W13050610>.

Ouammi, A. (2021). Model predictive control for optimal energy management of connected cluster of microgrids with net zero energy multi-greenhouses. *Energy*, 234, 121274. <https://doi.org/10.1016/J.ENERGY.2021.121274>.

Patil, R., & Gawande, R. (2016). A review on solar tunnel greenhouse drying system. *Renewable and Sustainable Energy Reviews*, 56, 196–214. <https://doi.org/10.1016/J.RSER.2015.11.057>.

Petersen, L. N., Poulsen, N. K., Niemann, H. H., Utzen, C., & Jørgensen, J. B. (2017). Comparison of three control strategies for optimization of spray dryer operation. *Journal of Process Control*, 57, 1–14. <https://doi.org/10.1016/J.JPROCONT.2017.05.008>.

Singh, S., Gill, R. S., Hans, V. S., & Mittal, T. C. (2022). Experimental performance and economic viability of evacuated tube solar collector assisted greenhouse dryer for sustainable development. *Energy*, 241, 122794. <https://doi.org/10.1016/J.ENERGY.2021.122794>.

Tham, T. C., Ng, M. X., Gan, S. H., Chua, L. S., Aziz, R., Chuah, L. A., Hii, C. L., Ong, S. P., Chin, N. L., & Law, C. L. (2017). Effect of ambient conditions on drying

of herbs in solar greenhouse dryer with integrated heat pump. *Drying Technology*, 35(14), 1721–1732. <https://doi.org/10.1080/07373937.2016.1271984>.

Tiwari, A. (2016). A Review on Solar Drying of Agricultural Produce. *J Food Process Technol*, 7(9), 623. <https://doi.org/10.4172/2157-7110.1000623>.

Vengsungle, P., Jongpluempiti, J., Srichat, A., Wiriyasart, S., & Naphon, P. (2020). Thermal performance of the photovoltaic–ventilated mixed mode greenhouse solar dryer with automatic closed loop control for Ganoderma drying. *Case Studies in Thermal Engineering*, 21, 100659. <https://doi.org/10.1016/J.CSITE.2020.100659>.

Verma, P. (n.d.). A Review Paper on Solar Greenhouse Dryer.

## 6 ADVANCES IN MODELING WITH COMPUTATIONAL FLUID DYNAMICS OF GREENHOUSE-TYPE SOLAR DRYERS

FOR SUBMISSION TO RENEWABLE ENERGY JOURNAL

Jose Olaf Valencia-Islas, Irineo Lorenzo Lopez-Cruz\*, Murat Kacira, Gene Giacomelli, Agustin Ruiz-Garcia, Peiwen Li

### 6.1 ABSTRACT

Solar drying systems are used to preserve perishable products, although the wide variability of solar dryers, the greenhouse type has significant benefits over other types of dryers and allows a high control of variables, opening the possibility to use them on an industrial scale. However, to enhance drying is necessary to use mathematical modeling techniques for understanding the phenomenon, optimize, improve designs, and propose new solutions that reduce time and gain drying quality. So far, the numerical approach of Computational Fluid Dynamics has been understudied, with advances in the sense of assessing the behavior of temperature, humidity, and wind speed within the dryer to determine if the conditions could produce good dehydration. Nevertheless, it is necessary to model the dryer with the product inside to have a complete understanding of what happens during the loss of water from the product. The objective of the present is to provide a review of the state of the art of modeling through CFD in solar greenhouse-type dryers focusing on how to build the model and which processes need to be considered to address the drying problem.

**Keywords:** CFD, greenhouses, drying, modeling, renewable energies.

## 6.2 INTRODUCTION

Food waste worldwide is a vital issue given the conditions of poverty in the world and the increase in population each year. Just in 2016, the total percentage of food loss in the world was around 15% considering the stages after harvest until distribution, most of the percentage is distributed in Central and South Asia (>20%), North America, and Europe (>15%), and Sub-Saharan Africa (>14%) (FAO, 2019). Most agricultural products exhibit a waste of less or equal to 25% of what is harvested (Figure 6-1), in Latin America, 127 million tons of food are wasted per year, which would be enough to feed 300 million people. The highest percentage of waste occurs in production and consumption with 28% of total production, followed by handling and storage with 22%. These losses generate a carbon footprint and water consumption, with cereals, meats, and vegetables being the main contributors to the percentage (FAO, 2015).

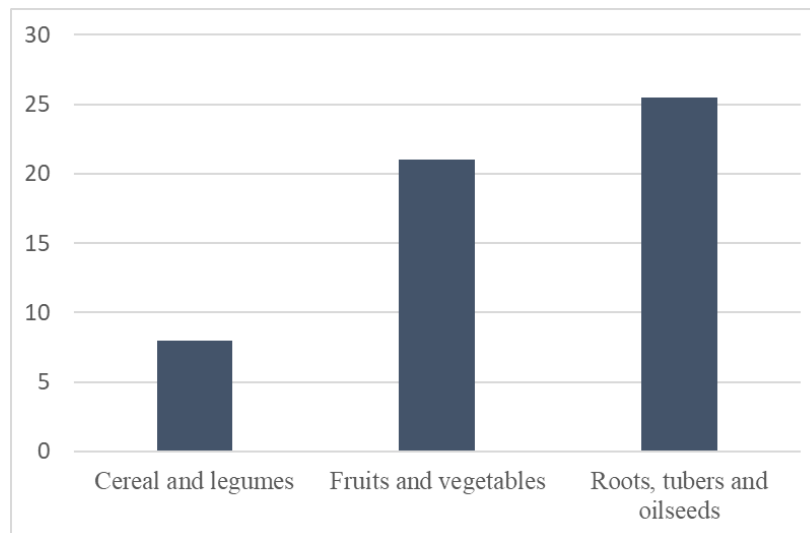


**Figure 6-1.** Most wasted agricultural products after harvest and during distribution stages (Adapted from FAO, 2019).

In Mexico, as an example, it is estimated that 925 thousand tons of tomatoes, 99 thousand tons of fish, and 41 thousand tons of pork are wasted, in total, 37% of what is produced in the country (Rivera, 2018). Among the most wasted foods in Mexico are those with short shelf life, these losses correspond to

an approximate cost for Mexico of 25,000 million US dollars (Forbes, 2018), another example is the US where the food lost and wasted can feed more than 120 million people on a 2000 kcal daily basis (Vittuari et al., 2020).

Two ways to contribute reduce food waste are to minimize production by increasing the shelf life of perishable products (Mahapatra & Tripathy, 2019; Patel & Patel, 2014; Tham et al., 2017) and improving transportation. The dehydration process allows the elimination of water contained in food, increasing the time it takes to decompose and reducing its volume for transportation. Solar drying is one of the oldest techniques, however, when it is performed in outdoor conditions, there are problems such as the inability to control factors that affect drying, for example, duration of drying, uncertainty in weather conditions, and the contamination of the products with dust, bacteria, and fungi spores (Kooli et al., 2007).

Several authors have carried out reviews on the types of solar dryers that exist today (El-Sebaei & Shalaby, 2012), some of them focus just on greenhouse-type dryers (Kumar & Shrivastava, 2017; Patil & Gawande, 2016; Verma, n.d.) and discuss the advantages and disadvantages of each design (Tiwari, 2016), as well as its possible applications. Nonetheless, no one considers if mathematical modeling is done for describing the drying process.

Greenhouse solar dryers have become of great interest not only because it is possible to use them for a double purpose, that is, as a greenhouse for crop production in seasons in which temperatures and humidity are controllable in the optimum range for plants and as a dryer when temperatures outside the greenhouse are too high and it is very expensive to control these variables making crop production economically unfeasible (Condorí et al., 2001; Jain, 2005; Sethi & Dubey, 2011); It also has the benefits of requiring less space compared to other dryers, being a technology suitable for small and medium growers since no electricity or other type of fuel is needed (Tiwari, 2016); maintains the quality of

dehydrated products; facilitates transport after having dehydrated the product (Leon et al., 2002); the cover and structure protects the product from external contamination such as dust or animals and is economically viable (Condorí & Saravia, 1998; Koyuncu, 2006).

Even though greenhouse solar dryers had been investigated and there is some research on their design, improvement, and operation (Prakash & Kumar, 2013), there is not a complete understanding of the behavior of the dehydration process under greenhouse conditions. Much of this lack of knowledge is the problem of modeling solar drying. The drying process is highly demanding in energy (Jamaledine & Ray, 2010; Tanwanichkul et al., 2013) and simultaneous processes of mass and heat transfer are involved. In addition, it is a multi-scale process, where macro-metric variables describing the behavior of the air inside and outside the dryer considerably affect the microscopic conditions within the product to be dehydrated (Defraeye, 2014). This multi-scale and unbalanced behavior that involves simultaneous transfer processes makes the process of mathematical modeling complex (Kemp, 2007; Kooli et al., 2007a).

Most of the models developed for solar greenhouse-type dryers are based on energy balances, using ordinary differential equations (ODEs) to model the humidity and temperature behavior of the air inside the dryer (Jain & Tiwari, 2004; Janjai et al., 2011, 2014; Kumar & Tiwari, 2006); however, when the product is involved, the so-called “thin layer” models are the most widely used. Thin layer models are based on regressions over data taken from the dehydration process during certain days and fitted with exponential or algebraic expressions that are based on Newton's law of cooling, diffusion, or exponential decay behavior approximations (Defraeye, 2014; Verma, n.d.). Both approaches with ODEs and Thin-layer modeling are developed considering there is no spatial variation in the inner conditions of the greenhouse; this assumption could be valid for small-volume greenhouses but for volumes greater than 10 m<sup>3</sup> this assumption is not

hold anymore as a great heat and mass exchange is occurring inside the dryer at the same time heat is collected from the sun radiation. Therefore, another type of modeling is needed to address the problem when spatial variations in the air inside the greenhouse are considered.

The objective of this review is to present an overview of the state-of-art in Computational Fluid Dynamics (CFD) applied to solar greenhouse-type dryers, the limitations, and future research that is needed to understand and optimize these systems.

### **6.3 PHYSICAL PHENOMENA THAT OCCUR IN GREENHOUSE-TYPE SOLAR DRYERS**

The solar drying problem is complex. Here we will first define a complex system and discuss how it is related to the Greenhouse-Type Solar Dryer System (called GTSDS hereafter).

According to Holland & Torres (2004), complex systems have 4 properties and 3 mechanisms. The properties are 1) Aggregation, which is the basic characteristic of complex systems and is a standard way of simplifying complexity. For the GTSDS, each material inside the dryer itself creates the drying system, the tables, the floor, the product, and the gases (could be just humid air but some fruits produce other gases) all of them interacting during the drying process; 2) Non-linearity, the drying behavior at different scales, as well as the multiphase interaction produces a highly non-linear behavior; 3) Flows, the movement of the fluids itself, the humidity inside the product that vaporizes to the dry air, the wind flow inside the dryer, and the heat by radiation of the solids inside the GTSDS; 4) Diversity, although this property contemplates a more historical diversity of the appearance of each element of the system, within the GTSDS there is a mixture of gases in different proportions, together with the diversity of materials that get into for dehydration.

The mechanisms of complex systems are 1) Labeling, which consists essentially to label the elements in the system that have the same likeness, although in the drying process each product behaves differently as it depends on the specific characteristics, they can be treated as the same if the dimensions are quite equal; 2) Internal models, "the structure from which we infer the environment also actively determines the behavior of its agent" (Holland & Torres, 2004), the air inside the greenhouse affects and interact with the product, this determines the drying of the product; 3) Building blocks, small blocks that can be combined to create a complex object or system. In the GTSDS there are products with different phases, dimensions, and scales that constitute a block when considered. Then, the GTSDS could be understood as a complex system to model with accuracy given the non-linear interactions and diversity of its elements.

Greenhouses are structures that trap short-wave solar radiation and store long-wave thermal radiation to create a favorable microclimate, mainly for growing crops (Morad et al., 2017); however, due to their climate control and heat retention capacity, their use as solar dryers have become widespread (Patil & Gawande, 2016; Verma, n.d.). The Greenhouse-Type Solar Dryer System consists of well-defined elements that act as an adiabatic system for heat and mass transfer simultaneously. Some of the elements that are generally found in GTSDS are 1) Support structure for the roof, depending on the dimensions it can be made of wood, galvanized steel, or aluminum; 2) Cover material, it can be plastic, glass, or polycarbonate sheets; 3) Floor, made of heat absorbing material, it can be concrete or some plastic, the cover is used as a barrier so dust, soil or plants do not contaminate the product; 4) Air inlets and outlets, allow the entry of new air with lower humidity and temperature compared to the air inside the dryer; 5) Exhaust fans to cause forced airflow, renew the air and homogenize the internal conditions of the dryer. The number of fans depends on the size of the dryer and the capacity of each fan. Some GTSDS have used Photovoltaic panels for powering the fans. 6) Trays or beds for placing the product, depending on the space available inside, several materials could be used, but in general, they are

fine meshing that allow the product to aerate mainly of stainless steel due to food safety requirements. 7) Drying chamber, is composed of the air inside the dryer that is heated as the sun rises. Depending on the volume of the dryer, this air mass could keep a temperature for some time even if the conditions outside change drastically, serving as a temperature buffer. Normally, the air has high temperature and low relative humidity which favor desorption. The product to be dried, here in after named just product, is placed inside the drying chamber over the trays or benches.

The GTSDS can be operated actively or passively referring to the function of the fans, the active ones are good for products with high water content, reducing drying time and enhancing product quality. In those with the passive operation, the humidity from the air is extracted due to the thermosyphon effect through the outlet window, it presents an advantage over the active operation due to the low costs of operation and maintenance (Kumar et al., 2017).

Within the GTSDS, physical processes occur that aid in the dehydration of products (Figure C-2). First, the roof receives solar radiation, some of this energy is absorbed by the covering material, and a certain percentage of the total radiation passes through the covering material while the rest is reflected into the atmosphere. The energy that is trapped inside the greenhouse is longwave radiation, some absorbed by the soil, some reflected from the soil and absorbed by the cover, and then the cover reflects most of this energy inside, and finally the rest is lost to sky by the cover. This process, also known as the greenhouse effect, raises the air temperature above 20 °C compared to the outside air temperature. In addition, the cover, due to its shape, losses heat on the surface that is in contact with the wind. The ground, for example, concrete, absorbs heat from the surrounding air, working as a thermal mass for storing heat during the day and as a heat supplier during periods of low radiation, more specifically, at night. The increase in air temperature generates heat transfer by convection with the product, benches, and floor, moving the hot air to the top and the cold air to the

ground. The tables, benches, or trays, absorb heat and release it by conduction to the mesh and by radiation to the product. The product begins to gain heat, energy makes the free water evaporate and the bounded water starts detaching from the molecules inside the product and moving to the surface of the product (Figure C-3). Usually, on both sides of the dryer's door, there are air inlets, covered with anti-aphid mesh, which allow the renewal of air from the outside depending on the type of ventilation, the exhaust fans, and the inlets should be open at the same time, otherwise, the inlets could be closed to increase the heat collected inside the greenhouse. This flow of air could be laminar or turbulent, depending on the type of flow, drying and moisture content will be affected or benefited.

All the energy used inside the dryer (lamps, as the dryer, usually is filled during no sunshine hours; exhaust fans, and sensors) needs to be considered. Some GTSDS uses photovoltaic systems to be off-grid and provide energy to all the dryer components.

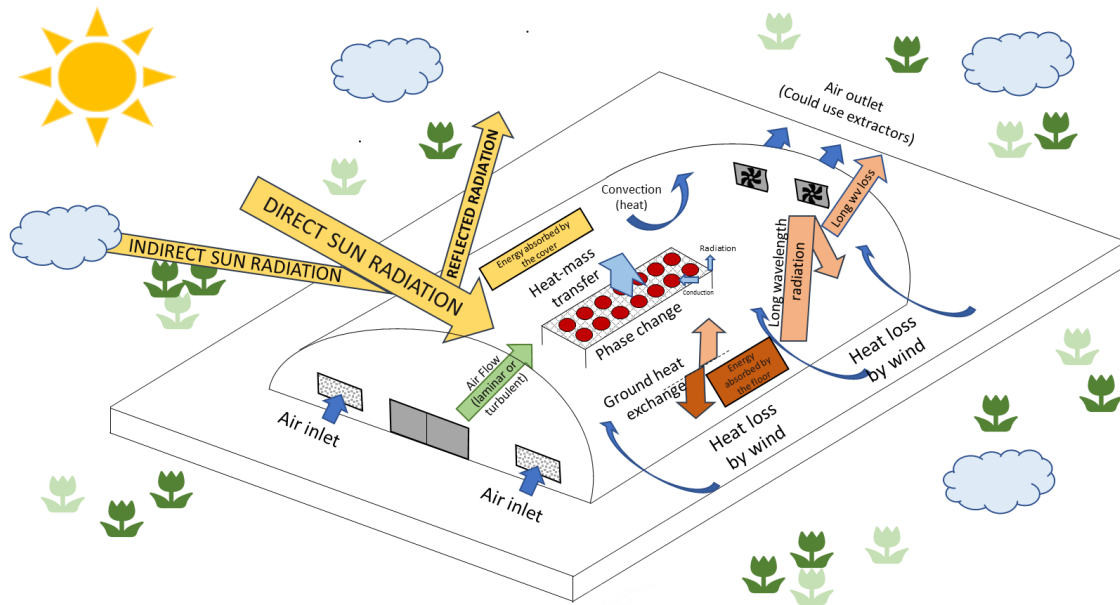


**Figure 6-2.** Physical processes involved in drying within a Greenhouse-Type Solar Dryer System (GTSDS).

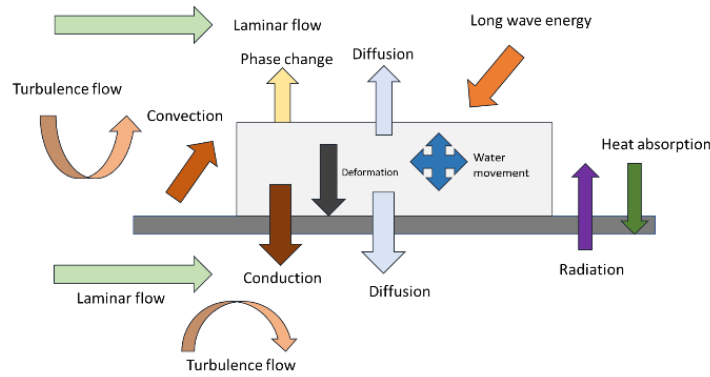


**Figure 6-3.** A closer look at the heat and mass transfer in a product under drying.

## 6.4 COMPUTATIONAL FLUID DYNAMICS

Computational Fluid Dynamics (CFD) is a branch of fluid mechanics that uses computer based numerical analysis (using Navier-Stokes equations) and algorithms to simulate, analyze and solve problems related to behavior of fluid flow, heat transfer, and associated chemical reactions using conservation of mass, conservation of momentum, and conservation of energy. The CFD approach replaces the governing equations with numbers and those approximations advance through time and space to find the final numerical description of the fluid field under study (Anderson, 2009). Some benefits of CFD simulations are the ability to simulate systems that are difficult to understand and that involve expensive or hazardous experiments; test improvements and new designs in real systems; understand the physics behind the fluid flow. As CFD involves a computational simulation we can define then as CFD code. Different software is used to make the CFD code packages used as numerical algorithms in a user interface which help with the construction of a specific CFD code. In general, CFD codes have three main stages i) Pre-processing, ii) Solver, and iii) post-processing all of them could be introduced in the same software or could need a specific computer program for each step.

### **6.4.1 Pre-Processing stage**

The pre-processing stage involves the statement of the problem, as a first step the CFD codes need a domain to solve the problem, in modern software, the domain is established by a geometric model of the real system. The following steps are the mesh of the geometric model, commonly known as grid generation as it sub-divides the volume into small sub-domains or cells; selection of the physics and chemics that drive the process, in other words, the mathematical models, physical and chemical laws and the assumptions needed to complete a mathematical definition of the problem; definition of the fluid properties; definition of the initial and boundary conditions in the domain.

### **6.4.2 Solver**

After defining the problem, the next step is to solve them in the domain, thus, the first step involves the integration of the governing equations of the fluid flow; next, the discretization step consists of converting the integral equations into a system of algebraic equations; finally, the solution is found from the algebraic equations through an iterative method. All modern CFD software contains each step in a well-presented manner and the user interface helps to do them without too much trouble. Some of the most used CFD codes are CFX, FLUENT, PHOENICS, STAR-CD, and Open FOAM.

### **6.4.3 Post-Processing**

The post-processing steps have been improved in modern software, and the availability of the computational capacity and new processors improve the tools to analyze and view the solutions of the governing equations in each cell at the system's domain. The main steps include the mesh and geometry display; plots

of the vector's fields; Contour, 2D, 3D, and surface plots to visualize the data matrices, and manipulation tools to scale, rotate, rotate, and display the results.

## 6.5 HOW TO BUILD A CFD MODEL FOR DRYING

The conservation equation has the general form (Versteeg & Malalasekera, 1996):

$$\frac{\partial \varphi}{\partial t} + \vec{\nabla} \cdot \varphi \vec{v} = \vec{\nabla} \cdot (\Gamma_{\varphi} \vec{\nabla} \varphi) + S_{\varphi} \quad (\text{Eq. 6-1})$$

where,  $\rho$  is the fluid density,  $\vec{v}$  is the vectorial velocity,  $\Gamma_{\varphi}$  is the diffusion coefficient, and  $S_{\varphi}$  is the source term. The symbol  $\varphi$  represents the concentration of the property under study.

In extended form, the conservation equations are:

Conservation of mass or continuity equation

$$\frac{\partial \rho}{\partial t} + \nabla(\rho U) = 0 \quad (\text{Eq. 6-2})$$

Momentum conservation

$$\frac{\partial}{\partial t}(\rho U) + \nabla(\rho U U) = \nabla p + \mu \nabla U^2 + \rho g + S_h \quad (\text{Eq. 6-3})$$

Energy conservation

$$\nabla(-k \nabla T + \rho C_p T U) = S_T \quad (\text{Eq. 6-4})$$

where  $\partial t$  is a partial derivative in terms of time,  $T$  is the temperature,  $U$  is the velocity vector,  $g$  is the gravity force,  $p$  is the pressure,  $C_p$  is the specific heat,  $k$  is the thermal conductivity,  $\mu$  is the dynamic viscosity,  $S_h$  and  $S_T$  are the source terms for heat transfer and momentum.

### 6.5.1 Radiation model

Radiation is an important term for the Greenhouse-type Solar dryer, the energy conservation equation needs to be coupled with a source of radiation and of course, the high temperatures involve radiative heat transfer. The CFD codes have different options to simulate the radiation of bodies but in general terms, the model needs to consider the option for semi-transparent boundaries as the greenhouses commonly use covers with those properties.

The Discrete Ordinates (DO) Radiation Model is the only one that considers semi-transparent boundaries, scattering, specular reflection, and accounts for the exchange of radiation between gas and particles, all their properties needed for modeling the drying process in greenhouses. Other models have some limitations and should be avoided if the properties listed above are considered for a simulation.

The energy model coupled with the DO model when integrated into a control volume  $i$ , yield the discrete energy equation (ANSYS, 2011a):

$$\sum_{j=1}^N \mu_j^T T_j - \beta_i^T T_i - \alpha_i^T \sum_{k=1}^L I_i^k \omega_k - S_i^T S_i^h \quad (\text{Eq. 6-5})$$

where,

$$\alpha_i^T = k\Delta V_i, \quad \beta_i^T = 16k\sigma T_i^{*3} \Delta V_i, \quad S_i^T = 12k\sigma T_i^{*4} \Delta V_i.$$

$$k = \text{absorption coefficient}, \Delta V = \text{control volume}$$

The  $\mu_j^T$  coefficient and the source term  $S_i^h$  are due to the discretization of the convection and diffusion terms.

### 6.5.2 Species Model

The study of the air inside the greenhouse dryer is not enough to increase the knowledge of the drying problem, the multi-nature of the drying problem should be faced taking into account the product to be dried. The different gases and solids interacting during the process of drying involve the mixing and transport into the conservation equations, the species model is suitable to simulate those processes without any issues.

The main advantage of this model is that it treats the air as a mixture of air and water vapor. Some other gases could be considered if needed. Humid air depends on pressure, temperature, and humidity so it is important to define the correct working pressure in the dryer and the initial or boundary conditions regarding temperature and mass fraction of water vapor.

The species model predicts the local mass of each specie specified  $Y_i$ , through the solution of a convection-diffusion equation for the  $i$ -th species. The conservation mass equation is then modified in general terms (ANSYS, 2011a):

$$\frac{\partial}{\partial t}(\rho Y_i) + \nabla \cdot (\rho U Y_i) = -\nabla \cdot J_i + R_i + S_i \quad (\text{Eq. 6-6})$$

Where,  $R_i$  is the net rate of production of species  $i$  by chemical reaction,  $S_i$  is the rate of creation by addition from the dispersed phase plus any user-defined sources,  $J_i$  is the diffusion flux of species  $i$ ,  $U$  is the velocity vector and  $Y_i$  is the  $i$ -th species.

### 6.5.3 Turbulence Model

The turbulence model completes the mathematical description of the system. In heated systems, the fluid flow will be of interest as the heat exchange depends on the turbulence and the properties of the fluid. According to (Yadav & Bhagoria, 2013) for 2-Dimensional heat exchangers, the best model is the Renormalization-group  $k - \varepsilon$  turbulence model as it predicts close to the

experimental results. The Reynolds-Averaged Navier-Stokes (RANS) models are preferred to simulate the turbulence for greenhouse dryers, the governing equations are solved in an averaged form and include the dissipation rate and the turbulence kinetic energy. The  $k - \varepsilon$  and  $k - \omega$  models are part of the RANS; thus, they are preferred for simulations but there are some considerations for picking a suitable model.

According to (Rodriguez, 2019) The Standard  $k - \varepsilon$  (SKE) is the most widely used model and is good for isotropic flows with high Reynolds numbers and simple flows, but it has some bad results with strongly curved surfaces, flow separation, and low-Re. The Renormalization group  $k - \varepsilon$  (RNG) improves the SKE model for low Re but is not as stable as the SKE. The Realizable  $k - \varepsilon$  (RKE) model differs from the standard as constraints only yield positive normal stresses allowing boundary flows, separated and swirling flows. The RKE is better than the RNG for separated flows and secondary flows. Finally, the  $k - \omega$  model is great for adverse pressure gradients, separated flows, turbulent heat transfer, and low Re, but it requires a fine mesh of the wall as it does not use wall functions. There is still further research needed in terms of turbulence modeling, but the most common model used for greenhouse-type solar dryers is the RKE, although, the RNG could be a good option as dryers involving heat exchange.

#### **6.5.4 Assumptions and Boundary Conditions**

Some assumptions should be considered that are relevant to specific problems. A common assumption in CFD codes to reduce the complexity of the governing equations is the Boussinesq model. This model treats the density as constant in all solved equations, except for the buoyancy term in the momentum equation (ANSYS, 2011b):

$$(\rho - \rho_0)g \approx -\rho_0 \beta(T - T_0)g \quad (\text{Eq. 6-7})$$

where,  $\rho_0$  is the constant density of the flow,  $\beta$  is the thermal expansion coefficient, and  $T_0$  is the operating temperature.

In general, without the Boussinesq approximation, the density is treated as dependent on the temperature, and the larger the temperature differences in the domain, the greater the influence of the change in density over the physical process. In specific, for dryers, it is important to consider these big differences if the natural convection is the main heat transfer process and if the volume is big enough to allow a poor mixture of the air inside the dryer. Some well-known limitations of the Boussinesq equations are that cannot be used with species calculations, combustion, or reacting flows (ANSYS, 2011b) as well as if the temperature difference is bigger than 15°C (Ferziger & Perić, 2002). Then, the recommendation is to avoid the Boussinesq approximation for greenhouse-type solar dryers.

The boundary conditions depend on the geometry, materials, orientation of the greenhouse, and properties of the product, but some general conditions to be considered are the following: the atmospheric pressure is an important factor as humid air changes according to the pressure and temperature, thus, it is important to place the correct value; cover and floor properties, it is important to have the coefficients of the covering material and the floor; For the inlet, air temperature and humidity are both parameters needed for the simulations; the density of air should be considered as an ideal gas with the pressure and temperature given.

## **6.6 STATE OF ART WITH CFD APPLICATION IN SOLAR DRYING**

Scopus is one of the largest literature databases, has about 5,000 publishers, and has search, analysis, and visualization tools (Spiroski, 2013). It is possible to perform searches by title, keywords, author, journal, topic, or knowledge area. If a quest is carried on with the word “drying” and the filter to search in “Article title, abstract, keywords” for the whole range of years and focus

on “Article or Review”, the result is 207,450 papers published from 1826 to 2021 (Figure 6-4). There is an increasing trend in the publication of articles related to drying since the year 1971. However, this result contains not only drying articles in the food area but also Medicine, Health Sciences, Chemistry, and Materials. That is why it is necessary to apply another filter to the areas that correspond to Agronomic Sciences or Agriculture and discard those that do not correspond to the subject.

When searching with more extensive filters and using words such as "CFD", "solar" and "greenhouse", with "drying", more precise and representative result are obtained on the number of items that correspond to solar drying in greenhouses and that use computational fluid dynamics modeling approach (Figure 6-5). Of the total drying studies, only 0.007% corresponds to CFD modeling of greenhouse-type solar dryers, which means 15 items. Through this simple search, it is possible to get an idea of the lack of research in CFD modeling in greenhouse dryers.

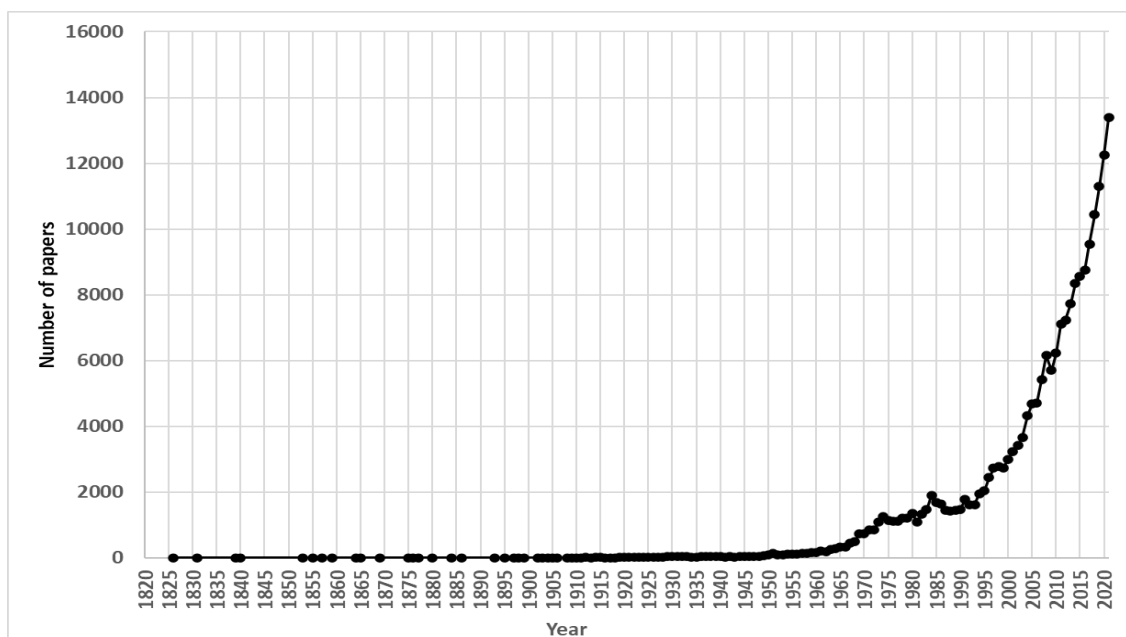


**Figure 6-4.** Number of drying papers per year, data from Scopus, 2019.

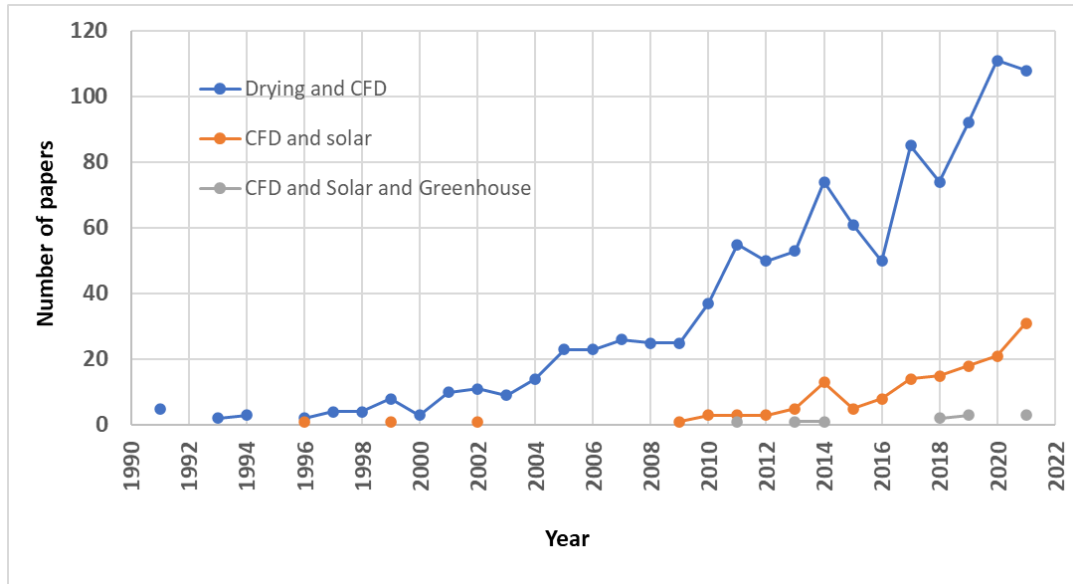


**Figure 6-5.** Paper growth publications per year in drying, CFD, and greenhouse-type solar dryers, data from Scopus, 2019.

Although CFD has indeed been worked in greenhouses for crop growth, and it is possible to use this knowledge if the behavior of the air inside the dryer is analyzed without considering the product, or crops in the case of greenhouses with agronomic purposes, the special interactions in both processes differ mainly due the energy needed for heating and the air temperature safe values. New proposals in greenhouse-type dryers, as Kumar & Shrivastava (2017) point out, are focused on specifically designing geometries and equipment that can produce a better energy conservation effect and a more homogeneous distribution of temperature and air-wind profiles with constant speeds.

### 6.6.1 Products studied in Greenhouse-type solar Dryers

The selection of products for dehydration is based on the high moisture content they possess since they are susceptible to fungi and decomposition. In most cases, those that represent an economic income or that by their nature require this drying process to be consumed, such as coffee, are selected for drying (Janjai et al., 2011).

Although various fruits, plants, and crops have been studied in drying around the world (Table 6-1), most studies were conducted in India and Thailand (31% and 15%, respectively); in Latin America, just Argentina and Brazil had research in drying.

**Table 6-1.** Products dehydrated in greenhouse-type solar dryers around the world.

Product	Author	Drying model	Greenhouse type	Country	Volume (m <sup>3</sup> )
Bamboo	Ong (2007)	-	kiln type	Malaysia	4.1
Vanilla	Abdullah & Mursalim, (2007)	Henderson's equation	Steel frame, polyethylene cover	Indonesia	35.1
Rice	Rachmat & Horibe (1999)	-	Fiber Reinforced Plastic Drying House	Japan	4.9
Alfalfa	Condorí & Saravia (1998)	Condori & Saravia	Greenhouse solar drier with forced ventilation, single and double chamber, plastic film cover.	Argentina	--
Beans	Condorí & Saravia (1998)	Condori & Saravia	Greenhouse solar drier with forced ventilation, single and double	Argentina	--

---

				chamber, plastic film cover.		
Grapes	Condorí & Saravia (1998)	& Condori & Saravia	Greenhouse solar drier with forced ventilation, single and double chamber, plastic film cover.	Argentina	--	
Oregano	Condorí & Saravia (1998)	& Condori & Saravia	Greenhouse solar drier with forced ventilation, single and double chamber, plastic film cover.	Argentina	--	
Mustard	Manohar Chandra (2000)	& Page Model	Greenhouse solar dryer with natural and forced ventilation	India	2.5	
Garlic	Condorí et al. (2001)	Condori & Saravia	Tunnel greenhouse	Argentina	336.7	
Pineapple	Bala et al. (2003)	-	Tunnel greenhouse	Bangladesh	--	
Cabbage	Jain & Tiwari (2004)	Exponential curve fitting	Roof type even span greenhouse with effective	India	0.6	

---

---

					floor covering.		
Casuarina (wood)	Helwa (2007)	et al.	-		Semi-greenhouse solar dryer, steel frame structure covered by a galvanized iron sheet.	Egypt	16.8
Peas	Jain & (2004)	Tiwari	Exponential curve fitting		Roof type even span greenhouse with effective floor covering.	India	0.6
Grapes	Fadhel (2005)	et al.	-		Natural convection solar tunnel greenhouse	Tunisia	--
Onion	Jain (2005)		Lewis (1921)		Greenhouse with packed bed thermal storage	India	60
Bombay Duck fish	Bala & (2005)	Janjai,	Single exponential equation		Tunnel greenhouse	Bangladesh	---
Jaggery	Kumar & (2006)	Tiwari	Thin layer based on a balance of energy		Roof type even span greenhouse with effective floor covering.	India	0.5
Organic tomato	Sacilik (2006)	et al.	Approximation of diffusion model		Tunnel greenhouse	Turkey	36

---

Pepper	Koyuncu (2006)	-		Two greenhouses were designed by the author. Polyethylene glazing of 0.15 mm thickness.	Turquía	1
Onion	Kumar & Tiwari (2007)	Malik, Kumar & Tiwari, Sodha (1982)		Roof type even span greenhouse with effective floor covering.	India	0.5
Red pepper	Kooli et al. (2007b)	Kooli et al. 2007		Tunnel greenhouse with a polyethylene cover	Tunisia	0.06
Hot chili	Hossain & Bala (2007)	Regression equations		Tunnel greenhouse	Bangladesh	--
Grapes	Barnwal & Tiwari (2008)	Linear and multilinear regressions.		Photovoltaic-thermal greenhouse drier (PV/T) roof type even span	India	9.3
Mangoes	Rankins et al. (2008)	-		Gable roofed and plastic-covered structure supported by wooden	Senegal	62
Bitter gourd flakes	Sethi & Arora (2009)	-		Greenhouse with inclined	India	73.2

---

						north wall reflection		
Banana	Janjai et al. (2011)	Thin layer equation with coefficients from Smitabhindu et al. (2008)	Greenhouse with polycarbonate cover, parabolic roof shape, and concrete floor.	Thailand	349.7			
Chilli	Janjai et al. (2011)	Thin layer equation with coefficients from Hossain (2003)	Greenhouse with polycarbonate cover, parabolic roof shape, and concrete floor.	Thailand	349.7			
Coffee	Janjai et al. (2011)	Thin layer equation with coefficients from Berbert et al. (1995)	Greenhouse with polycarbonate cover, parabolic roof shape, and concrete floor.	Thailand	349.7			
Onion	Kadam et al. (2011)	Newton	Low-cost greenhouse, Quonset shape Bamboo structure	India	32.8			
Chilli	Kaewkiew et al. (2012)	-	Greenhouse with polycarbonate cover, parabolic roof	Thailand	373.5			

---

---

			shape, and concrete floor		
Sludge	Lima et al. (2012)	-	Greenhouse meets the standard adopted by Comparni (2001), 150- micron translucent plastic	Brazil	180
Rubber	Tanwanichkul et al. (2013)	Tanwanichkul, Thepa & Rordprapat (2013)	Sandwich & greenhouse	Thailand	9.7
Chamomile flowers	Aghbashlo et al. (2015)	Halsey's equation	Forced convection Deep-Bed Solar Greenhouse	Serbia	120
Pepper	Akin et al. (2014)	Lewis (Newton), Henderson and Pabis, Logarithmic, Two-term, Page, Modified Page, Two-Term Exponential, Wang and Sing, Modified Henderson and Pabis, Verma	Solar tunnel dryer with forced convection	Turkey	23.4

---

Tomato	Prakash & Kumar (2013)	Newton, Henderson and Pabis, Page, Logarithmic, Two-Term, Wang and Singh, Modified Henderson and Pabis, Prakash and Kumar model.	Even span roof-type modified greenhouse dryer under active mode	India	1.07
Grapes	Tiwari et al. (2016)	Thin layer based on a balance of energy	Greenhouse mixed-mode solar dryer with the whole roof made by photovoltaic and extra glazing below the photovoltaic module.	India	0.71
Sludge	Belloulid et al. (2017)	-	Tunnel-type open greenhouse with transparent polycarbonate sheet	Morocco	0.62
Wood chips of <i>Pinus Pinaster</i>	(Perea-Moreno et al. (2016)	Logarithmic and Exponential	Tunnel greenhouse with a plastic film cover	Spain	304.3
Rubber	Jitjack et al. (2016)	Jitjack, Thepa, Sudaprasert & Namprakai	Parabolic greenhouse with an additional	Thailand	15.8

---

					area of enhanced panels		
Pepper	Azaizia et al. (2017)	Kooli et al. 2007			Flat plate solar collector and chapel-shaped greenhouse	Tunisia	0.6
<i>Orthosiphon aristatus</i>	Tham et al. (2017)	Thin layer equation			Greenhouse with integrated heat pump	Malaysia	-----
Amla candy	Patil & Gawande (2018)	Newton, Modified Henderson Pabis, Thompson	Page, Page, &		Forced convection tunnel greenhouse dryer	India	2.7
Bitter gourd flakes	Chauhan et al. (2018)	Lewis, Henderson Pabis, Logarithmic, Wang and Singh, Two-term exponential, Approximation of diffusion, Midilli-Kucuk & Prakash and Kuma.	Page, and		Greenhouse with solar collector forced ventilation and north wall with iron laminate	India	0.9
<i>Clinacanthu s nutans</i>	Tham et al. (2017)	Thin layer equation			Greenhouse with integrated heat pump	Malaysia	-----
Coconut	Ayyappan (2018)	-			Natural convection solar greenhouse	India	70.6

---

---

					dryer with biomass backup heater		
Organic fertilizer from olive mill wastewater	Galliou et al. (2018)		-		Greenhouse with plastic cover film, metallic structure, and with a concrete chamber inside.	Greece	1.5
Litchi	Toshing et al. (2018)		Artificial Neural Network (ANN)		Greenhouse with polycarbonate cover, parabolic roof shape, and concrete floor.	Thailand	105
Groundnuts	Sahdev et al. (2018)		Lewis, Modified Henderson, Pabis.	Page, Page, and	Even span roof-type greenhouse plastic pipe and Ultraviolet film cover of two hundred microns.	India	0.5
Tomato slices	Mahapatra & Tripathy (2019)		CFD 2-D, Heat equation		Kiln type	India	----
Cayenne pepper	Hempattarasuwan et al. (2019)		Page, Henderson, Pabis, Kucuk	Newton, & Midillo-	Greenhouse with polycarbonate cover, parabolic roof	Thailand	106.5

---

---

				shape, and concrete floor		
<i>Eucalyptus delegatensis</i>	Phonetip et al. (2019)	-		Kiln type with polyethylene film	Australia	--
Red pepper	Condorí et al. (2001); Condorí & Saravia (1998, 2003)	Condori & Saravia		Greenhouse solar drier with forced ventilation, single and double chamber, plastic film cover	Argentina	--

---

There is high variability in the volume of greenhouses that have been used for research. Most of them are less than 50 m<sup>3</sup> (Table 6-1), and a few are studied in high-volume greenhouses (Figure 6-6). The volume not only affects the heat stratification and variation in wind speed but also determines the drying capacity. If the volume is small, the influence of the geometry is not high in turbulence and infiltration.

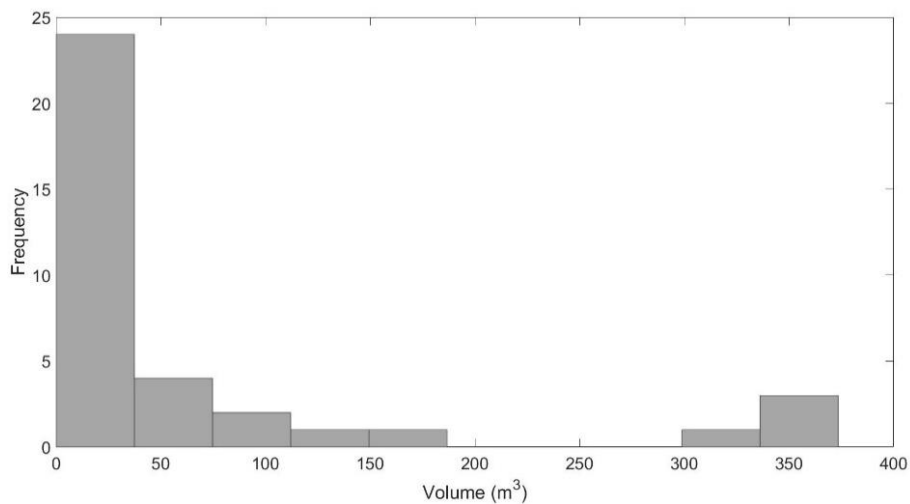


**Figure 6-6.** Volume of all greenhouses used in research, so far.

Fifty-two products were studied in the range of years from 1996-2019, the principal product in the studies is pepper, followed by grapes, onions, tomatoes, chilies, wood, and medicinal plants. Most of the products under study were of high economic importance, e.g., for Mexico pepper is translated into 0.22 billion dollars of income due to exportation (Maálaga et al., 2001). If food loss and waste are considered, pepper does not appear among the main products wasted in Mexico, even for the products most wasted in Mexico, just mangoes and bananas appear in the list but with one study each (Table 1) (FAO, 2015).

In most cases, semi-empiric models such as the Thin-layer models have been used (Ertekin & Firat, 2017). However, the scope of these models has limitations as they depend on the conditions from which are calibrated and are not extensible to other conditions, in each case, the parameters need to be recalculated and tested by statistics for the specific product to be dehydrated. Only one paper was found to use a CFD model approach in 2-D, to simulate the behavior of tomato slices during convection, radiation, and conduction heat transfer (Mahapatra & Tripathy, 2019).

A limitation in the use of CFD models coupled with simultaneous heat and mass transfer during the drying process is the presence of turbulence flow, this approach does not allow an accurate solution. Furthermore, when modeled, the behavior of air there is observed as a reduction in the drying curve on the edges of dryers due to the behavior of fluids in the boundary layer. This phenomenon is hard to simulate and couple with the air-solid interface equations (Jamaleddine & Ray, 2010). Another important issue to consider is the mesh in the model, as it is a multi-scale process the dimensions of the product in comparison with the dryer differ in the order of  $10^3$ , the software used for producing the mesh could make a smaller element mesh in the product and a bigger one for the air, these different elements could produce again, an inaccurate solution and will lead to a high computational cost (Norton & Sun, 2006).

Alternatives have emerged that allow the modeling of the product with different scales so it can be coupled together with the macro-metric flow equations. One of the alternatives is the use of the so-called “Meshless methods”, capable of simulating the behavior of water within the product at a micrometric scale of pore size. Models such as Lattice-Boltzman, Dissipative Particle Dynamics, and Pore Network, offer the advantages of obtaining an accurate three-dimensional image of the water inside the product and its movement to the air, as well as the possibility of predicting the behavior of water in a phase change or the presence of gas-liquid interfaces (Frank & Perré, 2010). With the increase in computing capacity, more models will likely be developed, or new techniques will be attempted that allow the simulation and estimation of the properties of agricultural products in the drying process as changes within them occur (Datta, 2007a, 2007b; Gulati & Datta, 2013). Another approach is to divide the behavior of the product by the function of the type of process studied, there is the case of a non-homogeneous porous material, convective drying, and storage in wet beds, among others. Through this type of modeling, the macroscopic or mesoscopic equations are adjusted to a particle level to allow the modeling and simulation of simultaneous multi-scale mass transfer (Datta, 2008; Perré, 2010).

## **6.7 CFD MODELING OF GREENHOUSE-TYPE SOLAR DRYERS**

The biggest problem when analyzing the macroscopic scale of the dryers is that even the simplest processes involved in drying are highly non-linear, and therefore, it is difficult to scale the results in small dryer experiments to dryers with larger dimensions (Strumillo, 2007). Some of the advantages of using CFD in dryers is that it is possible to reduce this scaling problem since you can evaluate geometries and answer questions of the form, what would happen if? And the ability to get values of each point in the space so is possible to compare what is happening during a process (Bakker et al., 2001). Up to now, CFD models have been focused only on the moving air inside the greenhouse-type dryer is studied. Through the search in Scopus, only 12 works related to the words "CFD",

"greenhouses", "drying" and "solar" were found, but only 11 are related to CFD simulations of greenhouse dryers (Table C-2).

Krawczyk & Badyda (2011) studied the process of drying sludge from waste inside a chapel-type greenhouse with dimensions of 3 m high, and 3.12 m long, the width is not reported. The study was in two dimensions, and simulate the behavior of humidity, the temperature of sludge, and air within the dryer with FLUENT software. They reported the difficulty of solving simultaneously the phenomena of transport and the use of fine mesh in the vicinity of the greenhouse walls. Lokeswaran & Eswaramoorthy (2013a), analyzed a hemicylindrical greenhouse with a concrete floor with an area of 40 m<sup>2</sup>, and transparent polyethylene covers of 200 microns thick. They used FLUENT 6.3.26 and a mesh of 914,905 elements. They found that the behavior of the air inside the dryer is not homogeneous, and to improve it is necessary to add a fan so that temperatures do not vary so much. Somsila & Teeboonma (2014), evaluated the behavior of a greenhouse with a sloping roof for drying para rubber. They found that the air had almost constant speeds throughout the dryer, which causes no temperature stratification. The temperature inside the dryer was between 55-60 °C, and the highest temperature was found in the ceiling.

Gupta et al. (2018) simulated the behavior of the air inside a chapel-type greenhouse with natural ventilation, produced by a small hole located in the opposite wall of the air inlet. They used ANSYS 15.0 software for simulation. The results indicated that the air could circulate throughout the geometry at an almost constant speed; however, the temperature has significant differences, being higher in the side walls. Noh et al. (2018) studied an industrial-scale solar dryer that consists of evacuated tubes, a heat exchanger blower, and a drying chamber. The dimensions of the drying chamber were 1.25 m in height, 1.7 m in width, and 17 m long. For simulation, five pallets were stacked up on top of each other, and three different ventilations were considered: the first being passive, passive with active combination, and passive with intermittent active ventilation. They found

that the optimal condition was passive with intermittent active ventilation which produce the highest temperature inside the sericite mica.

Srichat et al. (2019) used the benefits offered by CFD modeling to test a hypothesis about dryer geometry. They tested a roof with sinusoidal geometry compared to the parabolic shape roof. They found that the sinusoidal shape had higher temperatures in any of the axes where the solution is simulated. This shows that sinusoidal geometry would be an improved design of a solar greenhouse-type solar dryer, reducing drying time and increasing product quality. Román-Roldán et al. (2019) studied the behavior of a chapel-type greenhouse, with a plastic cover and a coupled air heater. They tested the number of elements in the mesh, going from 1 to 7 million, to determine the quality of the mesh in the geometry. 6 million mesh size provided better results. Also, it was found that if the volume is reduced by 36.5%, the temperature distribution and the air speed inside the dryer were improved.

Purusothaman et al. (2019) studied three different roof shapes in greenhouse dryers for free and forced convection. The research simulated the period from 10 am to noon. They found that the trapezoidal roof greenhouse achieves a higher temperature than the triangle or hemispherical roof greenhouses. Vivekanandan et al. (2021) studied six different small greenhouse dryers, the CFD results were compared with experimental data of 7.5 hours for winter and summer sessions. They found that the Quonset shape is the ideal shape; from maximum to minimum, the shapes were found to be Quonset, Tropical, Pyramid, Parabola, Modified Quonset, and Igloo.

Villagran et al. (2021) studied four different greenhouse dryer designs. Three of them had polyethylene covers and the last one uses insect-proof porous mesh inside the greenhouse. All greenhouses were placed in a computational domain around the greenhouse, it is a small box with a minimum of 10 times the height of the greenhouse. A wind profile was used as an inlet, solar radiation was

considered at the top, and as an outlet a pressure equal to the atmospheric pressure. The results found by the researchers were that the greenhouse with a double polyethylene film has the highest microclimate dynamics and thus the highest temperature and lowest relative humidity.

Finally, Román-Roldán et al. (2021) researched a new prototype for air recirculation of a chapel-type greenhouse dryer with a polyethylene cover. Six different configurations with fans were tested by the authors and compared to experimental results. The two main objectives were to study air distribution and air temperature in each configuration. They found that fans above 15 m/s are required to improve a better distribution of air, also if fan velocity was kept between 5 to 20 m/s the temperature of the drying chamber varies from 51 to 81°C. In Table 6-2 there is a summary of the solver, boundary conditions, and possible assumptions used in each research with CFD.

**Table 6-2.** CFD papers found in a literature review.

<b>Authors</b>	<b>CFD code and methodology</b>	<b>Product modeling</b>	<b>Greenhouse</b>	<b>Variables results</b>
(Krawczyk & Badyda, 2011b)	<ul style="list-style-type: none"> <li>• Solver: Ansys Fluent, 2D.</li> <li>• Turbulence model: -</li> <li>• Radiation model: -</li> <li>• Inlet: Velocity</li> <li>• Outlet: Pressure</li> </ul>	<ul style="list-style-type: none"> <li>• Sewage sludge</li> <li>• CFD through UDF</li> </ul>	<ul style="list-style-type: none"> <li>• Chapel-type but considered a small part of it</li> </ul>	<ul style="list-style-type: none"> <li>• Air/product temperature</li> <li>• Air/product relative humidity</li> <li>• Velocity</li> </ul>
(Lokeswaran & Eswaramoorthy, 2013b)	<ul style="list-style-type: none"> <li>• Solver: Ansys Fluent, 3D, steady state, SIMPLE algorithm.</li> <li>• Turbulence model: -</li> <li>• Radiation model: DO</li> </ul>	-	<ul style="list-style-type: none"> <li>• Hemi-cylindrical with polyethylene film</li> </ul>	<ul style="list-style-type: none"> <li>• Solar insolation</li> <li>• Air temperature</li> </ul>

---

	<ul style="list-style-type: none"> <li>• Inlet: Air temperature and velocity</li> <li>• Outlet: Pressure</li> <li>• Boussinesq Approximation</li> </ul>			
(Somsila & Teeboonma, 2014b)	<ul style="list-style-type: none"> <li>• Solver: Ansys, CFX, 3D.</li> <li>• Turbulence model: RNG k-epsilon</li> <li>• Radiation model: DO</li> <li>• Inlet: Pressure</li> <li>• Outlet: Pressure</li> </ul>	<ul style="list-style-type: none"> <li>• Para rubber but no modeling</li> </ul>	<ul style="list-style-type: none"> <li>• Inclined roof type</li> </ul>	<ul style="list-style-type: none"> <li>• Air temperature</li> <li>• Air velocity</li> </ul>
(Gupta et al., 2018)	<ul style="list-style-type: none"> <li>• Solver: Ansys CFX</li> <li>• Turbulence model: SST</li> <li>• Radiation model: -</li> <li>• Inlet: Air velocity</li> <li>• Outlet: Pressure</li> </ul>	<ul style="list-style-type: none"> <li>• Tomato flakes but not specified if modeled</li> </ul>	<ul style="list-style-type: none"> <li>• Even span roof</li> </ul>	<ul style="list-style-type: none"> <li>• Air velocity</li> <li>• Air temperature</li> </ul>
(Noh et al., 2018)	<ul style="list-style-type: none"> <li>• Solver: Ansys Fluent, 3D.</li> <li>• Turbulence model: k-epsilon</li> <li>• Radiation model: ASHRAE Equation</li> <li>• Inlet: Air velocity</li> <li>• Outlet: Passive, active and combine ventilation</li> </ul>	<ul style="list-style-type: none"> <li>• Sericite mica but modeled as an obstruction to air</li> </ul>	<ul style="list-style-type: none"> <li>• Industrial scale dryer with polycarbonate sheet</li> </ul>	<ul style="list-style-type: none"> <li>• Air velocity</li> <li>• Air temperature</li> </ul>

---

(Román-Roldán et al., 2019)	<ul style="list-style-type: none"> <li>• Solver: Ansys Fluent, 3D, SIMPLE algorithm.</li> <li>• Turbulence model: k-epsilon realizable</li> <li>• Radiation model: DO</li> <li>• Inlet: mass Flow rate and temperature</li> <li>• Outlet: Pressure</li> </ul>	-	<ul style="list-style-type: none"> <li>• Chapel-type with solar air heaters</li> </ul>	<ul style="list-style-type: none"> <li>• Turbulence</li> <li>• Air temperature</li> </ul>
(Purusothaman et al., 2019)	<ul style="list-style-type: none"> <li>• Solver: Ansys Fluent, 3D.</li> <li>• Turbulence model: -</li> <li>• Radiation model: -</li> <li>• Inlet: mass flow rate</li> <li>• Outlet: -</li> </ul>	-	<ul style="list-style-type: none"> <li>• Hemispherical, triangular, and trapezoidal roof greenhouses</li> </ul>	<ul style="list-style-type: none"> <li>• Air temperature</li> </ul>
(Srichat et al., 2019)	<ul style="list-style-type: none"> <li>• Solver: Ansys Fluent, 3D, SIMPLE algorithm.</li> <li>• Turbulence model: Standard k-epsilon</li> <li>• Radiation model: -</li> <li>• Inlet: -</li> <li>• Outlet: -</li> </ul>	-	<ul style="list-style-type: none"> <li>• Sinusoidal and parabolic roofs</li> </ul>	<ul style="list-style-type: none"> <li>• Air temperature</li> </ul>
(Vivekanandan et al., 2021)	<ul style="list-style-type: none"> <li>• Solver: -</li> <li>• Turbulence model: -</li> <li>• Radiation model: -</li> <li>• Inlet: -</li> <li>• Outlet: -</li> </ul>	-	<ul style="list-style-type: none"> <li>• Modified quonset, quonset, pyramid, Igloo, tropical, parabola</li> </ul>	<ul style="list-style-type: none"> <li>• Air temperature</li> </ul>
(Villagran et al., 2021)	<ul style="list-style-type: none"> <li>• Solver: Ansys Fluent, 3D, steady state, SIMPLE algorithm.</li> <li>• Turbulence model:</li> </ul>	-	<ul style="list-style-type: none"> <li>• Dual-roof tunnel type, Tunnel type two-span, Chapel-type with a flat roof on two sides,</li> </ul>	<ul style="list-style-type: none"> <li>• Air velocity</li> <li>• Air temperature</li> <li>• Relative humidity</li> </ul>

---

	<ul style="list-style-type: none"> <li>Standard k-epsilon</li> <li>• Radiation model: DO</li> <li>• Inlet: wind speed profile</li> <li>• Outlet Pressure</li> <li>• Boussinesq approximation</li> <li>• Species transport model</li> <li>• Computational domain around the dryer</li> </ul>		and Tunnel-type roof structure with different heights,	
(Román-Roldán et al., 2021)	<ul style="list-style-type: none"> <li>• Solver: Ansys Fluent, 3D, SIMPLE algorithm.</li> <li>• Turbulence model: Standard k-epsilon</li> <li>• Radiation model: DO</li> <li>• Inlet: Mass flow rate and temperature</li> <li>• Outlet: Pressure</li> </ul>	-	<ul style="list-style-type: none"> <li>• Chapel-type polyethylene film with external air heater collectors</li> </ul>	<ul style="list-style-type: none"> <li>• Air velocity</li> <li>• Solar heat flux</li> <li>• Air temperature</li> </ul>
(Duong et al., 2021)	<ul style="list-style-type: none"> <li>• Solver: Ansys Fluent, 3D, transient state.</li> <li>• Turbulence model: k-epsilon Realizable</li> <li>• Radiation model: DO</li> <li>• Inlet: Velocity and mass fraction</li> <li>• Outlet: Pressure</li> <li>• Boussinesq approximation</li> </ul>	<ul style="list-style-type: none"> <li>• Porous media as product as airflow resistant</li> </ul>	<ul style="list-style-type: none"> <li>• Parabolic roof shape with polycarbonate sheet and concrete floor.</li> </ul>	<ul style="list-style-type: none"> <li>• Air temperature</li> <li>• Air velocity</li> <li>• Air relative humidity</li> </ul>

---

Among the papers presented in the Table C-2, Lokeswaran and Eswaramoorthy (2013) modeled the behavior of air inside the greenhouse-type solar dryers with a product as a load of the system in 2D; Noh et al. (2018) and Duong et al. (2021) modeled the product but just as an obstruction for airflow. Apart from Lokeswaran and Eswaramoorthy (2013), the product was not modeled as a source of humidity or heat exchange. The list above contains information about the turbulence models used so far, given the discussion in the section “How to build a CFD model for drying,” the RANS models are identified as suitable for CFD codes for greenhouse solar dryers, and this was observed from all the studies reviewed with almost all the authors used k-epsilon models except one. The most commonly used k-epsilon model is the standard model and as mentioned it is recommended that the realizable or the RNG models are more suited for drying modeling compared to the standard k-epsilon model. Only one research deals with a transient state whereas all the other simulate a steady state, because of the drying complexity, it is recommended to study the transient behavior when the product is considered. The use of Boussinesq approximation is not recommended if the air temperature difference in the problem domain is high, but some of the papers reviewed used this assumption which should have been avoided.

Most of the research found in literature have been focused on the air velocity and temperature inside the greenhouse for different roof shapes. However, it is not common to find the influence of the product on the relative humidity and air temperature in the greenhouse. Only few studies evaluated the flow pattern due to the product, thus there is need for further research. Evaluating alternative designs to improve airflow patterns, product interaction with air inside the greenhouse, and new roof and cover designs deserve future research in solar greenhouse dryers.

## 6.8 CONCLUSIONS

Greenhouse-Type Solar Dryer System is a complex system, and its study involves multiphase and multiscale phenomena that need to be considered when modeling. Further research is needed on CFD modeling in greenhouse-type solar dryers. The great variability of types of solar dryers is the result of a lack of knowledge in the general drying process. Due to the nature of drying, scaling the results obtained with small-volume greenhouses to high-volume dryers is difficult, thus it is necessary to consider turbulence in the models and the behavior of the indoor air to obtain improved results. Using small greenhouses does not offer significant impact with research for the development of industrial-scale drying. The models developed so far are based on data, and few use theoretical and CFD models. Although alternatives have been proposed to solve the problem of simultaneous transfer processes, involving various phases and scales, so far, the behavior of the product and the air have not been modeled together. It is necessary to consider the most wasted products, not only those that are of economic importance.

## 6.9 REFERENCES

Abdullah, K., & Mursalim. (2007). Drying Of Vanilla Pods Using A Greenhouse Effect Solar Dryer. *Drying Technology*, 15(2), 685–698. <https://doi.org/10.1080/07373939708917254>.

Aghbashlo, M., Müller, J., Mobli, H., Madadlou, A., & Rafiee, S. (2015). Modeling and Simulation of Deep-Bed Solar Greenhouse Drying of Chamomile Flowers. *Drying Technology*, 33(6), 684–695. <https://doi.org/10.1080/07373937.2014.981278>

Akin, A., Gurlek, G., & Ozbalta, N. (2014). Mathematical Model of Solar Drying Characteristics For Pepper (*Capsicum Annuum*). *J. of Thermal Science and Technology*, 34, 99–109.

Anderson, J. D. (2009). Basic philosophy of CFD. Computational Fluid Dynamics, 3–14.

[https://doi.org/10.1007/978-3-540-85056-4\\_1/COVER/](https://doi.org/10.1007/978-3-540-85056-4_1/COVER/)

ANSYS, Inc. (2011a). ANSYS FLUENT Theory Guide.

ANSYS, Inc. (2011b). ANSYS FLUENT User's Guide.

Ayyappan, S. (2018). Performance and CO<sub>2</sub> mitigation analysis of a solar greenhouse dryer for coconut drying: Energy & Environment, 29(8), 1482–1494.

<https://doi.org/10.1177/0958305X18781891>

Azaizia, Z., Kooli, S., Elkhadraoui, A., Hamdi, I., & Guizani, A. A. (2017). Investigation of a new solar greenhouse drying system for peppers. International Journal of Hydrogen Energy, 42(13), 8818–8826.

<https://doi.org/10.1016/J.IJHYDENE.2016.11.180>

Bakker, A., Haidari, A. H., & Oshinowo, L. M. (2001). Realize greater benefits from CFD. Chemical Engineering Progress, 97(3), 45–53.

Bala, B. K., & Janjai, S. (2005). Solar Drying of Fish (Bombay Duck) Using Solar Tunnel Drier Home About Log In Register Search Current Archives. International Energy Journal, 6(2).

<http://www.rericjournal.ait.ac.th/index.php/eric/article/view/44>

Bala, B. K., Mondol, M. R. A., Biswas, B. K., das Chowdury, B. L., & Janjai, S. (2003). Solar drying of pineapple using solar tunnel drier. Renewable Energy, 28(2), 183–190. [https://doi.org/10.1016/S0960-1481\(02\)00034-4](https://doi.org/10.1016/S0960-1481(02)00034-4)

Barnwal, P., & Tiwari, G. N. (2008). Grape drying by using hybrid photovoltaic-thermal (PV/T) greenhouse dryer: An experimental study. *Solar Energy*, 82(12), 1131–1144. <https://doi.org/10.1016/J.SOLENER.2008.05.012>

Belloulid, M. O., Hamdi, H., Mandi, L., & Ouazzani, N. (2017). Solar Greenhouse Drying of Wastewater Sludges Under Arid Climate. *Waste and Biomass Valorization*, 8(1), 193–202. <https://doi.org/10.1007/S12649-016-9614-1/TABLES/4>

Chauhan, P. S., Kumar, A., Nuntadusit, C., & Mishra, S. S. (2018). Drying Kinetics, Quality Assessment, and Economic Analysis of Bitter Gourd Flakes Drying Inside Forced Convection Greenhouse Dryer. *Journal of Solar Energy Engineering, Transactions of the ASME*, 140(5). <https://doi.org/10.1115/1.4039891/368298>

Condorí, M., Echazú, R., & Saravia, L. (2001). Solar drying of sweet pepper and garlic using the tunnel greenhouse drier. *Renewable Energy*, 22(4), 447–460. [https://doi.org/10.1016/S0960-1481\(00\)00098-7](https://doi.org/10.1016/S0960-1481(00)00098-7)

Condorí, M., & Saravia, L. (1998). The performance of forced convection greenhouse driers. *Renewable Energy*, 13(4), 453–469. [https://doi.org/10.1016/S0960-1481\(98\)00030-5](https://doi.org/10.1016/S0960-1481(98)00030-5)

Condorí, M., & Saravia, L. (2003). Analytical model for the performance of the tunnel-type greenhouse drier. *Renewable Energy*, 28(3), 467–485. [https://doi.org/10.1016/S0960-1481\(01\)00137-9](https://doi.org/10.1016/S0960-1481(01)00137-9)

Datta, A. K. (2007a). Porous media approaches to studying simultaneous heat and mass transfer in food processes. I: Problem formulations. *Journal of Food Engineering*, 80(1), 80–95. <https://doi.org/10.1016/J.JFOODENG.2006.05.013>

Datta, A. K. (2007b). Porous media approaches to studying simultaneous heat and mass transfer in food processes. II: Property data and representative results. *Journal of Food Engineering*, 80(1), 96–110. <https://doi.org/10.1016/J.JFOODENG.2006.05.012>

Datta, A. K. (2008). Status of Physics-Based Models in the Design of Food Products, Processes, and Equipment. *Comprehensive Reviews in Food Science and Food Safety*, 7(1), 121–129. <https://doi.org/10.1111/J.1541-4337.2007.00030.X>

Defraeye, T. (2014). Advanced computational modelling for drying processes – A review. *Applied Energy*, 131, 323–344. <https://doi.org/10.1016/J.APENERGY.2014.06.027>

Duong, Y. H. P., Vo, N. T., Le, P. T. K., & Tran, V. T. (2021). Three-Dimensional Simulation of Solar Greenhouse Dryer. *Chemical Engineering Transactions*, 83, 211–216. <https://doi.org/10.3303/CET2183036>

El-Sebaili, A. A., & Shalaby, S. M. (2012). Solar drying of agricultural products: A review. *Renewable and Sustainable Energy Reviews*, 16(1), 37–43. <https://doi.org/10.1016/J.RSER.2011.07.134>

Ertekin, C., & Firat, M. Z. (2017). A comprehensive review of thin-layer drying models used in agricultural products. *Critical Reviews in Food Science and Nutrition*, 57(4), 701–717. <https://doi.org/10.1080/10408398.2014.910493>

Fadhel, A., Kooli, S., Farhat, A., & Bellghith, A. (2005). Study of the solar drying of grapes by three different processes. *Desalination*, 185(1–3), 535–541. <https://doi.org/10.1016/J.DESAL.2005.05.012>

FAO. (2015, April). Pérdidas y Desperdicios de Alimentos en América Latina y el Caribe. . <https://www.fao.org/publications/card/es/c/I4655S/>

FAO. (2019). El estado mundial de la agricultura y la formalización. <http://www.fao.org/3/ca6030es/ca6030es.pdf>

Ferziger, J. H., & Perić, M. (2002). Computational Methods for Fluid Dynamics. Computational Methods for Fluid Dynamics. <https://doi.org/10.1007/978-3-642-56026-2>

Forbes México. (2018). Desperdicio de alimentos en México cuesta 25,000 mdd al año • Actualidad. <https://www.forbes.com.mx/desperdicio-de-alimentos-en-mexico-cuesta-25000-mdd-al-ano/>

Frank, X., & Perré, P. (2010). The Potential of Meshless Methods to Address Physical and Mechanical Phenomena Involved during Drying at the Pore Level. Drying Technology, 28(8), 932–943. <https://doi.org/10.1080/07373937.2010.497077>

Galliou, F., Markakis, N., Fountoulakis, M. S., Nikolaidis, N., & Manios, T. (2018). Production of organic fertilizer from olive mill wastewater by combining solar greenhouse drying and composting. Waste Management, 75, 305–311. <https://doi.org/10.1016/J.WASMAN.2018.01.020>

Gulati, T., & Datta, A. K. (2013). Enabling computer-aided food process engineering: Property estimation equations for transport phenomena-based models. Journal of Food Engineering, 116(2), 483–504. <https://doi.org/10.1016/J.JFOODENG.2012.12.016>

Gupta, V., Sharma, A., & Gupta, K. S. (2018). Numerical Analysis of Direct Type Greenhouse Dryer. ASME 2017 Gas Turbine India Conference, GTINDIA 2017, 2. <https://doi.org/10.1115/GTINDIA2017-4784>

Helwa, N. H., Khater, H. A., Enayet, M. M., & Hashish, M. I. (2007). Experimental Evaluation of Solar Kiln for Drying Wood. *Drying Technology*, 22(4), 703–717. <https://doi.org/10.1081/DRT-120034258>

Hempattarasuwan, P., Somsong, P., Duangmal, K., Jaskulski, M., Adamiec, J., & Srzednicki, G. (2019). Performance evaluation of parabolic greenhouse-type solar dryer used for drying of cayenne pepper. *Drying Technology*, 38(1–2), 48–54. <https://doi.org/10.1080/07373937.2019.1609495>

Holland, J. H., & Torres Alexander, E. (2004). *El orden oculto: de cómo la adaptación crea la complejidad*. Fondo de Cultura Económica.

Hossain, M. A., & Bala, B. K. (2007). Drying of hot chilli using solar tunnel drier. *Solar Energy*, 81(1), 85–92. <https://doi.org/10.1016/J.SOLENER.2006.06.008>

Jain, D. (2005). Modeling the performance of greenhouse with packed bed thermal storage on crop drying application. *Journal of Food Engineering*, 71(2), 170–178. <https://doi.org/10.1016/J.JFOODENG.2004.10.031>

Jain, D., & Tiwari, G. N. (2004). Effect of greenhouse on crop drying under natural and forced convection I: Evaluation of convective mass transfer coefficient. *Energy Conversion and Management*, 45(5), 765–783. [https://doi.org/10.1016/S0196-8904\(03\)00178-X](https://doi.org/10.1016/S0196-8904(03)00178-X)

Jamaledine, T. J., & Ray, M. B. (2010). Application of Computational Fluid Dynamics for Simulation of Drying Processes: A Review. *Drying Technology*, 28(2), 120–154. <https://doi.org/10.1080/07373930903517458>

Janjai, S., Intawee, P., Kaewkiew, J., Sritus, C., & Khamvongsa, V. (2011). A large-scale solar greenhouse dryer using polycarbonate cover: Modeling and testing in a tropical environment of Lao People's Democratic Republic. *Renewable Energy*, 36(3), 1053–1062. <https://doi.org/10.1016/J.RENENE.2010.09.008>

Janjai, S., Phusampao, C., Nilnont, W., & Pankaew, P. (2014). Experimental performance and modeling of a greenhouse solar dryer for drying macadamia nuts. *International Journal of Scientific & Engineering Research*, 5(6). <http://www.ijser.org>

Jitjack, K., Thepa, S., Sudaprasert, K., & Namprakai, P. (2016). Improvement of a rubber drying greenhouse with a parabolic cover and enhanced panels. *Energy and Buildings*, 124, 178–193. <https://doi.org/10.1016/J.ENBUILD.2016.04.030>

Kadam, D. M., Nangare, D. D., Singh, R., & Kumar, S. (2011). Low-Cost Greenhouse Technology For Drying Onion (*Allium Cepa* L.) Slices. *Journal of Food Process Engineering*, 34(1), 67–82. <https://doi.org/10.1111/J.1745-4530.2008.00337.X>

Kaewkiew, J., Nabnean, S., & Janjai, S. (2012). Experimental investigation of the performance of a large-scale greenhouse type solar dryer for drying chilli in Thailand. *Procedia Engineering*, 32, 433–439. <https://doi.org/10.1016/J.PROENG.2012.01.1290>

Kemp, I. C. (2007). Drying Software: Past, Present, and Future. *Drying Technology*, 25(7–8), 1249–1263. <https://doi.org/10.1080/07373930701438709>

Kooli, S., Fadhel, A., Farhat, A., & Belghith, A. (2007). Drying of red pepper in open sun and greenhouse conditions.: Mathematical modeling and experimental validation. *Journal of Food Engineering*, 79(3), 1094–1103. <https://doi.org/10.1016/J.JFOODENG.2006.03.025>

Koyuncu, T. (2006). An Investigation on the performance Improvement of greenhouse-type agricultural dryers. *Renewable Energy*, 31(7), 1055–1071. <https://doi.org/10.1016/J.RENENE.2005.05.014>

Krawczyk, P., & Badyda, K. (2011). Two-dimensional CFD modeling of the heat and mass transfer process during sewage sludge drying in a solar dryer. *Archives of Thermodynamics*, 32(4), 3–16. <https://doi.org/10.2478/V10173-011-0028-Y>

Kumar, A., Deep, H., Prakash, O., & Ekechukwu, O. v. (2017). Advancement in greenhouse drying system. *Green Energy and Technology*, 0(9789811038327), 177–196. [https://doi.org/10.1007/978-981-10-3833-4\\_5](https://doi.org/10.1007/978-981-10-3833-4_5)

Kumar, A., & Shrivastava, V. (2017). Historical Trends and Recent Developments in Solar Greenhouse Dryer Operated Under Active Mode: A Review. *Indian Journal of Science and Technology*, 10(33), 1–16. <https://doi.org/10.17485/IJST/2017/V10I33/116988>

Kumar, A., & Tiwari, G. N. (2006). Thermal Modeling and Parametric Study of a Forced Convection Greenhouse Drying System for Jaggery: An Experimental Validation. *International Journal of Agricultural Research*, 1(3), 265–279. <https://doi.org/10.3923/IJAR.2006.265.279>

Kumar, A., & Tiwari, G. N. (2007). Effect of mass on convective mass transfer coefficient during open sun and greenhouse drying of onion flakes. *Journal of Food Engineering*, 79(4), 1337–1350. <https://doi.org/10.1016/J.JFOODENG.2006.04.026>

Leon, M. A., Kumar, S., & Bhattacharya, S. C. (2002). A comprehensive procedure for performance evaluation of solar food dryers. *Renewable and Sustainable Energy Reviews*, 6(4), 367–393. [https://doi.org/10.1016/S1364-0321\(02\)00005-9](https://doi.org/10.1016/S1364-0321(02)00005-9)

Lima, M. R. P., Zandonade, E., & Sobrinho, P. A. (2012). Characteristics of WWTP sludge after drying in greenhouse for agricultural purposes. *Water*

Science and Technology, 66(7), 1460–1466.  
<https://doi.org/10.2166/WST.2012.326>

Lokeswaran, S., & Eswaramoorthy, M. (2013). An Experimental Analysis of a Solar Greenhouse Drier: Computational Fluid Dynamics (CFD) Validation. *Energy Sources, Part A: Recovery, Utilization, and Environmental Effects*, 35(21), 2062–2071. <https://doi.org/10.1080/15567036.2010.532195>

Maálaga, J. E., Williams, G. W., & Fuller, S. W. (2001). US–Mexico fresh vegetable trade: the effects of trade liberalization and economic growth. *Agricultural Economics*, 26(1), 45–55. [https://doi.org/10.1016/S0169-5150\(00\)00101-8](https://doi.org/10.1016/S0169-5150(00)00101-8)

Mahapatra, A., & Tripathy, P. P. (2019). Experimental investigation and numerical modeling of heat transfer during solar drying of carrot slices. *Heat and Mass Transfer/Waerme- Und Stoffuebertragung*, 55(5), 1287–1300. <https://doi.org/10.1007/S00231-018-2492-2/FIGURES/11>

Manohar, k., & Chandra, P. (2000). Drying of agricultural procedure in a greenhouse type solar dryer. *International Agricultural Engineering Journal*, 9(3), 139–150.

Mitchell, M. (2009). *Complexity: a guided tour*. Oxford University Press.

Morad, M. M., El-Shazly, M. A., Wasfy, K. I., & El-Maghawry, H. A. M. (2017). Thermal analysis and performance evaluation of a solar tunnel greenhouse dryer for drying peppermint plants. *Renewable Energy*, 101, 992–1004. <https://doi.org/10.1016/J.RENENE.2016.09.042>

Noh, A. M., Mat, S., & Ruslan, M. H. (2018). CFD simulation of temperature and air flow distribution inside industrial scale solar dryer. *Journal of Advanced Research in Fluid Mechanics and Thermal Sciences*, 45(1), 156–164.

Norton, T., & Sun, D. W. (2006). Computational fluid dynamics (CFD) – an effective and efficient design and analysis tool for the food industry: A review. *Trends in Food Science & Technology*, 17(11), 600–620. <https://doi.org/10.1016/J.TIFS.2006.05.004>

Ong, K. S. (2007). Experimental Investigation of a Solar Bamboo Dryer. *Drying Technology*, 14(10), 2411–2417. <https://doi.org/10.1080/07373939608917213>

Patel, A., & Patel, G. (2014). Operational Augmentation of Forced Circulation Type Solar Dryer System Using CFD Analysis. *Journal of Engineering Research and Applications Wwww.Ijera.Com*, 4(4), 265–268. [www.ijera.com](http://www.ijera.com)

Patil, R. C., & Gawande, R. R. (2018). Drying characteristics of amla candy in solar tunnel greenhouse dryer. *Journal of Food Process Engineering*, 41(6), e12824. <https://doi.org/10.1111/JFPE.12824>

Patil, R., & Gawande, R. (2016). A review on solar tunnel greenhouse drying system. *Renewable and Sustainable Energy Reviews*, 56, 196–214. <https://doi.org/10.1016/J.RSER.2015.11.057>

Perea-Moreno, A. J., Juaidi, A., & Manzano-Agugliaro, F. (2016). Solar greenhouse dryer system for wood chips improvement as biofuel. *Journal of Cleaner Production*, 135, 1233–1241. <https://doi.org/10.1016/J.JCLEPRO.2016.07.036>

Perré, P. (2010). Multiscale Modeling of Drying as a Powerful Extension of the Macroscopic Approach: Application to Solid Wood and Biomass Processing.

<https://doi.org/10.1080/07373937.2010.497079>, 28(8), 944–959.  
<https://doi.org/10.1080/07373937.2010.497079>

Phonetip, K., Ozarska, B., Harris, G., Belleville, B., & Brodie, G. I. (2019). Quality assessment of the drying process for Eucalyptus delegatensis timber using greenhouse solar drying technology. *European Journal of Wood and Wood Products*, 77(1), 57–62. <https://doi.org/10.1007/S00107-018-1364-2/TABLES/3>

Prakash, O., & Kumar, A. (2013). Historical Review and Recent Trends in Solar Drying Systems. *International Journey of Green Energy*, 10(7), 690–738. <https://doi.org/10.1080/15435075.2012.727113>

Purusothaman, M., Valarmathi, T. N., & Santhosh, P. S. (2019). CFD Analysis of Greenhouse Solar Dryer with Different Roof Shapes. 5th International Conference on Science Technology Engineering and Mathematics, ICONSTEM 2019, 408–412. <https://doi.org/10.1109/ICONSTEM.2019.8918788>

Rachmat, R., & Horibe, K. (1999). Solar heat collection characteristics of a fiber reinforced plastic drying house. *Transactions of the ASAE*, 42(1), 149–157. <https://doi.org/10.13031/2013.13190>

Rankins, J., Sathe, S. K., & Spicer, M. T. (2008). Solar Drying of Mangoes: Preservation of an Important Source of Vitamin A in French-Speaking West Africa. *Journal of the American Dietetic Association*, 108(6), 986–990. <https://doi.org/10.1016/J.JADA.2008.03.013>

Rivera O. L. (2018). ¿Sabes cuántas toneladas de comida tira México a la basura? <https://www.eluniversal.com.mx/nacion/sociedad/mexico-desperdicia-20-millones-de-toneladas-de-comida>

Rodriguez, S. (2019). Best Practices of the CFD Trade. *Applied Computational Fluid Dynamics and Turbulence Modeling*, 225–273. [https://doi.org/10.1007/978-3-030-28691-0\\_6](https://doi.org/10.1007/978-3-030-28691-0_6)

Román-Roldán, N. I., Ituna Yudsonago, J. F., López-Ortiz, A., Rodríguez-Ramírez, J., & Sandoval-Torres, S. (2021). A new air recirculation system for homogeneous solar drying: Computational fluid dynamics approach. *Renewable Energy*, 179, 1727–1741. <https://doi.org/10.1016/J.RENENE.2021.07.134>

Román-Roldán, N. I., López-Ortiz, A., Ituna-Yudsonago, J. F., García-Valladares, O., & Pilatowsky-Figueroa, I. (2019). Computational fluid dynamics analysis of heat transfer in a greenhouse solar dryer “chapel-type” coupled to an air solar heating system. *Energy Science & Engineering*, 7(4), 1123–1139. <https://doi.org/10.1002/ESE3.333>

Sacilik, K., Keskin, R., & Elicin, A. K. (2006). Mathematical modelling of solar tunnel drying of thin layer organic tomato. *Journal of Food Engineering*, 73(3), 231–238. <https://doi.org/10.1016/J.JFOODENG.2005.01.025>

Sahdev, R. K., Kumar, M., & Dhingra, A. K. (2018). Development of empirical expression for the groundnuts drying inside a greenhouse. *International Food Research Journal*, 25(5), 1858–1863.

Sethi, V. P., & Arora, S. (2009). Improvement in greenhouse solar drying using inclined north wall reflection. *Solar Energy*, 83(9), 1472–1484. <https://doi.org/10.1016/J.SOLENER.2009.04.001>

Sethi, V. P., & Dubey, R. K. (2011). Development of dual purpose greenhouse coupled with north wall utilization for higher economic gains. *Solar Energy*, 85(5), 734–745. <https://doi.org/10.1016/J.SOLENER.2011.01.004>

Somsila, P., & Teeboonma, U. (2014). Investigation of temperature and air flow inside Para rubber greenhouse solar dryer incline roof type by using CFD technique. *Advanced Materials Research*, 931–932, 1238–1242. <https://doi.org/10.4028/WWW.SCIENTIFIC.NET/AMR.931-932.1238>

Spiroski, M. (2013). Analysis of Macedonian medical scientific papers in the Scopus database. *Macedonian Journal of Medical Sciences*, 6(1), 5–10. <https://doi.org/10.3889/MJMS.1857-5773.2013.0284>

Srichat, A., Vengsungle, P., Hongtong, K., Kaewka, W., & Jongpluempiti, J. (2019). A Comparison of Temperature for Parabola and Sinusoidal Greenhouse Solar Dryer by CFD. *IOP Conference Series: Materials Science and Engineering*, 501(1), 012006. <https://doi.org/10.1088/1757-899X/501/1/012006>

Strumiłło, C. (2007). Perspectives on Developments in Drying. *https://Doi.Org/10.1080/07373930600778056*, 24(9), 1059–1068. <https://doi.org/10.1080/07373930600778056>

Tanwanichkul, B., Thepa, S., & Rordprapat, W. (2013). Thermal modeling of the forced convection Sandwich Greenhouse drying system for rubber sheets. *Energy Conversion and Management*, 74, 511–523. <https://doi.org/10.1016/J.ENCONMAN.2013.06.020>

Tham, T. C., Ng, M. X., Gan, S. H., Chua, L. S., Aziz, R., Chuah, L. A., Hii, C. L., Ong, S. P., Chin, N. L., & Law, C. L. (2017). Effect of ambient conditions on drying of herbs in solar greenhouse dryer with integrated heat pump. *https://Doi-Org.Ezproxy2.Library.Arizona.Edu/10.1080/07373937.2016.1271984*, 35(14), 1721–1732. <https://doi.org/10.1080/07373937.2016.1271984>

Tiwari, A. (2016). A Review on Solar Drying of Agricultural Produce. *Journal of Food Processing & Technology*, 7(9). <https://doi.org/10.4172/2157-7110.1000623>

Tiwari, S., Tiwari, G. N., & Al-Helal, I. M. (2016). Performance analysis of photovoltaic–thermal (PVT) mixed mode greenhouse solar dryer. *Solar Energy*, 133, 421–428. <https://doi.org/10.1016/J.SOLENER.2016.04.033>

Toshing, K., Lamlert, N., Mundpookhier, T., Chanaalert, W., & Bala, K. (2018). Experimental performance and artificial neural network modeling of solar drying of litchi in the parabolic greenhouse dryer. *Journal of Renewable Energy and Smart Grid Technology*, 13(1), 1–12.

Verma, P. (n.d.). A Review Paper on Solar Greenhouse Dryer. *Journal of Mechanical and Civil Engineering*. Retrieved July 12, 2022, from <https://www.iosrjournals.org/iosr-jmce/papers/Conf15010/Vol-2/8.%2043-48.pdf>

Versteeg, H. K., & Malalasekera, W. (1996). *An introduction to computational fluid dynamics: the finite volume method*, 1995. Harlow-Longman Scientific & Technical, London, M, 503.

Villagran, E., Henao-Rojas, J. C., & Franco, G. (2021). Thermo-Environmental Performance of Four Different Shapes of Solar Greenhouse Dryer with Free Convection Operating Principle and No Load on Product. *Fluids* 2021, Vol. 6, Page 183, 6(5), 183. <https://doi.org/10.3390/FLUIDS6050183>

Vittuari, M., Pagani, M., Johnson, T. G., & de Menna, F. (2020). Impacts and costs of embodied and nutritional energy of food waste in the US food system: Distribution and consumption (Part B). *Journal of Cleaner Production*, 252, 119857. <https://doi.org/10.1016/J.JCLEPRO.2019.119857>

Vivekanandan, M., Periasamy, K., Babu, C. D., Selvakumar, G., & Arivazhagan, R. (2021). Experimental and CFD investigation of six shapes of solar greenhouse dryer in no load conditions to identify the ideal shape of dryer. *Materials Today*:

Proceedings, 37(Part 2), 1409–1416.  
<https://doi.org/10.1016/J.MATPR.2020.07.062>

Yadav, A. S., & Bhagoria, J. L. (2013). Heat transfer and fluid flow analysis of solar air heater: A review of CFD approach. *Renewable and Sustainable Energy Reviews*, 23, 60–79. <https://doi.org/10.1016/J.RSER.2013.02.035>

# 7 TWO NEW AIR DISTRIBUTION SYSTEMS TO ENHANCE DRYING IN GREENHOUSES

FOR SUBMISSION TO BIOSYSTEMS ENGINEERING JOURNAL

Valencia-Islas J. O., Kacira M.\* , Lopez-Cruz I.L., Giacomelli G., Ruiz-Garcia A.,  
Li P.

## 7.1 ABSTRACT

The drying of agricultural products in greenhouses is a practice that has gained momentum due to the improvement in the quality of the product, as well as the possibility of controlling the microenvironment inside the greenhouse system. The present study first validated a CFD model for greenhouse-type dryer and then evaluated various air distribution design that can enhance drying process. The greenhouse solar type dryer used for model validation was located at the Universidad Autonoma Chapingo (Mexico), with dimensions 9 x 12 x 3.4 m. The greenhouse has a 6 mm polycarbonate cover, a 15 cm thick concrete floor, and four air inlets. Two Cases for air distribution system designs were evaluated including a double tubing row and three tubing rows with holes distributed in their lengths. The results indicated that the air in the attic of the greenhouse has a higher air temperature. Both air distribution systems to force the air in the attic to flow under the drying tables tested provided satisfactory results in the homogeneity of the air temperature at the vertical level in the greenhouse. The mean air temperature in the experimental greenhouse is 45°C and with the newly designed systems it was further enhance to 52 °C. The air temperature and velocity in the greenhouse obtained from the new design were suitable for drying. The density and air distribution homogeneities were improved with the two new designs proposed, but the air distribution design with three tubes provided

improved environmental uniformity and much improved air temperatures especially at the product tray levels. The study considers the case where no exhaust fans were activated as a first stage of control before evacuating the indoor air

**Keywords:** Optimization, CFD, solar drying, mathematical modeling

## 7.2 INTRODUCTION

Solar drying in greenhouses has been studied in recent years as an alternative to conventional solar drying systems and those whose natural convection is the driving force. Due to their size, greenhouse-type solar dryers need fans that can extract moist air and produce forced convection to improve temperature and humidity uniformity, which is linked to the quality of the product to be dried (Deng et al., 2021; Noh et al., 2018).

The development of greenhouse-type solar dryers with forced ventilation responds to the fact that natural convection dryers are not the best to be used for drying fish, fruits, and vegetables on a semi-industrial or industrial scale (Janjai & Bala, 2012). However, the modeling of forced convection with a special focus on the air temperature and velocity distribution inside the greenhouse becomes complex due to the number of variables involved in the process. Being able to describe how the air behaves inside the greenhouse volume can be used to improve the design and, therefore, the solar drying in these systems (Duong et al., 2021a; Román-Roldán et al., 2019).

The computational fluid dynamics approach can be very useful for the purposes to redesign and improve actual conditions (Rodriguez, 2019). However, much remains to be done to understand the dynamics of drying in greenhouse-type solar dryers, considering that each greenhouse has a different size, location, roof shape, and equipment (Srinivasan & Muthukumar, 2021). Krawczyk &

Badyda (2011) focused on a 2D study on a greenhouse dryer for sludge. The air velocity was not studied just the air and product temperatures. The 2D studies lack velocity and turbulence reports and are not common for greenhouse-type dryers.

On the other hand, some 3D studies have been carried out to evaluate the air distribution temperature (Duong et al., 2021a; Srichat et al., n.d.; Villagran et al., 2021), air velocity (Duong et al., 2021b; Román-Roldán et al., 2021; Villagran et al., 2021), geometry testing (Purusothaman et al., 2019; Villagran et al., 2021; Vivekanandan et al., 2021), and different materials in its construction (Deng et al., 2021; Srinivasan & Muthukumar, 2021). Not enough work has been done to report solar radiation (Lokeswaran & Eswaramoorthy, 2013; Román-Roldán et al., 2019; Somsila & Teeboonma, 2014) and turbulence, except for (Gupta et al., 2018; Román-Roldán et al., 2019; Somsila & Teeboonma, 2014); and the product to be dried in 3D. The only way to improve the drying process in greenhouses is to study all the variables at once.

Therefore, the objectives of the present study were 1) to develop and validate a CFD model that is suitable for predicting the indoor environment in a greenhouse-type solar dryer; 2) to evaluate alternative air distribution system designs using the validated CFD model for improving the drying process and homogenizing the air temperature and velocity and air distributions in the greenhouse solar dryer system.

## **7.3 MATERIALS AND METHODS**

### **7.3.1 Experimental Setup**

The greenhouse is located at the Universidad Autonoma Chapingo, Mexico (2250 meters above sea level, 19°29' N, 98°53' W). The city of Chapingo is in the center of the country with temperate weather. The greenhouse cover is made of polycarbonate and has a 6 mm thick parabolic shape, a 15 cm thick concrete floor,

four air inlets covered with anti-aphid mesh, and a double door to prevent heat from escaping when it is closed. The total volume of the greenhouse is 211 m<sup>3</sup> and an area of 108 m<sup>2</sup> (Figure 7-1). The height of the two upper air inlets coincides with the height of the drying tables. The experiment from which the measurements were obtained was carried out on May 3rd, 2021, without a product inside the dryer.

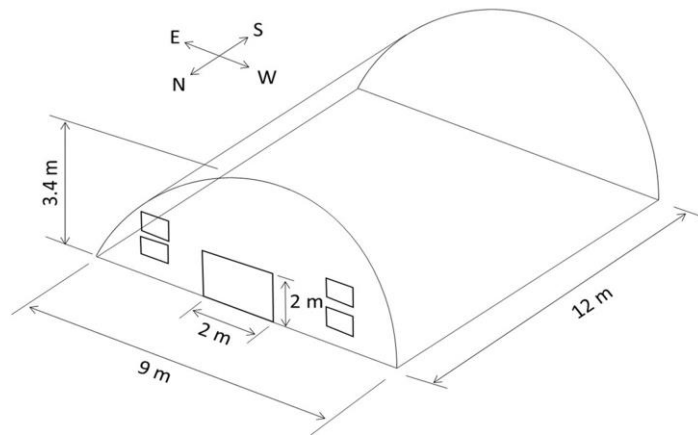


**Figure 7-1.** Greenhouse-type solar dryer used for this study. Orientation and dimensions.

### 7.3.2 Instrumentation

Measurements were made inside and outside the greenhouse and variables were recorded every five minutes. The variables measured inside the greenhouse were the air temperature and relative humidity, with a CS215L sensor (Campbell Sci,  $\pm 2\%$ ,  $\pm 0.4^\circ\text{C}$  accuracies) in different locations inside the greenhouse (Figure 7-2); solar radiation, with a CMP3 pyranometer (Kipp & Zonen,  $5 \mu\text{V} / \text{W} / \text{m}^2$  accuracy); wind speed was measured with a WINDSONIC4 sensor (Campbell Sci,  $\pm 2\%$  Accuracy) placed between one of the air inlets and the drying tables. To measure the temperature and relative humidity of the air outside the greenhouse, an HMP60 digital sensor (Vaisala,  $\pm 3\%$ ,  $\pm 0.6^\circ\text{C}$ , accuracy) was used, and a Hukseflux pyranometer (LP02-L, Campbell Sci.) was used for solar radiation. The sensors were placed in a location near the greenhouse but at a height higher than the greenhouse cover. The data time used

for the comparison was with the solar radiation from 10 am, where the solar radiation started to raise the temperature, but the exhaust fans are not activated.

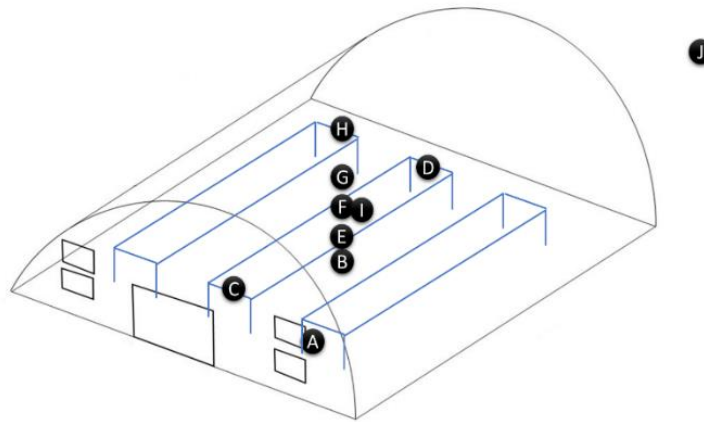


**Figure 7-2.** Sensor distribution in the greenhouse-type solar dryer. A) WINDSONIC4, B) CS215-L floor, C) North wall 0.95 m, D) South wall 0.95 m, E) Cs215-L 0.6m, F) CS215-L 0.95 m, G) CS215-L 1.9m, H) CS215-L 2.65 m, I) CMP3 pyranometer and J) Sensors outside the greenhouse.

### 7.3.3 Meshing and Simulations

For the evaluation case, the greenhouse geometry was meshed with tetrahedral elements with good quality and some refinement on the top of the cover (Figure 7-3). The element refinement was considered as the geometry of the greenhouse cover has a parabolic shape and the study of solar radiation as the main source of heat was an important part of the study. Compared to the next cases, the geometry was just the greenhouse with the cover and the inlets.

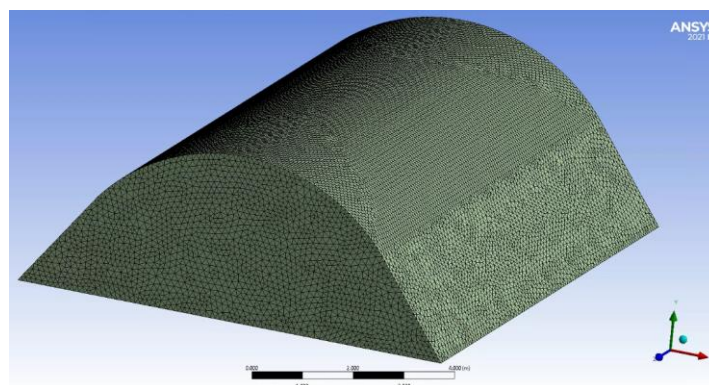


**Figure 7-3.** Evaluation Case mesh.

The geometric models used contemplate the greenhouse as a model for evaluation, called case A (Figure 7-1); the greenhouse with a recirculation system with two lines and a single hole (Figure 7-4), called case B; and the greenhouse with the recirculation system with three lines (Figure 7-5), called case C. Each geometric model has the same measurements of the greenhouse located at the Universidad Autonoma Chapingo and was only simplified by extracting the interior volume in ANSYS Workbench SpaceClaim. For this study, the geometry of the lines was selected as squares (Figure 7-6).

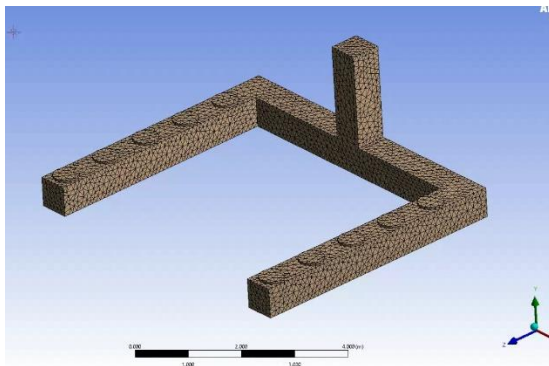


**Figure 7-4.** First design proposal for air distribution system with 2 lines. Case B.

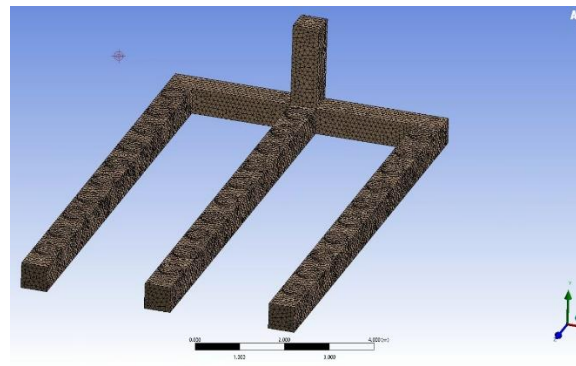


**Figure 7-5.** Second design proposal for air distribution system with 3 lines. Case C.

The mesh was generated with the Fluent meshing software in each of the three geometries (Figure 7-7) with a different number of nodes when the redistribution systems were added all of them with tetrahedral elements. According to ANSYS (2010), the acceptable ranges for each mesh quality statistic are as follows: the aspect ratio should be in general  $\leq 5$ ; the skewness range for excellent is from 0 to 0.25 and for good quality 0.25 to 0.5; for orthogonality, the acceptable range is from 0.15 to 1.0, the close to 0 the worst. The meshes were analyzed and the values of the statistics were found within the favorable range in each case (Table 7-1).

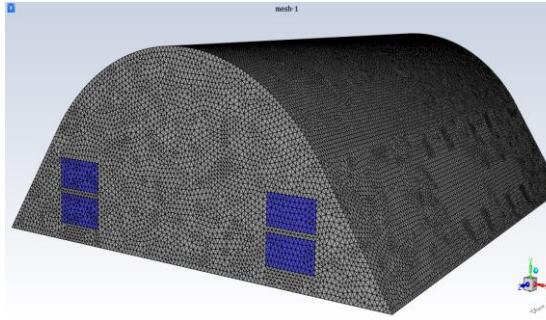


**Figure 7-6.** Greenhouse mesh with the inlets (blue) done by the Fluent meshing program.

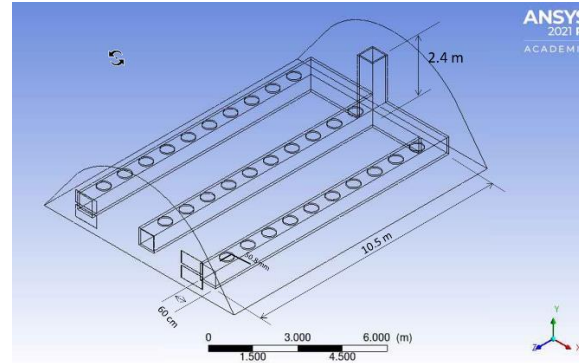


**Figure 7-7.** Dimensions of the B and C systems. The B system is located at the half of the greenhouse while the C is located at the south wall.

For the simulations, a computer with the following specifications was used: CPU – Intel Xeon E5-2630 v4@2.2GHz; 64GB RAM memory; NVIDIA Quadro M2000 36GB and SSD SanDisk 12G1001. Each simulation of the Evaluation Case had a computational cost of 24 hours with the selected mesh. For geometries B and C, the PC took 48 hours and 52 hours, respectively.

**Table 7-1.** Mesh quality statistics for all geometries under study.

Case	Nodes	Elements	Aspect ratio	Skewness	Orthogonality
<b>A</b>	570167	388816	<4.68 ( $\mu = 1.88,$ $\sigma = 0.356$ )	0-0.39 ( $\mu =$ 0.26, $\sigma = 0.095$ )	0.61-0.96 ( $\mu = 0.75, \sigma = 0.093$ )
<b>B</b>	100980	489253	<3 ( $\mu = 1.89,$ $\sigma = 0.37$ )	0-0.42 ( $\mu = 0.26, \sigma =$ 0.099)	0.5-0.96 ( $\mu = 0.74, \sigma = 0.097$ )
<b>C</b>	212769	1072424	<2.4 ( $\mu = 1.86,$ $\sigma = 0.47$ )	0.04-0.42 ( $\mu = 0.24, \sigma =$ 0.091)	0.58-0.95 ( $\mu = 0.76, \sigma = 0.090$ )

The CFD model was first validated by comparing the model predictions against the experimental data. with the Case A shown above. The air temperature

was the main variable for comparison for the evaluation due to its significant affect in the drying process (Duong et al., 2021). For testing the new designs, the fan velocity was calculated to be 5 m s<sup>-1</sup> that ensured sufficient flow through the system and distributed the air effectively to the whole greenhouse volume.

## 7.4 THEORY/CALCULATIONS

### 7.4.1 Mathematical Models

The solar dryer was considered as a system at steady state, with turbulence, in 3D, and with an atmospheric pressure of 77993 Pa (Chapingo, Mexico). It is important to mention that the change in pressure generates a change in the properties of humid air, which were calculated using the equations provided by ASHRAE in its manual (American Society of Heating, 1989). The equations that represent the transport inside the greenhouse, better known as Navier Stokes, were the following (Versteeg & Malalasekera, 1996):

Conservation of mass or continuity equation

$$\frac{\partial \rho}{\partial t} + \nabla(\rho U) = 0 \quad (\text{Eq. 7-1})$$

Momentum conservation

$$\frac{\partial}{\partial t}(\rho U) + \nabla(\rho U U) = \nabla p + \mu \nabla U^2 + \rho g + S_h \quad (\text{Eq. 7-2})$$

Energy conservation

$$\nabla(-k \nabla T + \rho C_p T U) = S_T \quad (\text{Eq. 7-3})$$

where  $\partial t$  is a partial derivative in terms of time,  $T$  is the temperature,  $U$  is the velocity vector,  $g$  is the gravity force,  $p$  is the pressure,  $C_p$  is the specific heat,  $k$  is the thermal conductivity,  $\mu$  is the dynamic viscosity,  $S_h$  and  $S_T$  are the source terms for heat transfer and momentum.

The effect of turbulence through the dryer inlets was modeled with the realizable k- $\epsilon$  model, based on the turbulent kinetic energy ( $k$ ) and velocity ( $\epsilon$ ). Moist air was modeled with species transport as a mixture of air and water vapor at atmospheric pressure in Chapingo. The solar radiation model used was the discrete ordinates (DO) because it allows the use of semi-transparent boundary conditions. The radiation model can be used by coupling to the radiation transfer equation by equation (ANSYS, 2011):

$$\sum_{j=1}^N \mu_j^T T_j - \beta_i^T T_i - \alpha_i^T \sum_{k=1}^L I_i^k \omega_k - S_i^T S_i^h \quad (\text{Eq. 7-4})$$

where,  $\alpha_i^T = k \Delta V_i$ ,  $\beta_i^T = 16k\sigma T_i^{*3} \Delta V_i$ ,  $S_i^T = 12k\sigma T_i^{*4} \Delta V_i$ .  $k =$  absorption coefficient,  $\Delta V =$  control volume.

The  $\mu_j^T$  coefficient and the source term  $S_i^h$  are due to the discretization of the convection and diffusion terms.

#### 7.4.2 Boundary conditions

The boundary conditions included the solar radiation flux on the walls that correspond to the greenhouse cover; considered the ground as opaque; four air inlets with a constant speed during the simulation; natural convection inside the greenhouse and initial temperatures equal to ambient temperature (Table 7-2). The walls were considered stationary without a slip shear condition. The operating conditions are presented in Table 7-3. The Boussinesq approximation was not considered as the density depends on the temperature (Ferziger & Perić, 2002),

hence the assumption that density changes are negligible could be invalid at any time.

**Table 7-2.** Boundary conditions used for the simulations.

Case	Name	Boundary conditions	Material	Parameter	Value	Source
A	Cover	Wall (semi-transparent)	Polycarbonate	Thickness (m)	0.006	User-defined
				Emissivity	0.9	(Román-Roldán et al., 2019)
				Density (kg m <sup>-3</sup> )	1200	(Zhang & Xu, 2019)
				Heat transfer coeff. (W m <sup>-2</sup> K <sup>-1</sup> )	3.63	(Shultz, 1999)
				Specific heat (J kg <sup>-1</sup> K <sup>-1</sup> )	1200	(Shultz, 1999)
				Absorptivity	0.2	User-defined
				Transmissivity	0.8	(Serrano & Moreno, 2020)
	Floor	Wall (opaque)	Concrete	Thickness (m)	0.15	User-defined
				Density (kg m <sup>-3</sup> )	2200	(Asadi et al., 2018)
				Heat transfer coeff. (W m <sup>-2</sup> K <sup>-1</sup> )	2.25	(Asadi et al., 2018)
				Specific heat (J kg <sup>-1</sup> K <sup>-1</sup> )	880	(Villagran et al., 2021a)
	Inlet greenhouse	- Velocity inlet	Humid air	Velocity (m s <sup>-1</sup> )	0.1	Measured
				Temperature (°C)	24	Measured
				Specific mass (kg kg <sup>-1</sup> )	0.0061	Computed

	Ventilation inlet	Velocity inlet	Humid air	Velocity (m s <sup>-1</sup> )	5	User-defined
				Specific mass (kg kg <sup>-1</sup> )	0.0061	Computed
<b>B and C</b>	Body vent	Wall	Polyethylene	Thickness (mil)	6	User-defined
				Density (kg m <sup>-3</sup> )	920	(Villagran et al., 2021a)
				Thermal conductivity (W m <sup>-2</sup> K <sup>-1</sup> )	0.30	(Villagran et al., 2021a)
				Specific heat (J kg <sup>-1</sup> K <sup>-1</sup> )	1900	(Villagran et al., 2021a)
	Outlet vent	Pressure outlet	-	Pressure (Pa)	77993	User-defined

**Table 7-3.** Operating conditions used for the simulations.

<b>Solver</b>	3D simulation	Coupled
	Implicit formulation	
	Steady-state analysis	
	Pressure-based	
	Absolute formulation	
	Fluent Ansys 2021	
<b>Models</b>	Energy equation	activated
	Viscous model	k-ε Realizable, standard wall
	Species transport	H <sub>2</sub> O and air (ideal gas)
	Radiation	Discrete Ordinate (DO)
<b>Pressure</b>	77993 Pa	Chapingo, Mexico
<b>Date</b>	May 3rd, 2021	
<b>Gravity</b>	-9.81 m s <sup>-1</sup>	
<b>Outdoor Temperature</b>	24°C	

## 7.5 RESULTS

### 7.5.1 Evaluation

The measurements and simulations were compared (Table 7-4). In general, the results are below  $\pm 3^{\circ}\text{C}$  of uncertainty, which can be explained by the uncertainty associated with the sensors or because the metal drying tables were not modeled in Case A, however they were present when performing the measurements. Given the average temperature of  $45^{\circ}\text{C}$  and the average density  $0.88\text{ kg m}^{-3}$ , the average Enthalpy at product height was calculated as  $12.95\text{ kJ kg}^{-1}$ ; whereas the average energy available for at the product height was  $11.396\text{ kJ m}^{-3}$ .

**Table 7-4.** Evaluation points between measurements and simulations.

Measurements			Simulations		Difference
Sensor position	Position $(x, y, z)$	Temperature $(^{\circ}\text{C})$	Position	Temperature $(^{\circ}\text{C})$	$(^{\circ}\text{C})$
<b>B</b>	(0,0,-6)	40.69	(0,0,-6)	39.70	0.99
<b>E</b>	(0,0.6,-6)	45.66	(0,0.6,-6)	45.01	0.65
<b>F</b>	(0,1.9,-6)	49.62	(0,1.9,-6)	47.39	2.23
<b>G</b>	(0,2.65,-6)	47.64	(0,2.65,-6)	48.75	-1.11
<b>C</b>	(0,0.95,-1)	39.18	(0,0.95,-1)	41.20	-2.02
<b>D</b>	(0,0.95,-11)	43.88	(0,0.95,-11)	42.02	1.86

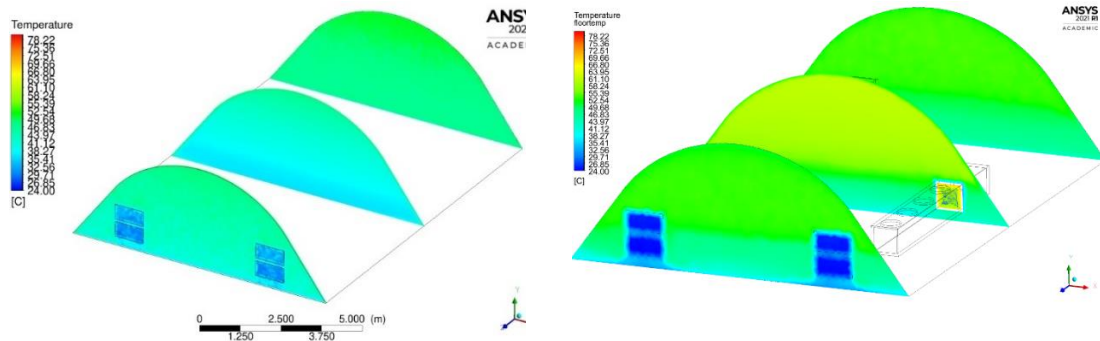
### 7.5.2 Air temperature

For the evaluation Case, the temperature distribution inside the greenhouse shows a vertical stratification with the data and simulations. The higher temperatures are in the attic of the greenhouse and at the south wall, at the far end of the dryer. The lowest temperatures are those found close to the inlets of the dryer as there is some mixing of the inside and outside air (Figure 7-8a). The

average temperature is 45 °C, but the disparity is noticeable both in the vertical and horizontal positions.

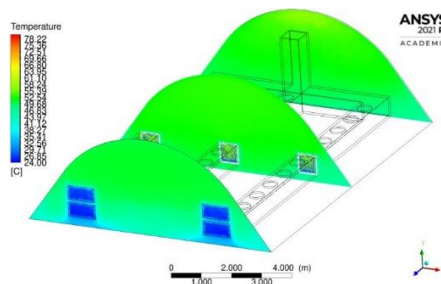
In Case B, the average temperature is 52 °C, more than sufficient for drying. Compared with the evaluation Case (Figure 7-8a), the increase in temperature at the level of the drying tables is noted, where the green color appears, to be specific (Figure 7-8b). Also, temperature stratification in both directions is reduced. The highest temperatures occur in the recirculation system (79 °C) and the lowest are found near the floor of the greenhouse (40 °C).

The air temperature with Case C showed better homogenization compared to both designs with two and three rows with holes. The average air temperature, at the height of the drying tables, was 52 °C (Figure 7-8c). By placing the air intake at the rear of the greenhouse, a space with a higher temperature concentrated near the south wall is observed, which did not occur with Case B.



a) Evaluation case. Case A.

b) Two lines design recirculation system. Case B.



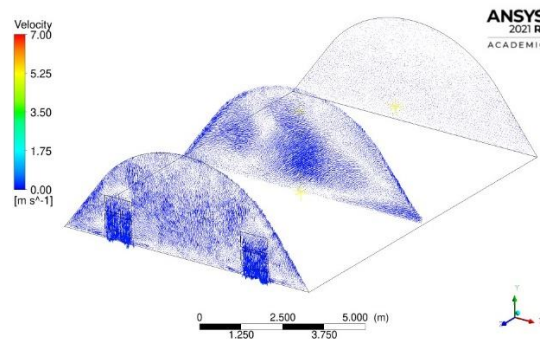
c) Three lines design recirculation system. Case C.

**Figure 7-8.** Air temperature distribution inside the greenhouse-type solar dryer with the different designs tested.

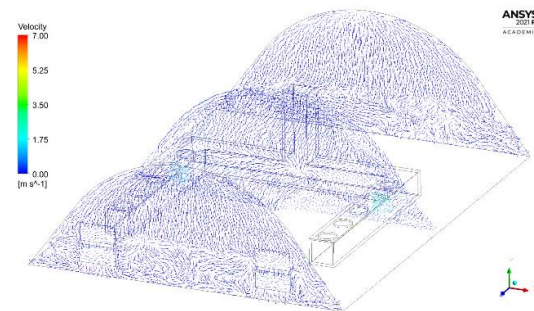
### 7.5.3 Air velocity

The evaluation results indicated that the highest speed occurred at the dryer inlet, more specifically at the lower inlets. The mixing of air due to the difference in densities caused a speed of approximately  $0.3 \text{ m s}^{-1}$  with places throughout the volume with lower speeds and stagnation of the air in the upper part of the greenhouse (Figure 7-9a). If Case B is considered, a higher speed was observed in the air recirculation system, due to the fan. However, an average velocity of  $0.4 \text{ m s}^{-1}$  can be found distributed in most of the volume with differences in some spots at the center, in the west cover (positive x-axis), and close to the back wall. This system takes the air from the central part and distributes it to the entire volume causing some differences. However, an improvement in the speed and distribution of the air at the level of the tables was observed (Figure 7-9b).

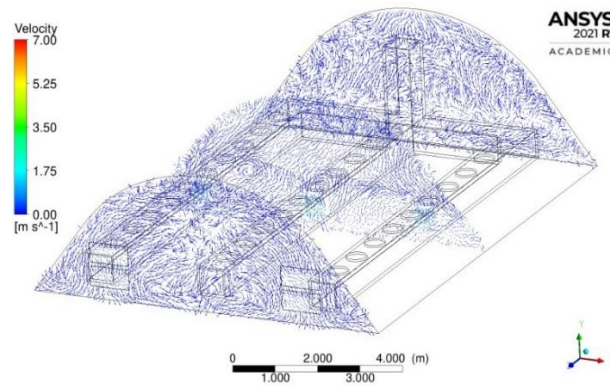
Finally, with Case C, satisfactory results are obtained when comparing them with the previous two. The average speed is  $0.35 \text{ m s}^{-1}$ , distributed throughout the volume of the greenhouse. The highest velocities occur within the recirculation system. However, when compared to the previous case, the length and arrangement of the three lines caused air velocity to be higher in the center than at the edges, and the air velocities at the end of the system were reduced (Figure 7-9c).



a) Evaluation case. Case A.



b) Two lines design recirculation system. Case B.



c) Three lines design recirculation system. Case C.

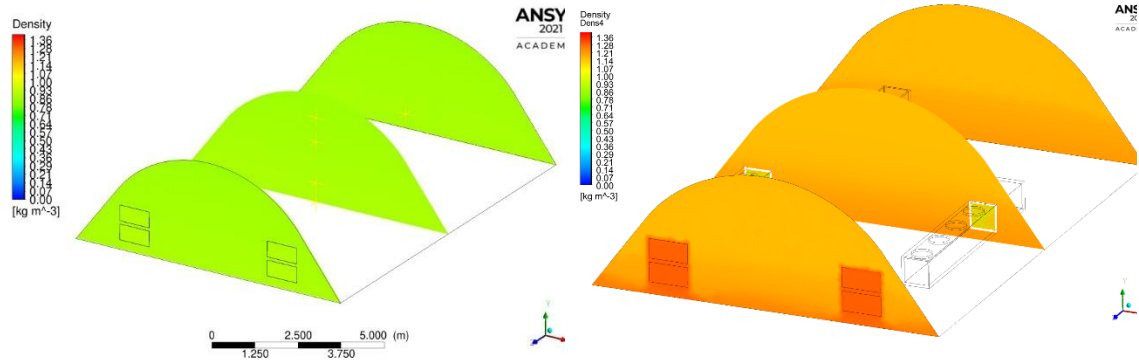
**Figure 7-9.** Air velocity distribution inside the greenhouse-type solar dryer.

#### 7.5.4 Air Density

The results for the air density are comparable to those of air temperature. Starting with Case A, the density ranges from 1.03 to 1.13 kg m<sup>-3</sup>. The greater values were found in the inlets of air as the outdoor temperature is lower than the indoor (Figure 7-10a). There is a stratification of the density due to the natural convection process and follows the results from air temperature; this makes sense as density depends on temperature.

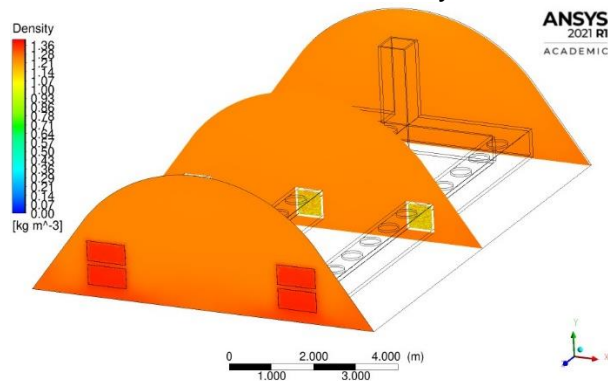
For the Case B, the mean density value is 1.2 kg m<sup>-3</sup>. The greater values were found in the lower part of the volume due to the lower temperatures, but the stratification was reduced when forced the air to flow below the drying tables (Figure 7-10b).

With Case C, the density shows a more homogenous density with a mean value of 1.22 kg m<sup>-3</sup>. Again, the stratification is the same as the air temperature. The greater values were found close to the floor and in the inlets (Figure 7-10c).



a) Evaluation case. Case A.

b) Two lines design recirculation system. Case B.



c) Three lines design recirculation system. Case C.

**Figure 7-10.** Air density distribution inside the greenhouse-type solar dryer.

## 7.6 DISCUSSION

### 7.6.1 Case A

The results indicated that the CFD model developed was sufficiently accurate to predict the air temperature based on comparisons with experimental data for the project greenhouse evaluated. The discrepancy in the obtained temperatures may be due to the same uncertainty and to the fact that in the real system there are materials that can absorb and emit heat during the day. An evaluation of the mesh was carried out in each case to determine that the results were reliable. Restrictions were placed on the maximum dimension of the elements in the mesh, considering the maximum as 0.1 m, achieving good results.

The temperature stratification that is observed in the dryer is due to the entry of air, mixing and producing that, being of lower temperature, it moves downwards while when heated and changes its density, it rises to the top in the greenhouse. The density of air in Case A closely resembles the temperature distribution of air. This makes sense since density depends on temperature and pressure; however, as it is a system that exchanges air with the outside, the pressure does not change, with the temperature being one of the most important variables in the greenhouse-type dryer. On average, the density presents a value of  $1.06 \text{ kg m}^{-3}$ , the cold air represents the lower part in the dryer and coincides with the air inlets, which physically happens in the real system. On the other hand, the airspeed has an average of  $0.3 \text{ m s}^{-1}$  without considering the velocity at the dryer inlet. The velocity is higher in the lower part of the dryer due to the effect of natural convection, being the part near the cover the one with the lowest speed. Again, this corroborates that the air temperature is higher in the upper part due to the natural convection process generating temperature stratification.

### **7.6.2 Case B**

Case B presents an improvement in air temperature distribution with less stratification from the height of the tables. On average, the temperature is  $52 \text{ }^{\circ}\text{C}$ , sufficient for drying. In the actual handling of the greenhouse during tomato drying (just as an example), the temperature of the product mustn't exceed  $50 \text{ }^{\circ}\text{C}$  to preserve the vitamins and lycopene (Khama et al., 2016). In addition, with the new system design, the necessary temperatures would be obtained in less time, greatly reducing the drying time (Janjai & Bala, 2012). The highest temperature was found in the recirculation system, the plastic during recirculation heated up and presented the highest temperatures on the scale. Materials that support this temperature should be considered to improve the design. Perhaps a smaller metal material can serve that purpose.

In terms of air velocity, it is observed that there are smaller stagnation spaces, the average speed is  $0.45 \text{ m s}^{-1}$ , and where higher speeds occur is in the redistribution system as expected. Something to note is that the length of the line is sufficient to keep the temperature homogeneous, but the speed is reduced at the end of the plastic channel, which should be considered for future designs. A lack of homogeneity is also observed, mainly in the center of the greenhouse. Concerning air density, a reduction in the stratification of values is observed both vertically and horizontally. The denser air continues to present itself at the inlets and concentrates at the bottom of the dryer. The average density is  $1.2 \text{ kg m}^{-3}$ .

### **7.6.3 Case C**

Finally, due to the lack of homogeneity in the center of the dryer, it was decided to improve the design with a tube in the middle and move the air intake to the back of the greenhouse. The temperature results indicated that the same temperatures are reached on average as with Case B but with a better distribution over the entire volume of the greenhouse, reducing the temperature near the ground to  $35 \text{ }^\circ\text{C}$ . Again, higher temperatures occur within the air recirculation system and must be considered for the correct selection of the material. Regarding the air velocities, it is observed that with this new geometry average speeds of  $0.35 \text{ m s}^{-1}$  are reached, the highest being found in the air recirculation system. About the system, it is observed that the tube in the middle is the one that presents higher speeds to those on the side and although the speed is reduced, the results in terms of air mixing were satisfactory.

The density presented a more constant value throughout the dryer with an average value of  $1.22 \text{ kg m}^{-3}$  in this new case, with a difference in the lower part of the dryer and of course in the inlets, which are exchanging air with the exterior. This result corroborates that the temperature is more homogeneous with this new system compared to Cases A and B. This system not only allows an optimal

temperature to be reached for drying within the entire volume but also places where there is a lower temperature are below the drying tables.

#### **7.6.4 Comparison between Cases**

If the real system is considered and comparing the three scenarios, with the same solar radiation on the same day and time, there is a higher temperature in the drying zone in both Cases B and C, with a better distribution in Case C. In both cases, the speed is also better distributed throughout the volume with acceptable values for the drying to produce good quality.

The results obtained with Case A, without an air recirculation system, showed a similar vertical air temperature stratification when compared to results from Duong et al. (2021); Román-Roldán et al. (2019); Srichat et al. (n.d.); Villagran et al. (2021). Obviously, the longer the greenhouse, the greater stratification will appear on the horizontal axis; however, the exact value reached by air inside the dryer depends on various factors such as location, the day the experiments were carried out, cloud coverage, solar radiation, ambient temperature, altitude and, of course, the geometry of the dryer. However, it is important to reiterate that in the greenhouses reviewed from the studies in the literature, uniformity of the air temperature and air velocity was lacking.

The drying process in greenhouses can be improved with systems that support forced convection. The best geometry for each design, materials, speeds, and control strategies for these systems must be considered and studied. The current study was carried out at a time when the exhaust fans were not activated since the average temperature was less than 50°C, established as the set point for tomato drying (just as an example). The use of exhaust fans in conjunction with this type of system should also be studied but forcing the air in the attic to move under the drying tables improves the internal conditions for solar drying in greenhouses.

Many authors do not document the pressure at which the calculations of the properties of moist air were made, but it should be noted that ANSYS by default uses the atmospheric pressure at sea level and must be updated for the place where the study is being carried out. As the dryers become greater for fulfilling the needs of a solar dryer at an industrial scale, CFD stands as a powerful tool for improving the designs and reduce the costs of experimentation.

## 7.7 CONCLUSIONS

CFD simulation is a valuable engineering tool to study various designs and evaluate “*what-if*” scenarios. This study first validated a CFD model for greenhouse-type dryer and then evaluated various air distribution design that can enhance drying process. The distribution of air temperature and velocity was investigated in a 3D greenhouse-type solar dryer. The use of ANSYS fluent allowed the incorporation of solar radiation with the DO model and the realizable k- $\epsilon$  turbulence model. The density of the original system varies concerning the volume, so using the Boussinesq approximation could lead to an error during the simulation of greenhouse-type solar dryers when it is not known if the temperature difference is greater than 15°C. The temperature distribution inside the greenhouse is improved when a recirculation system with three lines is used with a fan that can provide a speed of 5 m s<sup>-1</sup>. If a system with two lines is used, better air distribution is observed compared to the original system, however there are still regions in the greenhouse with temperature stratification. The temperature near the ground is lower than the one reached in the upper part at the height of the drying tables, this would allow the addition of a monitoring system inside the dryer without being affected or the installation of lights in the lower part of the dryer. Bearing in mind that if you want to make the most of solar radiation, it is a better option to introduce the product at dawn.

The average speed of the air in the three systems is 0.3 m s<sup>-1</sup>, which is desirable for a good quality product when drying. An improvement can be made

to the system by reducing the size of the holes and changing the layout to three holes per tube, which is an ongoing study by the authors. However, the factor of the tables and the product must be added to investigate the reduction in air velocity due to the obstruction of both.

## 7.8 REFERENCES

American Society of Heating, R. and A.-C. Engineers. (1989). ASHRAE handbook: fundamentals.

ANSYS, Inc. (2010). ANSYS Meshing User's Guide.

ANSYS, Inc. (2011). ANSYS FLUENT Theory Guide.

Asadi, I., Shafigh, P., Abu Hassan, Z. F. bin, & Mahyuddin, N. B. (2018). Thermal conductivity of concrete – A review. *Journal of Building Engineering*, 20, 81–93. <https://doi.org/10.1016/J.JOBE.2018.07.002>

Deng, Z., Li, M., Xing, T., Zhang, J., Wang, Y., & Zhang, Y. (2021). A literature research on the drying quality of agricultural products with using solar drying technologies. *Solar Energy*, 229, 69–83. <https://doi.org/10.1016/J.SOLENER.2021.07.041>

Duong, Y. H. P., Vo, N. T., Le, P. T. K., & Tran, V. T. (2021a). Three-Dimensional Simulation of Solar Greenhouse Dryer. *Chemical Engineering Transactions*, 83, 211–216. <https://doi.org/10.3303/CET2183036>

Duong, Y. H. P., Vo, N. T., Le, P. T. K., & Tran, V. T. (2021b). Three-Dimensional Simulation of Solar Greenhouse Dryer. *Chemical Engineering Transactions*, 83, 211–216. <https://doi.org/10.3303/CET2183036>

Ferziger, J. H., & Perić, M. (2002). Computational Methods for Fluid Dynamics. Computational Methods for Fluid Dynamics. <https://doi.org/10.1007/978-3-642-56026-2>

Gupta, V., Sharma, A., & Gupta, K. S. (2018). Numerical Analysis of Direct Type Greenhouse Dryer. ASME 2017 Gas Turbine India Conference, GTINDIA 2017, 2. <https://doi.org/10.1115/GTINDIA2017-4784>

Janjai, S., & Bala, B. K. (2012). Solar drying technology. Food Engineering Reviews, 4, 16–54. <https://doi.org/10.1007/s12393-011-9044-6>

Khama, R., Aissani, F., Alkama, R., Bennamoun, L., Fraikin, L., Salmon, T., Plougonven, E., & Leonard, A. (2016). CONVECTIVE DRYING OF CHERRY TOMATO: STUDY OF SKIN EFFECT. Journal of Engineering Science and Technology, 11(3), 443–457.

Lokeswaran, S., & Eswaramoorthy, M. (2013). An Experimental Analysis of a Solar Greenhouse Drier: Computational Fluid Dynamics (CFD) Validation. [Http://Dx.Doi.Org/10.1080/15567036.2010.532195](http://Dx.Doi.Org/10.1080/15567036.2010.532195), 35(21), 2062–2071. <https://doi.org/10.1080/15567036.2010.532195>

Noh, A. M., Mat, S., & Ruslan, M. H. (2018). CFD Simulation of Temperature and Air Flow Distribution inside Industrial Scale Solar Dryer. Journal of Advanced Research in Fluid Mechanics and Thermal Sciences, 45(1), 156–164. <https://www.akademiabaru.com/submit/index.php/arfmts/article/view/2192>

Purusothaman, M., Valarmathi, T. N., & Santhosh, P. S. (2019). CFD Analysis of Greenhouse Solar Dryer with Different Roof Shapes. 5th International Conference on Science Technology Engineering and Mathematics, ICONSTEM 2019, 408–412. <https://doi.org/10.1109/ICONSTEM.2019.8918788>

Rodriguez, S. (2019). Applied Computational Fluid Dynamics and Turbulence Modeling. Applied Computational Fluid Dynamics and Turbulence Modeling. <https://doi.org/10.1007/978-3-030-28691-0>

Román-Roldán, N. I., Ituna Yudonago, J. F., López-Ortiz, A., Rodríguez-Ramírez, J., & Sandoval-Torres, S. (2021). A new air recirculation system for homogeneous solar drying: Computational fluid dynamics approach. Renewable Energy, 179, 1727–1741. <https://doi.org/10.1016/J.RENENE.2021.07.134>

Román-Roldán, N. I., López-Ortiz, A., Ituna-Yudonago, J. F., García-Valladares, O., & Pilatowsky-Figueroa, I. (2019). Computational fluid dynamics analysis of heat transfer in a greenhouse solar dryer “chapel-type” coupled to an air solar heating system. Energy Science and Engineering, 7(4), 1123–1139. <https://doi.org/10.1002/ESE3.333>

Serrano, M. A., & Moreno, J. C. (2020). Spectral transmission of solar radiation by plastic and glass materials. Journal of Photochemistry and Photobiology B: Biology, 208. <https://doi.org/10.1016/J.JPHOTOBIO.2020.111894>

Shultz, A. R. (1999). PVT, Specific Heat, and Thermal Transitions. Handbook of Polycarbonate Science and Technology, 165–194. <https://doi.org/10.1201/9781482273694-15>

Somsila, P., & Teeboonma, U. (2014). Investigation of temperature and air flow inside Para rubber greenhouse solar dryer incline roof type by using CFD technique. Advanced Materials Research, 931–932, 1238–1242. <https://doi.org/10.4028/WWW.SCIENTIFIC.NET/AMR.931-932.1238>

Srichat, A., Vengsungnle, P., Hongtong, K., Kaewka, W., & Jongpluempiti, J. (n.d.). A Comparison of Temperature for Parabola and Sinusoidal Greenhouse Solar Dryer by CFD. <https://doi.org/10.1088/1757-899X/501/1/012006>

Srinivasan, G., & Muthukumar, P. (2021). A review on solar greenhouse dryer: Design, thermal modelling, energy, economic and environmental aspects. *Solar Energy*, 229, 3–21. <https://doi.org/10.1016/J.SOLENER.2021.04.058>

Versteeg, H. K., & Malalasekera, W. (1996). *An introduction to computational fluid dynamics: the finite volume method*, 1995. Harlow-Longman Scientific & Technical, London, M, 503.

Villagran, E., Henao-Rojas, J. C., & Franco, G. (2021a). Thermo-environmental performance of four different shapes of solar greenhouse dryer with free convection operating principle and no load on product. *Fluids*, 6(5). <https://doi.org/10.3390/FLUIDS6050183>

Villagran, E., Henao-Rojas, J. C., & Franco, G. (2021b). Thermo-Environmental Performance of Four Different Shapes of Solar Greenhouse Dryer with Free Convection Operating Principle and No Load on Product. *Fluids* 2021, Vol. 6, Page 183, 6(5), 183. <https://doi.org/10.3390/FLUIDS6050183>

Vivekanandan, M., Periasamy, K., Babu, C. D., Selvakumar, G., & Arivazhagan, R. (2021). Experimental and CFD investigation of six shapes of solar greenhouse dryer in no load conditions to identify the ideal shape of dryer. *Materials Today: Proceedings*, 37(Part 2), 1409–1416. <https://doi.org/10.1016/J.MATPR.2020.07.062>

Zhang, W., & Xu, Y. (2019). Experimental Studies of Mechanical Properties of Polycarbonate. *Mechanical Properties of Polycarbonate*, 1–28. <https://doi.org/10.1016/B978-1-78548-313-4.50001-7>